Compression Lap Splices of Straight Bars and Compression Development of Headed and Hooked Bars in Beam-Column Joints

By
© 2022
Guido Andrés Valentini
Ingeniero Civil, Universidad Nacional de Rosario, 2019

Submitted to the graduate degree program in Civil, Environmental & Architectural Engineering and the Graduate Faculty of the University of Kansas in partial fulfillment of the requirements for the degree of Master of Science in Civil (Structural) Engineering.

Chair: Rémy Lequesne

Andrés Lepage

David Darwin

Date Defended: 02 September 2022

The thesis committee for Guido Andrés Valentini certifies that this
is the approved version of the following thesis:

Compression Lap Splices of Straight Bars and Compression Development of Headed and Hooked Bars in Beam-Column Joints

_____

Chair: Rémy Lequesne

Date Approved: 04 September 2022

Abstract

ACI 318-19 Building Code provisions for compression lap splices and for headed and hooked bar development in special moment frame (SMF) joints were evaluated against databases of test results. Recommendations are made for simplifying and improving code requirements.

Compression lap splice length provisions (ACI 318-19 §25.5.5) were shown to produce calculated lengths longer than Class B tension lap splice lengths under certain design conditions and also to be a poor fit to a database of 89 test results (it must be emphasized that 72 specimens in the database violated the ACI 318-19 minimum lap splice length). It was shown that several equations exist that better fit the dataset, and that it may be possible to define the compression lap splice length as a function of the tension development length. Use of tension development length equations for compression lap splice design is a practical, more accurate alternative to §25.5.5 that eliminates the need to calculate both tension and compression development lengths and prevents design cases where calculated lengths are longer in compression than in tension.

Analyses show that ACI 318-19 §18.8.2.2 should not require that headed and hooked bars satisfy §25.4.9. Comparisons with results from exterior beam-column connections with headed or hooked beam reinforcement terminating in the joint show that satisfying §25.4.9 is not a necessary condition for preventing anchorage distress in SMF joints. None of the 55 specimens (36 with headed bars and 19 with hooked bars) with drift capacities above 3% and no evidence of anchorage distress satisfied §25.4.9. The analyses also show that complying with §18.8.5.2 is not a necessary condition for joints with headed bars to exhibit satisfactory behavior, suggesting that §25.4.4, which §18.8.5.2 refers to, may be overly conservative. Other equations were considered and found to better fit the data.

Acknowledgments

Support for this research was provided by the Concrete Reinforcing Steel Institute (CRSI) Education and Research Foundation.

This work would not have been possible without the many people that offered me their help and encouragement throughout my journey at the University of Kansas.

I want to thank my advisor Rémy Lequesne for taking me as his student and for believing in me even at the times when I would not. Your optimism, sense of humor, and unreasonable patience have been invaluable. I will be forever grateful for the countless opportunities you have sent my way.

Very special thanks to my thesis committee members for their support and input leading to the completion of this research project and thesis. Thanks to Andrés Lepage for his time invested in me and for his ever-meticulous insights. Thank you for the valuable lessons you have taught me inside and outside the classroom. Many thanks to David Darwin for his cheerful guidance and for encouraging meaningful debates through his expertise.

Thanks to my friends and colleagues at the University of Kansas for sharing a piece of your life with me between classes, and for supporting me as I almost became insane writing this thesis.

I owe the greatest thanks to my family for their unconditional support and love. Thank you to my parents, Claudia Saquino and Germán Valentini, for always seeing the best in me. Thank you to my sister and best friend, Chiara Valentini, for being always there for me.

Guido Valentini

September 4, 2022

Table of Contents

List of Figures

List of Tables

Chapter 1: Introduction

1.1 Background and Motivation

For reinforced concrete to function as a composite, concrete and steel bars must interact such that forces in one material can transfer into the other. This interaction is referred to as bond, which is understood to result from multiple mechanisms. Bond first manifests by mechanical adhesion between the two materials, but this is a relatively weak mechanism that is eliminated by small relative displacements (bar slip). Bar slip causes frictional forces to develop as a result of the roughness of the interface. Finally, in deformed bars, mechanical anchorage takes place due to bearing of bar deformations against the concrete. For bars in compression, a fourth mechanism is active: bearing of the end of the bar against concrete.

Bond research has been primarily focused on bars in tension [1]. ACI 408R-03 [1] and fib bulletin 72 [2] provide thorough reports on bond and development of straight reinforcing bars in tension. ACI 408R-03 states that bond of straight bars is primarily governed by:

- The mechanical properties of the concrete (tensile and bearing strength),
- The volume of concrete around the bars (related to concrete cover and bar spacing),
- The presence of confinement in the form of transverse reinforcement (ties, spirals), which controls crack propagation,
- The surface condition of the bar, and
- The geometry of the bar (deformation height, spacing, width, and face angle).

Comparatively little research has been conducted to investigate bond of bars in compression. In general, bond in compression is understood to be affected by the same factors as in tension, except that end bearing in compression is also important.

For design, the length required for a reinforcing bar embedded in concrete to transfer a force equal to $A_b f_y$ through bond is referred to as the *development length*. The force in question can be either tension and compression, leading to design requirements for *tension development length*, ℓ_d, and *compression development length*, ℓ_{dc}, for straight bars. The overlap length required to transfer force between bars is referred to as *lap splice length*. There are design requirements for *tension lap splice length*, ℓ_{st}, which are related to ℓ_d, and *compression lap splice length*, ℓ_{sc}, which are not related to ℓ_{dc}. Due to the beneficial contribution of end bearing to bond in compression, ℓ_{dc} and ℓ_{sc} should be no longer than ℓ_d and ℓ_{st}, respectively. However, as will be described in Chapter 2, the ACI 318-19 [1] provisions for ℓ_{dc} sometimes produce required lengths that are substantially longer than ℓ_d. This problem motivates the work in Chapter 2.

Headed and hooked bars, which are common in beam-column joints and other connections, transfer tension force in a bar to the concrete through a combination of bond along the straight portion of the bar and bearing of the head or hook against concrete. The development lengths of headed and hooked bars (ℓ_{dh} and ℓ_{dt}, respectively) are based on tests under direct tension. Due in part to the lack of tests of headed and hooked bars in compression, heads and hooks are not generally considered effective for transferring compression forces to concrete. Nevertheless, there are applications, such as in beam-column joints subjected to earthquake-induced shaking, where headed and hooked bars are subjected to cyclic tension and compression forces. Very little research has been aimed at understanding the behavior of headed and hooked bars in compression, and it is

unclear whether the design of headed and hooked bars in joints should consider compression force demands.

ACI 318-19 [1] governs the design of special moment frames (SMF) and prescribes that reinforcement terminating in a joint must be detailed so that both the tension and compression development lengths are satisfied. The work in Chapters 3 and 4 will show that it is not necessary for either headed or hooked bars to satisfy the compression development length requirements to obtain acceptable beam-column joint behavior under reversed cyclic displacements. Moreover, Chapter 3 will show that the tension development requirements for headed bars also appear exceedingly conservative in SMF joints.

1.2 Scope

In Chapter 2, the ACI 408R-03 database of compression lap splice test results [4] was used to evaluate ACI 318-19 provisions for compression development and lap splice length. ACI 318-19 provisions are shown to be imprecise and highly conservative. Equations from other design standards and researchers were evaluated and recommendations are made for improving and simplifying ACI 319-19 provisions for compression development.

In Chapter 3, databases compiled by Kang et al. [5] and Ghimire et al. [6] are used to evaluate development length provisions for headed bars in SMF joints. The databases include test results from exterior reinforced concrete beam-column joint specimens with headed bars subjected to reversed cyclic loading. Recommendations are made for improving ACI 318-19 provisions.

In Chapter 4, a database assembled by the author is used to evaluate development length provisions for headed bars in SMF joints. The database includes results from tests of exterior

reinforced concrete beam-column joint specimens with hooked bars that are subjected to reversed cyclic loading. Recommendations are made for improving ACI 318-19 provisions.

Chapter 5 provides a summary of major findings and recommendations from prior chapters.

Notation is defined within each chapter. Citations are provided for references in Chapter 6.

1.3 Notation

A_b	=	cross-sectional area of reinforcing bar (in.^{2})
f_y	=	specified yield stress for non-prestressed steel reinforcement (psi)
ℓ_d	=	tension development length (in.)
ℓ_{dc}	=	compression development length (in.)
ℓ_{sc}	=	compression lap splice length (in.)
ℓ_{st}	=	tension lap splice length (in.)
ℓ_{dh}	=	headed bar tension development length (in.)
ℓ_{dt}	=	hooked bar tension development length (in.)

Chapter 2: Development and Lap Splice Length of Straight Bars in Compression

2.1 Introduction

Section 25.5.5 of ACI 318-19 [3] requires that the compression lap splice length, ℓ_{sc}, satisfy Eq. (1), which is a function of the specified yield stress of the reinforcing steel and the bar diameter, with a minimum required length of 12 in. (300 mm).

$$\begin{array}{ll} \text{(a) } \max\{0.0005\, f_y\, d_b \text{ ; } 12 \text{ in.}\} & \text{for } f_y \le 60{,}000 \text{ psi} \\ \text{(b) } \max\{(0.0009\, f_y - 24)\, d_b \text{ ; } 12 \text{ in.}\} & \text{for } 60{,}000 \text{ psi} < f_y \le 80{,}000 \text{ psi} \\ \text{(c) } \max\{(0.0009\, f_y - 24)\, d_b \text{ ; } \ell_{st} & \text{for } 80{,}000 \text{ psi} < f_y \end{array} \qquad \text{Eq. (1) [lb-in.]}$$

The provisions are applicable to No. 11 or smaller deformed bars in compression. The calculated splice length is to be increased by one-third when the concrete compressive strength is less than 3000 psi (21 MPa), but otherwise the provisions do not account for concrete compressive strength. For compression lap splices in columns, Chapter 10 of ACI 318-19 (§10.7.5.2.1) allows the calculated lap splice length to be reduced by 17 or 25% if the splice is enclosed throughout its length by sufficient ties or spiral reinforcement. Sufficient refers, in this case, to an effective reinforcement ratio of ties greater or equal than 0.0015 in both directions throughout the splice length or spirals that meet ACI 318-19 requirements throughout the splice length, respectively. The provisions do not account for smaller quantities of transverse reinforcement in columns or for any quantity of transverse reinforcement for lap splices in members other than columns.

This contrasts with other ACI 318-19 equations related to bond, which do account for several of these variables. Consider the tension development length (§25.4.2), tension lap splice length (§25.5.2), and compression development length (§25.4.9) equations, shown in Eqs. (2) to (4), respectively. These equations not only include the steel reinforcement yield stress and bar diameter, but also the concrete compressive strength and factors accounting for lightweight

concrete and transverse reinforcement. Equations (2) and (3) furthermore include modification factors accounting for reinforcement grade, epoxy coating, bar size, reinforcement casting position, and concrete cover.

$$\ell_d = \max\left\{\left(\frac{3}{40}\frac{f_y}{\lambda\sqrt{f_c'}}\frac{\psi_t\psi_e\psi_s\psi_g}{\left(\frac{c_b + K_{tr,318}}{d_b}\right)}\right)d_b \ ;\ 12 \text{ in.}\right\} \qquad \text{Eq. (2)}\ [\text{lb-in.}]$$

$$\ell_{st} = \begin{cases} 1.0\ell_d & \text{(Class A splice)} \\ 1.3\ell_d & \text{(Class B splice)} \end{cases} \qquad \text{Eq. (3)}\ [\text{lb-in.}]$$

$$\ell_{dc} = \max\left\{\frac{f_y\psi_r}{50\lambda\sqrt{f_c'}}d_b \ ;\ 0.0003 f_y\psi_r d_b \ ;\ 8 \text{ in.}\right\} \qquad \text{Eq. (4)}\ [\text{lb-in.}]$$

Since tension development, compression development, and compression lap splicing provisions represent very similar physical phenomena, it would be reasonable to expect that these provisions account for the same variables. The fact that they do not can lead to questionable (and possibly inefficient) designs. One of the issues is that in certain cases the calculated compression lap splice length can be considerably longer than the respective tension lap splice length. For instance, a lap splice of No. 8 (25 mm) Grade 80 (550) uncoated bars in a column with a concrete compressive strength of 8000 psi (55 MPa) and closely spaced ties would be 48 in. (1220 mm) according to Eq. 1 (§25.5.5), 20% longer than the tension lap splice length of 40 in. (1020 mm) calculated with Eq. 3 (§25.5.2) for Class B lap splices. Even though §10.7.5.2 permits the calculated compression lap splice length to be reduced to 40 in. (1020 mm), that reduction is only permitted in columns. Furthermore, the compression lap splice length is almost three times the compression development length of 18 in. (457 mm) calculated with Eq. 4 (§25.4.9).

The fact that $\ell_{sc} > \ell_{st}$ in a reasonable design scenario is cause to question whether Section 25.5.5 (Eq. 1) can be improved. There is a need to identify equations for compression lap splice length that account for key variables (such as bar yield stress, bar diameter, concrete compressive strength, and transverse reinforcement) and produce calculated lengths that are less than tension lap splice lengths.

2.2 Database Description

This study examined the results in Group 1 of the ACI 408 compression lap splice database [4], which contains results from 91 tests of columns with lap-spliced bars subjected to monotonic compression. A summary of specimen variables is provided in Appendix A. The cross sections of columns in the database are shown in Figure 1. The distribution of important variables within the database are shown in Figures 2 through 7.

Most of the columns (87 out of 91) had rectangular cross-sections, and the ratio of wide-to-narrow cross-sectional dimension was nominally between 1.0 and 1.4. Four specimens had circular cross sections. All lap-spliced bars had bond and bearing interactions with the concrete and the reported bar stress at lap splice failure did not exceed the yield stress. To limit the scope to specimens exhibiting stresses similar to those observed in practice, the two specimens that failed with steel stresses below 40 ksi (275 MPa) were removed from the dataset, resulting in a set of results from 89 tests.

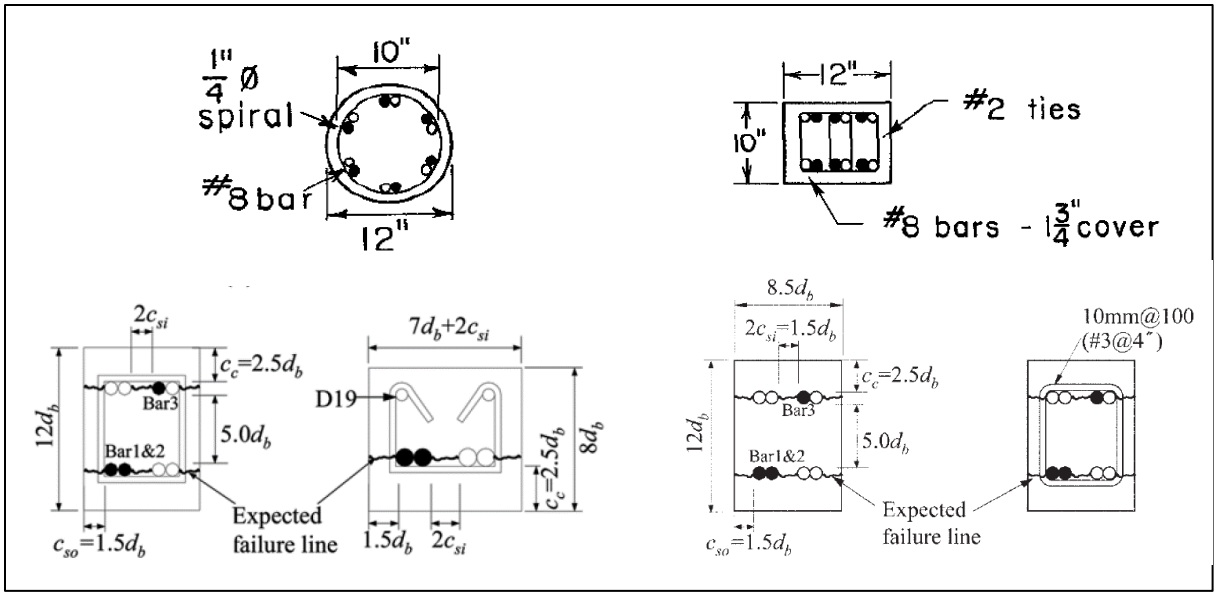

Figure 1 – Cross-sections of column specimens in database (from Refs. [7, 8, 9, 10])

The column longitudinal reinforcement, which was lap spliced, consisted of either No. 7, 8, or 9 (22, 25, or 29 mm) reinforcing bars (Figure 2). These bar sizes are reasonably representative of the bar sizes used in columns, walls, and beams where compression lap splices are common in practice. The rectangular columns in the database had either four or six longitudinal bars and the circular columns had six longitudinal bars. Either half or all the column bars were lap spliced, and there were no columns with staggered lap splices in this dataset.

Approximately half (47%) of the columns had transverse reinforcement within the lap splice consisting of evenly spaced ties or hoops in the rectangular columns or a spiral in the circular columns. Figure 3 shows the distribution of the value obtained from $(c_b + K_{tr,318})/d_b$, which ranged from 2.0 to 4.25, and Figure 4 shows the distribution of $K_{tr,318}/d_b$, which ranged from 0 to 1.75. In this database, c_b/d_b was greater than $K_{tr,318}/d_b$ in 80% of the specimens. In ACI 318-19, $(c_b + K_{tr,318})/d_b$ is part of the tension development length equation and does not apply for compression

development, but it is used here because no analogous term is available within the building code for compression lap splices.

The distribution of concrete compressive strengths and reinforcement stresses at failure are shown in Figure 5 and Figure 6, respectively. Concrete compressive strength was measured using either 4 by 8 in. (100 by 200 mm) or 6 by 12 in. (150 by 300 mm) cylinders. To reduce scatter in results associated with differences in cylinder size, the measured strengths were converted to an equivalent 6 by 12 in. (150 by 300 mm) cylinder using the method described by Reineck et al. [11] ($f_{1c,mod}$ was obtained by multiplying results from 4 by 8 in. (100 by 200 mm) or 6 by 12 in. (150 by 300 mm) cylinders by (0.92/0.95) and 1.00, respectively). The converted concrete compressive strengths ranged from 3.5 to 14.2 ksi (24 to 98 MPa). Specimens failed with bar stresses of 40 to 83 ksi (275 to 570 MPa), with most specimens (80%) failing at bar stresses between 50 and 70 ksi (345 to 482 MPa). Bar stresses were inferred from readings from strain gauges on the lap-spliced reinforcement, except for four specimens reported by Pfister and Mattock [7]. The bar stresses in these tests were inferred using a method calibrated against bar strain measurements.

The lap splices had lengths of 3.5 to 30 in. (89 to 760 mm) (Figure 7), but the majority were shorter than 14 in. (356 mm). Given this distribution, and to avoid reducing the number of tests in the database too severely, no minimum lap splice length was applied in the analyses even though ACI 318-19 requires a minimum length of 12 in. (300 mm).

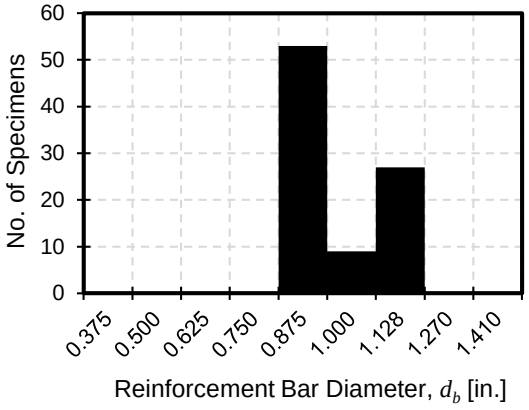

Figure 2 – Histogram of bar diameter
(1 in. = 25.4 mm)

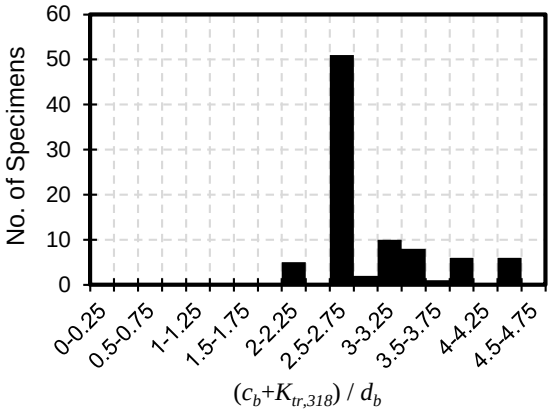

Figure 3 – Histogram of $(c_b + K_{tr,318})/d_b$ values

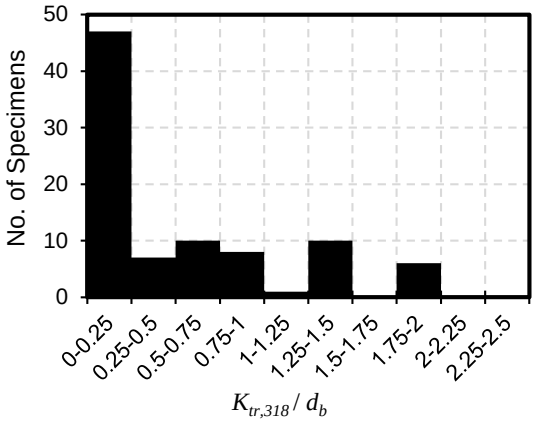

Figure 4 – Histogram of $K_{tr,318}/d_b$

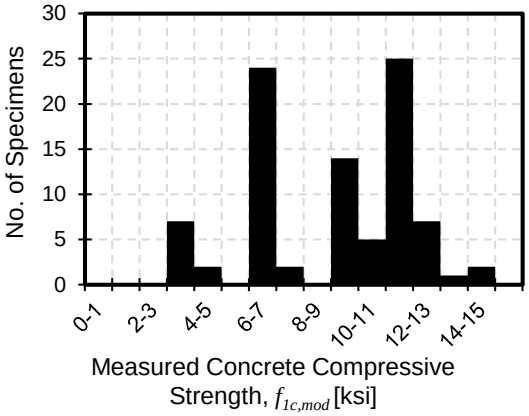

Figure 5 – Histogram of measured concrete compressive strength (1 ksi = 6.895 MPa)

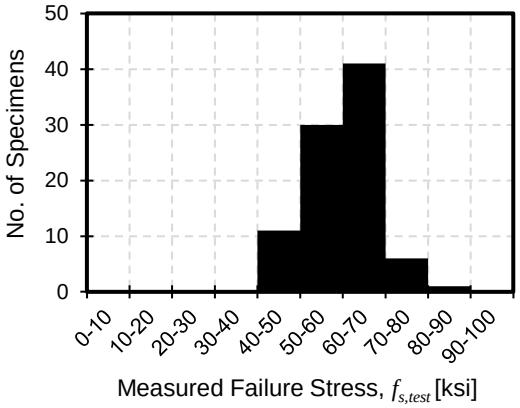

Figure 6 – Histogram of measured steel stress at failure (1 ksi = 6.895 MPa)

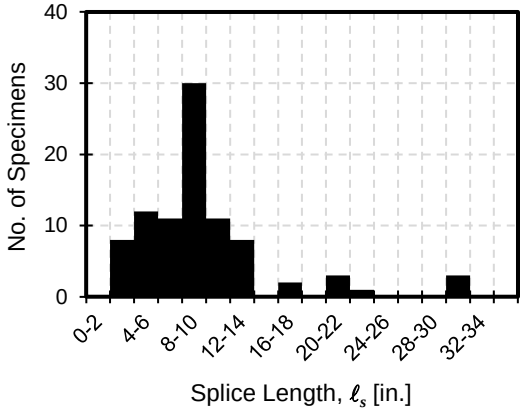

Figure 7 – Histogram of lap splice lengths
(1 in. = 25.4 mm)

When assessing equations using a dataset, it is important to acknowledge unintended biases within the dataset. Such biases can occur because, as shown in Figures 2 through 7, the variables are not randomly distributed. Decisions made by researchers can also, inadvertently, cause independent variables to be correlated within a database. For example, it was found that concrete compressive strength and lap splice length are somewhat correlated in this database (Figure 8). All specimens with a concrete compressive strength above 10 ksi (69 MPa) also had a lap splice length of not more than 12 in. (300 mm). No other correlations were observed among the variables plotted in Figures 2 through 7. Plots similar to Figure 8 for other sets of variables are in Appendix B.

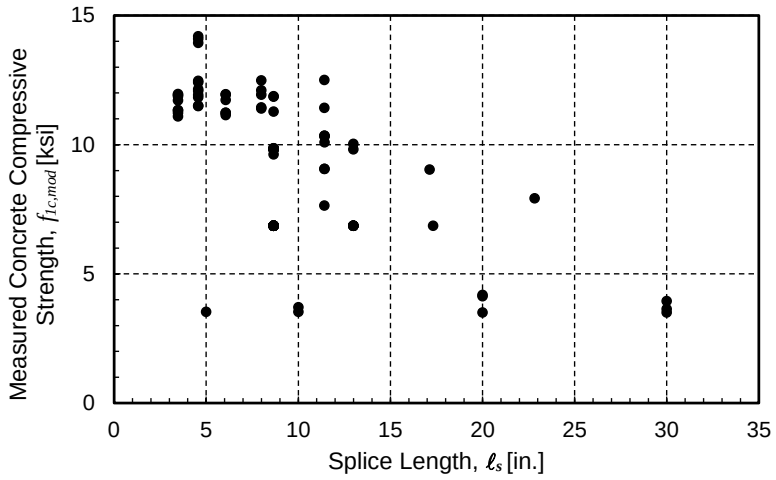

Figure 8 – Correlation between concrete compressive strength and lap splice length
(1 in. = 25.4 mm, 1 ksi = 6.895 MPa)

2.3 Comparisons with Design Equations

The database was used to evaluate the ACI 318-19 [3] compression lap splice provisions in Eq. (1) (§25.5.5). This was done by comparing the bar stress at failure, $f_{s,test}$, against $f_{s,calc}$, which was obtained by solving the design equations in Eq. (1) for bar stress and replacing f_y with $f_{s,calc}$ to obtain Eq. (5). The stress $f_{s,calc}$ is a function of the provided lap splice length and bar diameter, with the choice of equation (a), (b), or (c) based on the measured failure stress.

$$\begin{aligned} &\text{(a) } \ell_{sc}/(0.0005 d_b) && \text{for } f_{s,test} \le 60{,}000 \text{ psi} \\ &\text{(b) } (\ell_{sc} / d_b + 24)/0.0009 && \text{for } 60{,}000 \text{ psi} < f_{s,test} \le 80{,}000 \text{ psi} \\ &\text{(c) } (\ell_{sc} / d_b + 24)/0.0009 && \text{for } f_{s,test} > 80{,}000 \text{ psi} \end{aligned} \qquad \text{Eq. (5)}$$

A test-to-calculated stress ratio (T/C) was then calculated for each specimen as the quotient of $f_{s,test}$ and $f_{s,calc}$. The modification factor in ACI 318-19 §10.7.5.2.1 that accounts for transverse reinforcement was included where it was applicable. The mean T/C for the database for Eq. (5) was 2.58 with a coeficient of variation, CV, of 0.60, and values ranging from 0.97 to 6.50. This is a high mean and CV indicating that the ACI provisions are imprecise and sometimes overly conservative.

To better understand the trends, T/C values are plotted in Figures 9 through 12 versus several variables known to govern bond: $(c_b + K_{tr,318})/d_b$, $f_{1c,mod}$, $f_{s,test}$, and ℓ_s. Figure 9 includes no limits on $(c_b + K_{tr,318})/d_b$ because this term does not apply to compression lap splices (the limit of 2.5 for tension bar development is omitted). The ACI 318-19 minimum lap splice length of 12 in. (300 mm) was also not applied as a limit, although these plots do distinguish between specimens with lap splice lengths of at least $\ell_{sc,min}$ = 12 in. (300 mm) and those with shorter lap splices.

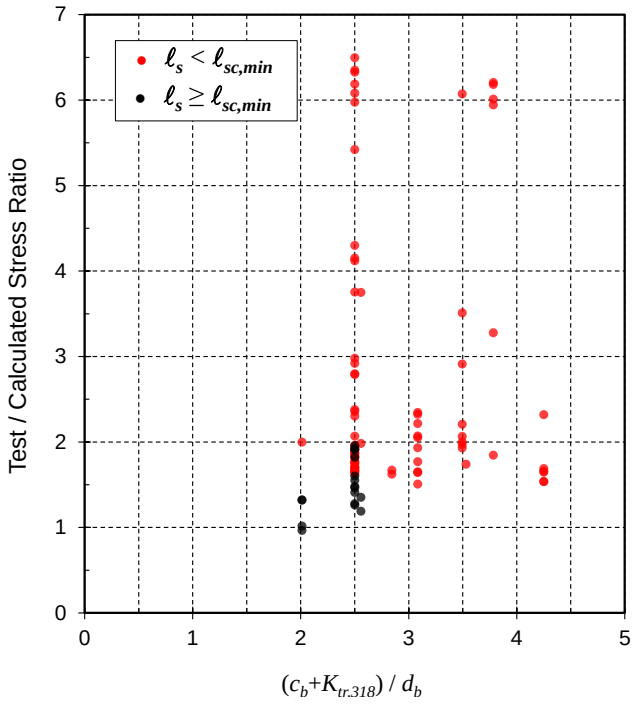

Figure 9 – ACI 318-19 Compression Lap Splice : T/C vs. $(c_b + K_{tr,318})/d_b$

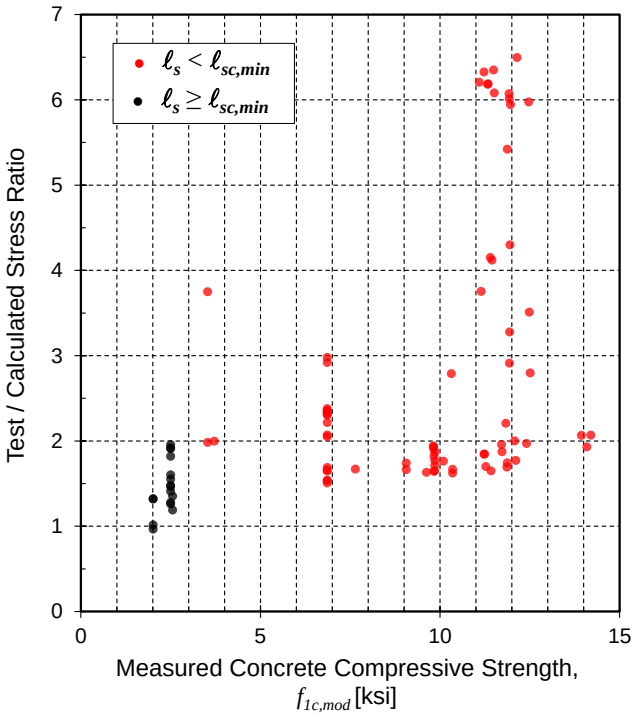

Figure 10 – ACI 318-19 Compression Lap Splice: T/C vs. measured concrete compressive strength, $f_{1c,mod}$

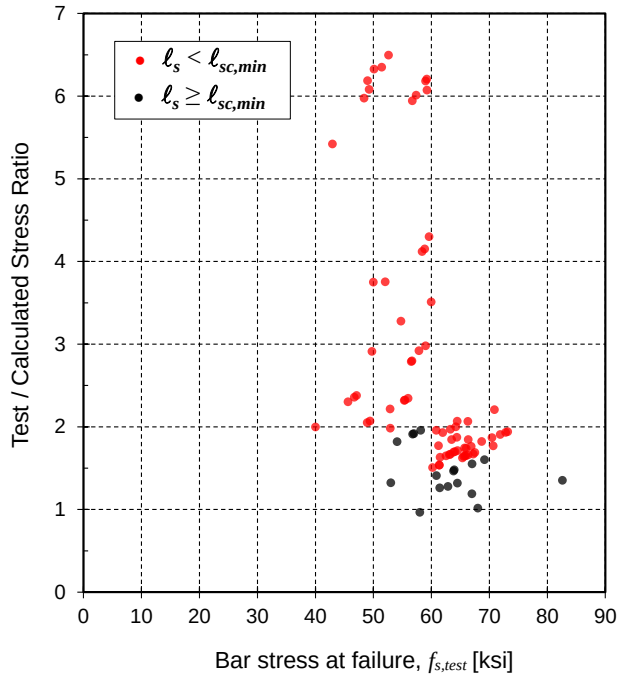

Figure 11 – ACI 318-19 Compression Lap Splice: *T*/*C* vs. bar stress at failure, $f_{s,test}$

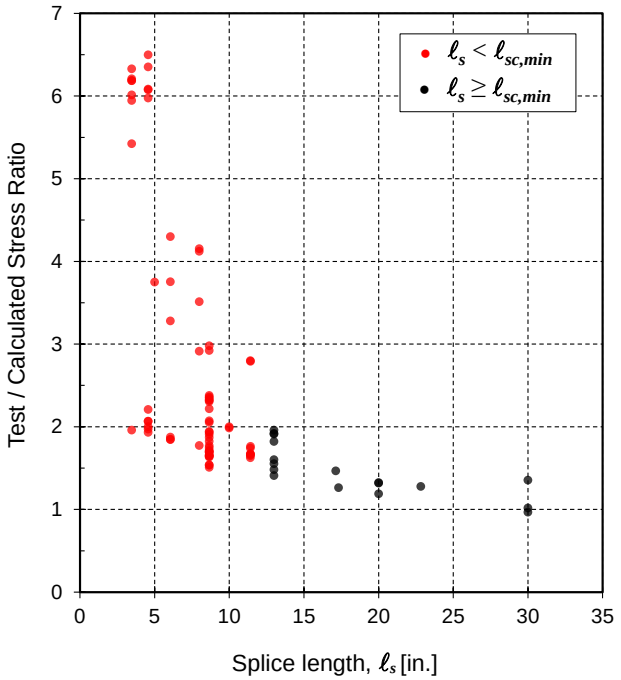

Figure 12 – ACI 318-19 Compression Lap Splice: *T*/*C* vs. provided lap splice length, ℓ_s

Figures 9 and 10 suggest that ACI 318-19 §25.5.5 tends to become more conservative as the provided confinement and the concrete compressive strength increase, although there is considerable scatter. Figure 11 shows that Eq. 5(b) produces substantially less scatter for bar stresses greater than 60 ksi than Eq. 5(a) produces for bar stresses less than 60 ksi. By inspection, it is also clear that Eq. 5(a) is considerably more conservative than Eq. 5(b). Figure 12 shows that the provisions become less conservative with longer lap splice lengths.

The scatter in Figures 9 through 12 increases for specimens with $f_{1c,mod}$ > 10,000 psi (69 MPa) and $f_{s,test}$ < 60,000 psi (420 MPa), which coincides with use of the equation applicable for $f_{s,test}$ < 60,000 psi. Many specimens with $f_{1c,mod}$ > 10,000 psi (69 MPa) tended to have short lap splice lengths (below the ACI minimum) and, thus, also had lower bar stresses at failure. The black

circles in Figures 9 through 12, representing the 17 specimens with ℓ_s > 12 in. (300 mm), had *T*/*C* values between 0.97 and 2.0. Among these 17 specimens, the scatter is still greater for $f_{s,test}$ < 60,000 psi than for $f_{s,test}$ > 60,000 psi (Figure 11). Given this scatter, and given that these equations sometimes produce calculated lap splice lengths that are longer for compression than tension, there is a need to consider alternative expressions for design of compression lap splices.

2.4 Comparisons with other Compression Development Length Equations

2.4.1 Equations Considered

In addition to the comparisons with the ACI 318-19 [3] provisions, *T*/*C* values were calculated for another six expressions for either compression development length or compression lap splice length. These include: part (b) of the compression lap splice provisions from ACI 318-19 § 25.5.5.1, the ACI 318-19 §25.4.9 compression development length provisions, the 'complex' equation proposed by Chun, Lee, and Oh [9], the 'simplified' equation proposed by Chun, Lee, and Oh [12], the equation proposed by Cairns [13], and the fib Model Code [14] provisions.

i) Expression (b) of ACI 318-19 §25.5.5.1 compression lap splice length provisions (with §10.7.5.2.1 modifiers for confinement)

The ACI 318-19 lap splice length provisions (Eq. (1)) prescribe three different expressions (a, b, and c) for length, depending on the value of the steel reinforcement yield stress. Here only expression (b), reproduced in Eq. (6), is considered, regardless of the steel stress at failure. The minimum required lap splice length of 12 in. was omitted for this comparison. The confinement modifiers from §10.7.5.2.1 were used where applicable.

$$\ell_{sc} = (0.0009\, f_y - 24)\, d_b \qquad \text{Eq. (6)}$$

ii) Development of straight bars in compression (ACI 318-19 §25.4.9)

Equation (4), which is repeated below, shows the ACI 318-19 [3] compression development length (§25.4.9) equations. The Code imposes a minimum compression development length of 8 in., which was omitted in these comparisons.

$$\ell_{dc} = \max\left\{ \frac{f_y \psi_r}{50\lambda\sqrt{f_c'}} d_b \; ; \; 0.0003 f_y \psi_r d_b \right\} \qquad \text{Eq. (4) [lb-in.]}$$

where $\sqrt{f_c'} \le 100$ psi. Factor λ was 1.0 because no specimens in this database had lightweight concrete. The confining reinforcement factor, ψ_r, was also always 1.0 except for the four circular column specimens reported in Pfister and Mattock [7].

iii) 'Complex' equation for compression lap splices from Chun, Lee, and Oh [9]

Chun et al. [8, 9, 10] report results from tests of columns with compression lap splices with and without confinement. They propose Eq. (7), referred to herein as the 'complex' equation, to distinguish it from the 'simplified' Eq. (8) proposed by the same authors.

$$\frac{l_s}{d_b} = \left(\frac{\dfrac{f_y}{0.82\sqrt{f_c'}} - 198 - 21\delta}{134 + 18\dfrac{K_{tr,318}}{d_b}} \right)^2 \qquad \text{Eq. (7) [lb-in.]}$$

where $\dfrac{K_{tr,318}}{d_b} \le 1.76$; $\dfrac{l_s}{d_b} \le \begin{cases} 0.0005 f_y & \text{if } f_y \le 60{,}000 \text{ psi} \\ 0.0009 f_y - 24 & \text{if } f_y > 60{,}000 \text{ psi} \end{cases}$

iv) ‘Simplified’ equation for compression lap splices proposed by Chun, Lee, and Oh. [12]

The simplified equation from Chun, Lee, and Oh [12], Eq. (8), is indeed much simpler than Eq. (7). Aside from simplicity, it is notable that Eq. (8) includes concrete compressive strength to the quarter power as opposed to its square root.

$$\frac{l_s}{d_b} = \frac{1.4 f_y}{\psi_{sc} f_c'^{1/4}} - 52$$

$$\text{with } \psi_{sc} = 1 + 0.084 \frac{K_{tr,318}}{d_b} \; ; \; \frac{l_s}{d_b} \leq \begin{cases} 0.071 f_y & \text{if } f_y \leq 420 \text{ MPa} \\ 0.13 f_y - 24 & \text{if } f_y > 420 \text{ MPa} \end{cases}$$

Eq. (8) [SI]

v) Compression lap splice equation proposed by Cairns [13]

Cairns [13] proposed Eq. (9) for compression lap splice strength based on tension splice equations using test data from different sources. The equation highlights the role of transverse reinforcement and end bearing in the compression problem. Based on the empirical finding that compression lap splices tend to fail when transverse reinforcement yields [14], this compression splice equation uses the yield stress of the transverse reinforcing steel, f_{yt}. Within the available database, this parameter was only measured and reported by Pfister and Mattock [7]. Where no information about the transverse reinforcing steel was reported, a yield stress of 60 ksi was assumed for calculating *T*/*C*.

$$f_{sc} = \left[16.9 \frac{\ell_s}{d_b} + 354 + 0.026 \frac{A_{tr} \cdot f_{yt} \cdot \ell_s}{s \cdot d_b^{\,2}} \right] \sqrt{f_c'} \qquad \text{Eq. (9) [lb-in.]}$$

vi) fib Model Code [15] provisions

The *fib* 2010 Model Code method is notably different from the other equations considered. First, a basic bond strength is calculated from the characteristic concrete compressive strength, f_{ck},

bar diameter, bar surface characteristics, bar position during casting, and characteristic strength of steel reinfocement. This basic bond strength is then modified to obtain a design bond strength, depending on concrete cover, bar spacing, and other factors affecting confinement. Finally, the design bond strength is used to determine a required length of lap splice in compression, l_b. These provisions are reproduced in Eq. (10) in the original SI units. A minimum lap length, $l_{b,min}$, is prescribed but has been omited in this work.

Length of lap in compression:

$$l_b = \frac{\varnothing}{4 f_{bd}} \left(f_{yd} - F_h / A_s \right); \quad f_{yd} = f_{yk} / \gamma_s ; \quad F_h = 60\, f_{bd} A_s ;$$

$$l_b \geq l_{b,\min} = \max \left\{ 0.7 \frac{\varnothing}{4} \frac{f_{yd}}{f_{bd}} \; ; 15\varnothing \; ; 200 \text{ mm} \right\} \text{(ignored)}$$

Design bond strength:

$$f_{bd} = \left(\alpha_2 + \alpha_3 \right) f_{bd,0} - 2\, p_{tr} / \gamma_c < 2.5\, f_{bd,0} - 0.4\, p_{tr} / \gamma_c < 1.5 \sqrt{f_{ck}} / \gamma_c \; ;$$

Eq. (10) [SI]

$$\alpha_2 = \left(c_{min} / \varnothing \right)^{0.5} \left(c_{max} / c_{min} \right)^{0.15} \text{ for ribbed bars;} \quad \alpha_3 = k_d \left(K_{tr,fib} - \alpha_t / 50 \right) \geq 0.0$$

$$K_{tr,fib} = n_t A_{st} / \left(n_b \varnothing s_t \right) \leq 0.05$$

Basic bond strength:

$$f_{bd,0} = \eta_1 \eta_2 \eta_3 \eta_4 \left(f_{ck} / 25 \right)^{0.5} / \gamma_c$$

2.4.2 Results

Figure 13 shows the range, mean, and *CV* of the *T*/*C* for each of these compression lap splice or development length equations, and well as for the already discussed ACI 318-19 compression lap splice provisions. To examine whether the equations considered reasonably

represent the effects of the considered variables on bond strength, a set of plots analogous to Figures 9 through 12 are in Appendix C for each of the equations considerd in Figure 13.

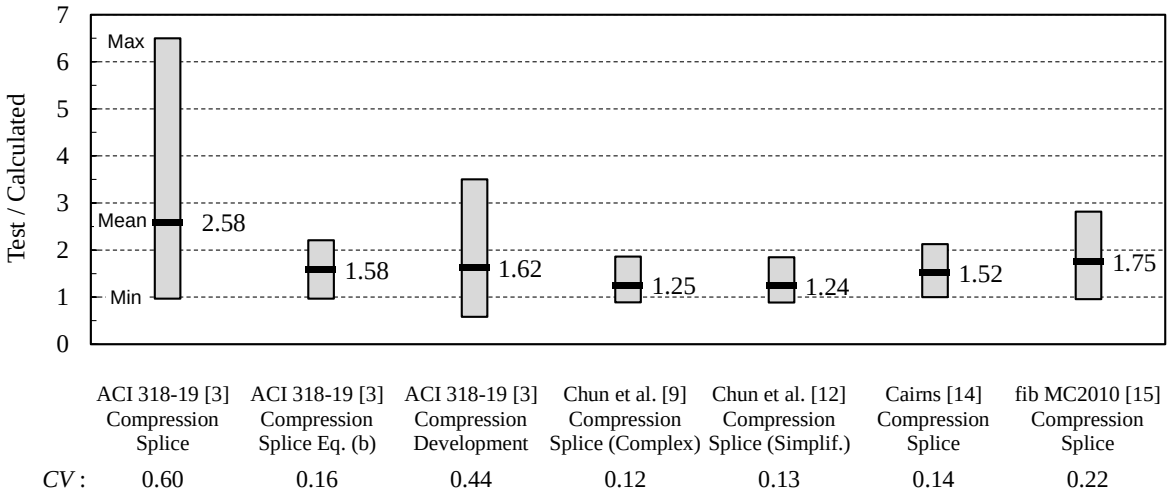

Figure 13 – *T*/*C* for compression lap splice and development length equations

The worst performance in terms of scatter is the ACI 318-19 compression lap splice provisions, with a *CV* of 0.60 (although it must be emphasized that all specimens with $T/C > 2.0$ violated the ACI 318-19 minimum lap splice length).

When solely applying Eq. (b) of the ACI 318-19 compression lap splice provisions to the entire database, as opposed to discriminating by steel failure stress, the calculated stresses are much closer to the measured values than when using the entire provision, with a mean of 1.58 and *CV* of 0.16. Figure 66 in Appendix C shows that, although the scatter is low, use of Eq. (b) of ACI 318-19 does not appear to properly account for effects of confinment or concrete compressive strength. Furthermore, it produces relatively low *T*/*C* values for lap splices longer than $20d_b$ and for the only specimen with a bar stress greater than 75 ksi.

The ACI 318-19 compression development length equations exhibited more scatter than Eq. (b) of the compression lap splice provisions, with a mean of 1.62 and *CV* of 0.44. Although

not shown here, removing the 100 psi (0.69 MPa) limit on $\sqrt{f_c'}$ did not result in a substantial improvement for the ACI 318-19 development length equation and is not recommended. Figure 67 in Appendix C shows the ACI 318-19 compression development length equations do not properly account for effects of confinment or concrete compressive strength. Furthermore, they produce *T*/*C* values below 1.0 for lap splices longer than $12d_b$ and for the only specimen with a bar stress greater than 75 ksi. It would not be acceptable to use the ACI 318-19 §25.4.9 compression development length provisions for compression lap splice design.

The two equations proposed by Chun, Lee, and Oh [9, 12] show similar results in terms of mean and *CV*, and they are the most accurate and precise of the equations referenced in Figure 13. The simplified equation in particular, which includes only four independent variables (f_y, f_c', d_b, and $K_{tr,318}$), provides a very good fit with the data given its simplicity. Figure 68 and Figure 69 in Appendix C show that the 'complex' equation properly accounts for effects of confinement, concrete compressive strength, and lap splice length, with *T*/*C* values that are similar across the range of these variables in the database. Furthermore, the 'complex' equation becomes slightly more conservative for higher bar stresses, which is desireable since only one test result is available for bar stresses greater than 75 ksi. The 'simplified' equation also does a good job accounting for effects of confinement and concrete compressive strength and tends to become more conservative for longer lap splices and higher bar stresses. It appears that either equation is a candidate for use in design.

The Cairns [13] equation also produces a very good fit to the data, with a mean of 1.52 and *CV* of 0.14. This equation is the only one considered that uses the yield stress of the transverse reinforcing steel, f_{yt}. Figure 70 in Appendix C shows that this equation also does a good job accounting for effects of confinement, concrete compressive strength, and lap splice length, with

T/*C* values that are similar across the range of these variables in the database. Furthermore, it becomes more conservative for higher bar stresses, which is desireable since only one test result is available for bar stresses greater than 75 ksi. This equation is a candidate for use in design.

The fib Model Code [15] design provisions have a mean *T*/*C* of 1.75 and *CV* of 0.22 and are more complex than the other equations considered. They are considerably more accurate and precise than the ACI 318-19 provisions but less accurate and precise than the equations proposed by researchers. Figure 71 in Appendix C shows that fib Model Code design provisions also do a good job accounting for effects of confinement, concrete compressive strength, bar stress, and lap splice length, with *T*/*C* values that are similar across the range of these variables in the database. These provisions appear appropriate for use in design.

2.5 Comparisons with Tension Development Equations

2.5.1 Equations Considered

The prior section demonstrates that several equations exist that fit the database of compression lap splice tests relatively well and might be candidates for use in design. Nevertheless, since the mechanics of bond are similar for bars in tension and compression, this section explores the potential to use existing tension development length equations for design of compression lap splices. Tension development has long been studied and designers are familiar using equations for tension development length. If feasible, use of the same or similar equations for design of compression and tension lap splices would simplify design.

Six equations were considered: the ACI 318-19 [3] tension development length equation; the ACI 408R-03 [1] tension development length equation; an equation proposed by Lepage, Yasso, and Darwin [16]; an equation proposed by Darwin, Lutz, and Zuo [17]; an equation

proposed by Canbay and Frosch [18]; and an equation proposed by Frosch, Fleet, and Glucksman [19].

i) ACI 318-19 [3] tension development length for deformed bars and wires

ACI 318-19 [3] §25.4.2 prescribes that the tension development length for deformed bars and wires shall be the greater of (a) and (b) in Eq. 11:

Development length shall be the greater of (a) and (b):

$$\text{(a) } \ell_d = \left(\frac{3}{40} \frac{f_y}{\lambda \sqrt{f_c'}} \frac{\psi_t \psi_e \psi_s \psi_g}{\left(\frac{c_b + K_{tr,318}}{d_b} \right)} \right) d_b \qquad \text{(b) 12 in. (ignored)}$$

with ψ_t, ψ_e, ψ_s, and ψ_g per Table 25.4.2.5 (with linear interpolation for ψ_g depending on the bar stress). For bars with $f_y \geq 80{,}000$ psi spaced ≤ 6 in. on center, transverse reinforcement shall be provided such that $K_{tr,318} \geq 0.5 d_b$

$$K_{tr,318} = \frac{40 A_{tr}}{sn} \; ; \; \sqrt{f_c'} \leq 100 \text{ psi} \; ; \; \left(\frac{c_b + K_{tr,318}}{d_b} \right) \leq 2.5 \; ; \; \psi_t \psi_e \leq 1.7$$

Eq. (11) [lb-in.]

ACI 318-19 defines $K_{tr,318}$ as a factor that represents the contribution of transverse reinforcement across potential splitting planes and whose determination involves the considereation of multiple splitting scenarios in seach of the most unfavorable case.

The values of the reinfocement grade factor ψ_g used for design are tabulated in ACI 318-19 and are a function of only bar grade. In this section, ψ_g was defined as a linear function of $f_{s,calc}$ rather than bar grade:

$$\psi_g = 0.55 + f_{s,calc}/40{,}000 \qquad \text{Eq. (12) [lb-in.]}$$

This required an iterative solution process to solve for $f_{s,calc}$, since $f_{s,calc}$ was both an input and output.

ii) ACI 408R-03 [1] tension development length equation

The recommendations for tension development length by ACI Committee 408 account for numerous parameters, including transverse reinforcement, concrete cover, bar geometry, bar stress, and concrete strength (Eq. (13)).

$$\frac{\ell_d}{d_b} = \frac{\left(\frac{f_y}{\phi\, f_c'^{1/4}} - 2400\omega\right)\alpha\beta\lambda}{76.3\left(\frac{c\omega + K_{tr,408}}{d_b}\right)}$$

$$\text{with: } \omega = 0.1\,\frac{c_{max}}{c_{min}} + 0.9 \le 1.25 \quad ; \quad t_r = 9.6\,R_r + 0.28 \le 1.72 \;;$$

$$t_d = 0.03\,d_b + 0.22 \quad ; \quad K_{tr,408} = \frac{0.52 t_r t_d A_{tr}}{sn}\, f_c'^{1/2} ; \quad f_c'^{1/4} \le 11.0 \;;$$

$$f_y \le 80 \text{ ksi} \qquad \left(\frac{c\omega + K_{tr,408}}{d_b}\right) \le 4.0 \quad ; \quad \frac{\ell_d}{d_b} \ge 16$$

Eq. (13) [lb-in.]

iii) Lepage, Yasso, and Darwin [16] equation

The equation recommended in Lepage, Yasso, and Darwin [16], shown as Eq. (14), is also derived from ACI 408R-03. It allows the use of higher-grade reinforcement and higher strength concrete than permitted by the base equations. A reinforcement yield stress modification factor, ψ_y, is introduced to account for the fact that lap splice length and bar grade are not proportional.

As with the ACI 318-19 §25.4.2 tension development length equation, solving for $f_{s,calc}$ in this case requires extra attention because the steel stress variable is present both as a proportional factor for ℓ_d and in the definition of ψ_y. An iterative solution process is required to solve for $f_{s,calc}$.

$$\frac{\ell_d}{d_b} = \frac{1}{90} \frac{f_y \psi_t \psi_e \psi_y}{\lambda \, f_c'^{1/4} \left(\frac{c_b \omega + K_{tr,318}}{d_b} \right)}$$

$$\text{with } \psi_y = 1.5 - \frac{30{,}000}{f_y} \geq 0.75 \; ; \; \left(\frac{c_b \omega + K_{tr,318}}{d_b} \right) \leq 4.0$$

Eq. (14) [lb-in.]

iv) Darwin, Lutz and Zuo [17] equation

The equation recommended in Darwin, Lutz and Zuo [17] (Eq. (15)) is based on the ACI 408R-03 tension development length equations. The variable $K_{tr,408}$ is replaced with K'_{tr}, which eliminates the term representing the effect of relative rib area. The upper limit for the confinement term, in this case ($c_b\omega+K'_{tr}/d_b$), is 4, similar to ACI 408R-03.

$$\ell_d = \frac{\left(\frac{f_y}{f_c'^{1/4}} - 2400\omega \right) \psi_t \psi_e \, \lambda}{1.5 \left(\frac{c_b \omega + K'_{tr}}{d_b} \right)} d_b$$

$$\text{with: } \omega = 0.1 \, \frac{c_{max}}{c_{min}} + 0.9 \leq 1.25 \quad ; \quad t_d = 0.03 \, d_b + 0.22$$

$$K'_{tr} = \frac{t_d A_{tr} \sqrt{f'_c}}{2sn} \; ; \; \left(\frac{c\omega + K'_{tr}}{d_b} \right) \leq 4.0$$

Eq. (15) [lb-in.]

v) Canbay and Frosch [18] equation

Canbay and Frosch [18] proposed a simplified design equation applicable for the design of beams and slabs. The proposed expression, which can be used to calculate either development or lap splice lengths, depends only on the yield stress and bar diameter of the longitudinal reinforcement and the concrete compressive strength.

$$\frac{\ell_d}{d_b} = \frac{0.9 \cdot 10^{-6} f_y^{\,2} \sqrt{d_b}}{\sqrt{f_c'}} \qquad \text{Eq. (16)} \quad [\text{lb-in.}]$$

vi) Frosch, Fleet, and Glucksman [19] equation

Frosch, Fleet, and Glucksman [19] recommend a design expression for bond strength (not development length). The first term deals with the contribution of concrete to bond strength, while the second term accounts for transverse reinforcement.

$$f_b = \left(f_c' \right)^{0.25} \left(\frac{l_s}{d_b} \right)^{0.5} \left(\frac{c_{so}}{d_b} \right)^{0.25} + \frac{30 N_s \left(N_l A_t \right)}{N_b A_b} \qquad \text{Eq. (17)} \quad [\text{lb-in.}]$$

2.5.2 Methods for Evaluating Tension Development Equations Against Database

There is an important difference between the mechanics of bond for bars in tension and compression: bars in compression benefit from end bearing of the bar against concrete. To develop the same bar force, a shorter lap splice length should be needed in compression than in tension.

Therefore, in addition to assessing *T*/*C* values for the tension equations (Table 1). Three methods for adjusting the tension development length equations were also considered. Each of these methods was calibrated to obtain a minimum *T*/*C* value of 1.0 when compared against the

database of compression lap splice tests. This minimum *T*/*C* value was selected for simplicity and consistency, and may not reflect the appropriate level of conservatism for design.

Method #1: r_1 length multiplier

Method 1 for converting the calculated length in tension to a calculated length in compression is shown in Eq. (18). Each calculated tension development length, ℓ_d, was multiplied by r_1, a constant that differs for each equation that was selected to produce a minimum *T*/*C* of 1.0 when compared with the test results in the database, that is, to achieve a 0% fractal.

$$\ell_{sc} = r_1 \, \ell_d \qquad \text{Eq. (18)}$$

For instance, for the ACI 408R-03 [1] equation, this results in:

$$\ell_{sc} = r_1 \cdot l_{d,408} = r_1 \frac{\left(\frac{f_y}{\phi \, f_c'^{1/4}} - 2400\omega \right) \alpha\beta\lambda}{76.3 \left(\frac{c\omega + K_{tr,408}}{d_b} \right)} d_b \qquad \text{Eq. (19) [lb-in.]}$$

This method is simple and intuitive, but also not exactly correct: the force transferred by end bearing is unlikely to be proportional to development length. This approach is still considered given its simplicity.

Method #2: r_2 bar stress multiplier

If a bar developed in compression transfers force to the concrete through end bearing, then for the same target yield stress, less force must transfer through bond in compression than in

tension. Method 2 assumes that the tension development length equations represent the length necessary to transfer a given force through bond. In Method 2, the calculated lap splice length in compression is obtained from the tension development length equations for a bar stress of $r_2 f_y$ (Eq. (20)). Multiplier r_2 affects f_y everywhere it may appear in the equations, including variables that are a function of f_y such as ψ_y in the Lepage, Yasso and Darwin equation.

$$\ell_{sc} = \ell_d \left(r_2 f_y \right) \qquad \text{Eq. (20)}$$

The r_2 value is a constant that differs for each equation that, as with r_1, was selected to produce a minimum T/C of 1.0, which corresponds to a 0% fractal.

As with Method 1, Method 2 is simple and intuitive, but also not exactly correct: the force transferred by end bearing is unlikely to be proportional to bar stress. This approach is still considered given its simplicity.

Method #3: ψ_y modifier in Lepage, Yasso. and Darwin equation [16]

The Lepage, Yasso, and Darwin [16] equation includes the reinforcement yield stress factor in Eq. (21). Their tension development length equation [Eq. (15)] is proportional to this factor, which has the form A – B / f_y, where A is 1.5 and B is 30,000 psi.

$$\psi_y = 1.5 - \frac{30,000}{f_y} \geq 0.75 \qquad \text{Eq. (21)}$$

Method 3 consists of modifying the constant B to obtain a minimum T/C of 1.0, which again corresponds to a 0% fractal. The calculated value of B is 55,600, which is rounded to 50,000.

2.5.3 Results

Table 1 summarizes the *T*/*C* statistics obtained for the six considered tension development length equations and shows how their behavior changes with the derived r_1, r_2, and ψ_y factors.

Table 1 – Summary of *T*/*C* statistics for original and altered tension development equations

	ACI 318-19 [3]	ACI 408R-03 [1]	Lepage et al. [16]	Darwin et al. [17]	Canbay and Frosch [18]	Frosch et al. [19]
	Original Equation					
mean	1.94	1.76	2.02	1.74	2.00	1.82
SD	0.64	0.23	0.35	0.21	0.42	0.37
CV	0.33	0.13	0.17	0.12	0.21	0.20
max	3.65	2.30	2.76	2.28	3.30	2.85
min	1.05	1.19	1.35	1.28	1.27	1.08
	with r_1					
r_1	0.94	0.69	0.66	0.63	0.62	0.85
mean	1.84	1.51	1.75	1.44	1.58	1.68
SD	0.60	0.24	0.36	0.23	0.33	0.34
CV	0.33	0.16	0.21	0.16	0.21	0.20
max	3.46	2.09	2.58	1.97	2.61	2.64
min	1.00	1.00	1.00	1.00	1.00	1.00
	with r_2					
r_2	0.96	0.84	0.74	0.78	0.79	0.93
mean	1.85	1.47	1.50	1.36	1.58	1.69
SD	0.61	0.19	0.26	0.16	0.33	0.34
CV	0.33	0.13	0.17	0.12	0.21	0.20
max	3.49	1.92	2.06	1.78	2.61	2.64
min	1.00	1.00	1.00	1.00	1.00	1.00
	with optimized ψ_y (A=1.5, B=50,000)					
mean			1.39			
SD			0.20			
CV			0.14			
max			1.82			
min			1.00			

Figures 14, 15, and 16 are analogous to Figure 13 and show the range, mean, and *CV* of the *T*/*C* for each tension development equation considered, including the value of r_1 and r_2 where applicable.

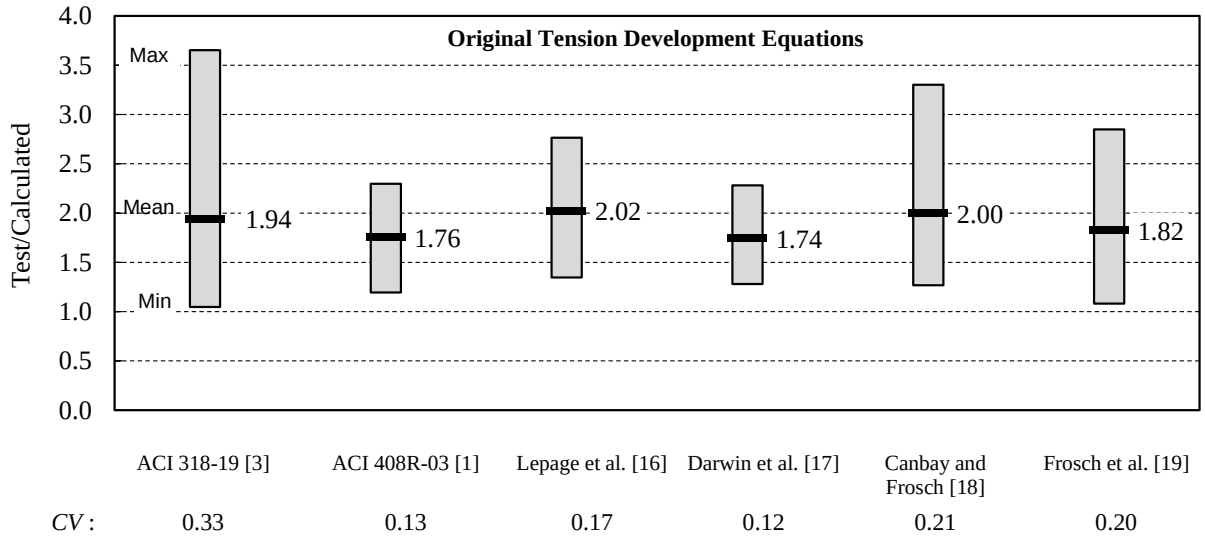

Figure 14 – *T*/*C* for tension development length equations with no modification

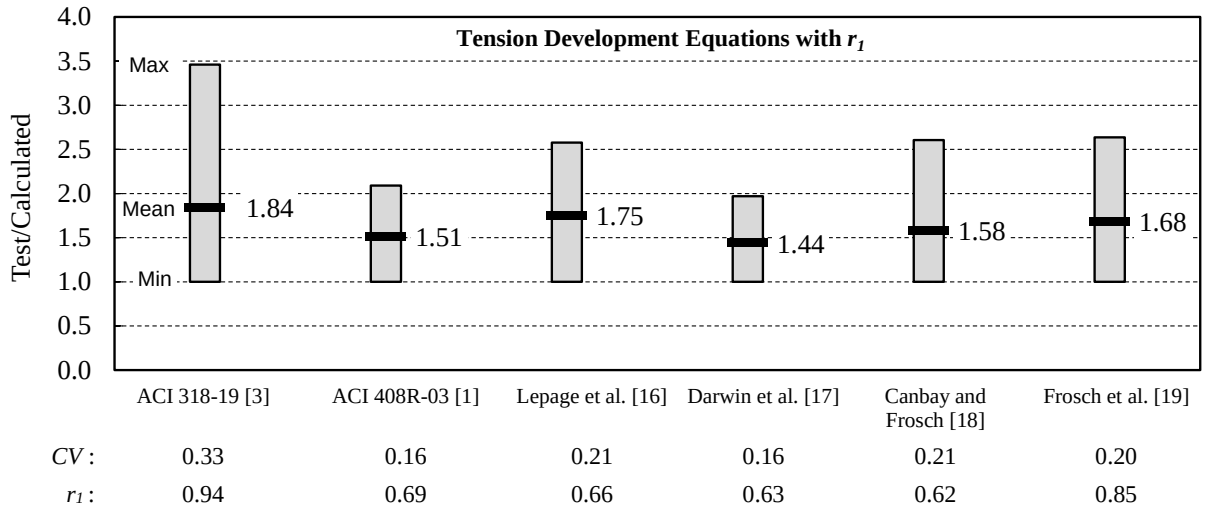

Figure 15 – *T*/*C* for tension development length equations including r_1 multiplier

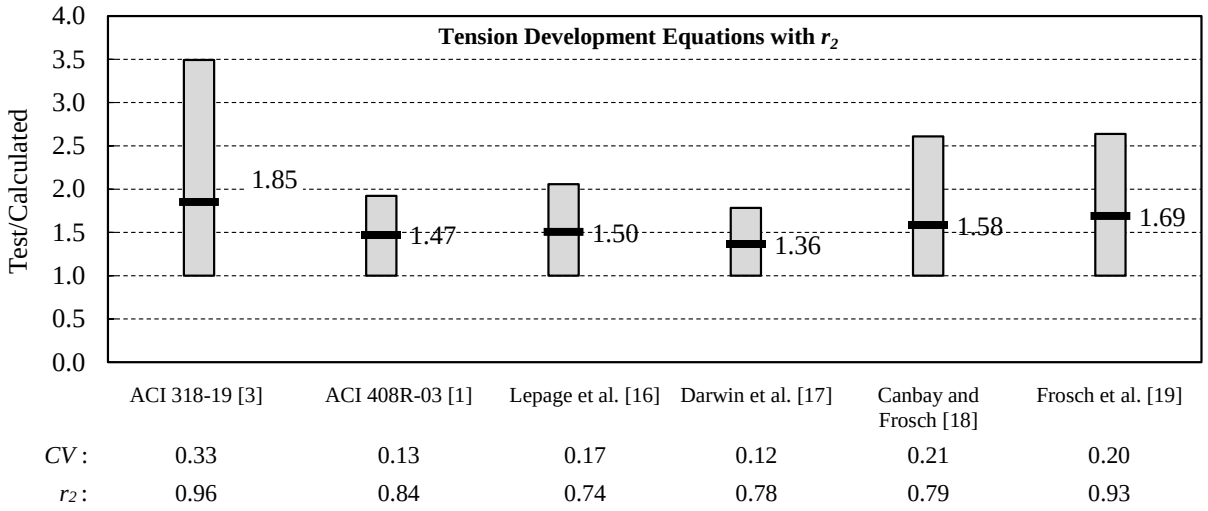

Figure 16 – T/C for tension development length equations including r_2 multiplier

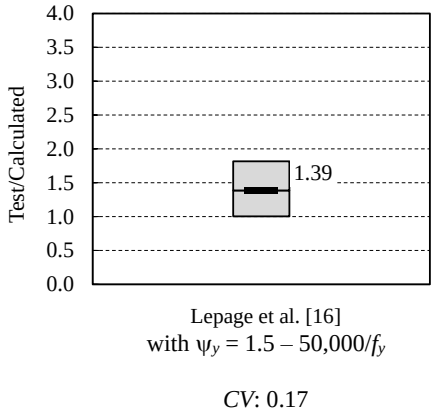

Figure 17 – *T*/*C* for Lepage et al. [16] recommended provisions with modified ψ_y

Table 1 and Figure 14 show that the unaltered tension development length equations all have lower mean and *CV* values than the current ACI 318-19 provisions for compression lap splices. The ACI 318-19 tension development length equation has the highest mean (1.94) and scatter (*CV* of 0.33) of the six tension development equations considered. The other five unmodified tension development length equations in Figure 14 have *CV* values that are similar to the most precise compression lap splice equations shown in Figure 13 (*CV* values were 0.12 to

0.21 for tension equations in Figure 14 and 0.12 to 0.22 for compression equations in Figure 13). These results strongly suggest that it may be possible to determine compression lap splice lengths as a function of tension lap splice lengths without losing precision.

Moreover, Figures 15, 16, and 17 suggest that all three methods for modifying the tension development length equations to obtain a 0% fractal have potential, with the bar stress (r_2) multiplier resulting in marginally better accuracy and precision than the bar length (r_1) multiplier for the ACI 408R-03, Lepage et al., and Darwin et al. equations. Both the r_1 and r_2 approaches produce the same result for the remaining equations.

Figure 18 shows T/C for the ACI 408R-03 tension development equation versus $f_{1c,mod}$ for (a) the original equation, (b) the equation with r_1, and (c) the equation with r_2. For the original equation, Figure 18(a), the values of T/C range from 1.19 to 2.30. In Figure 18(b), when r_1 is under effect, the minimum value of T/C becomes 1.00, as per the definition of r_1. Figure 18(c) with r_2 also has a minimum T/C value of 1.00, but the range of values is reduced compared to Figure 18(b). The trend line is also somewhat more horizontal in Figure 18(c) than in Figure 18(b), which along with the reduced scatter, shows that for this equation r_2 produces a marginally better fit to the data than either r_1 or the original equation.

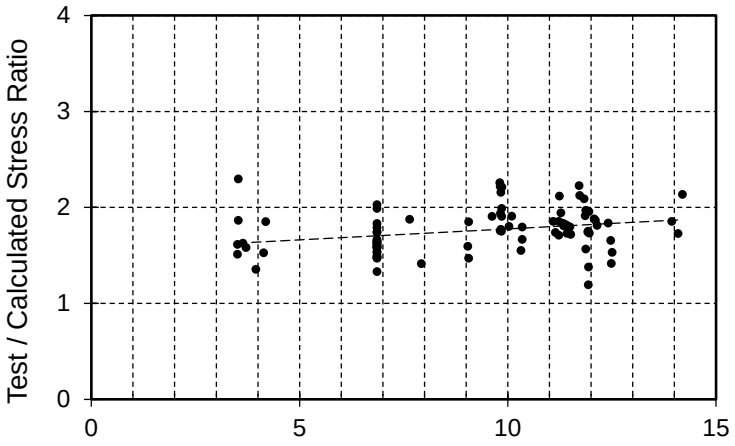

(a)

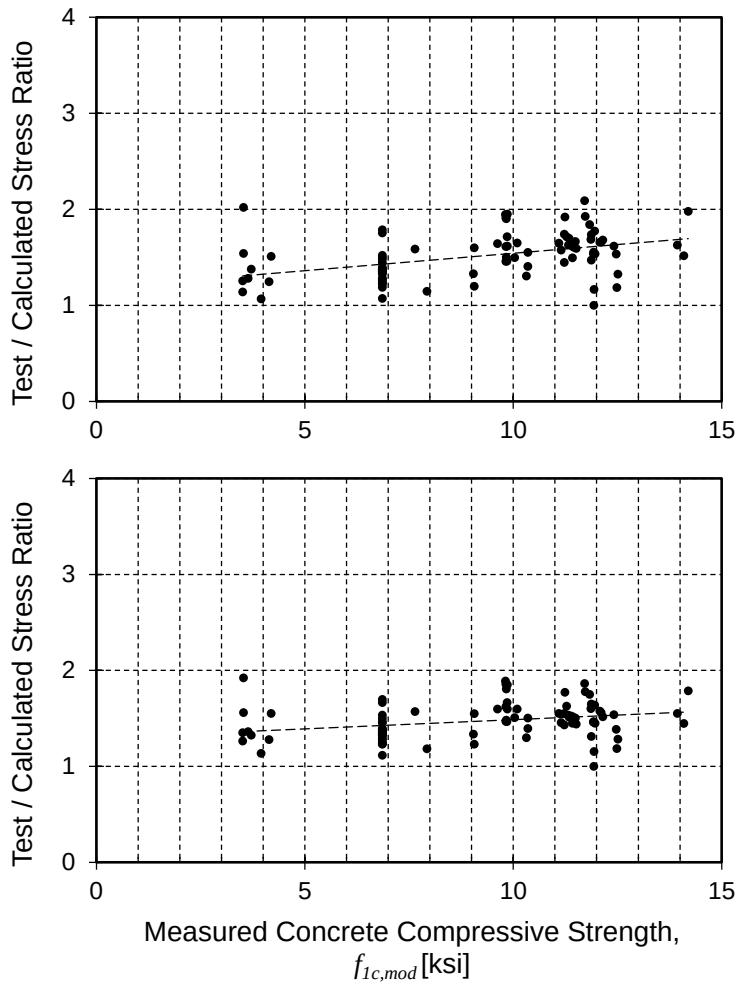

Figure 18 – Behavior of ACI 408R-03 [1] tension development length in terms of T/C against $f_{1c,mod}$: (a) original equation (b) with $r_1 = 0.69$ (c) with $r_2 = 0.84$

Appendix D has a set of plots analogous to those in Figures 9 through 12 that show the behavior of each equation in terms of T/C in relation to variables versus $(c_b + K_{tr,318})/d_b$, $f_{1c,mod}$, $f_{s,test}$, and ℓ_s.

Collectively, the plots in Appendix D show that all of the tension development equations considered more effectively account for the key variables than the ACI 318-19 compression lap splice provisions. Of the tension equations considered, the ACI 318-19 development length

equation is the least effective at representing the effects of $(c_b + K_{tr,318})/d_b$, $f_{1c,mod}$, $f_{s,test}$, and ℓ_s, as evidenced by the clearly sloped trendline in the Appendix D plots.

The ACI 408R-03, Lepage et al., Darwin et al., and Frosch et al. equations all have trendlines with nearly zero slope when T/C is plotted versus $(c_b + K_{tr,318})/d_b$, suggesting these equations effectively account for cover and transverse reinforcement.

Of the equations considered, the ACI 408R-03 and Darwin et al. equations are most effective at representing the effect of concrete compressive strength. The Lepage et al., Canbay and Frosch, and Frosch et al. equations behave similarly in terms of T/C versus $f_{1c,mod}$.

All of the equations considered, except for the ACI 318-19 tension development length equation, exhibit a positive trend between T/C and bar stress, indicating more conservatism for higher bar stresses. This is a fortunate trend given the sparse data for bar stresses greater than 70 ksi.

The six equations become less conservative as the provided lap splice length increases, similar to the compression equations, with the ACI 318-19 tension development length equation exhibiting the most extreme trend.

The plots in Appendix D show that the application of r_1, r_2, or the optimized ψ_y do not alter these general trends.

Collectively, these results show that it may be possible to base compression lap splice requirements on tension development length provisions. For example, it might be feasible to set the compression development length equal to r_1 times the tension development length. This approach simplifies the building code and ensures that calculated compression development lengths will never exceed the tension development length. Another appealing aspect of the length multiplier (r_1) method is that it avoids a separate length calculation for bar subjected to both tension

and compression. As most research on bond has been focused on the behavior in tension, tension development length equations tend to account for more relevant variables and to be supported by more experimental data than compression development length equations.

The bar stress (r_2) multiplier approach produces a somewhat better fit to the data than the r_1 approach, particularly for the ACI 408R-03, Lepage et al., and Darwin et al. equations. The improvement is evident from the somewhat lower mean and *CV* values obtained with the r_2 approach. Both the r_1 and r_2 approaches produce the same result for the remaining equations. Depending on the tension development length equation, the r_2 approach might produce more accurate and precise results, but also requires that the tension development length equation to be recomputed. This is slightly less convenient than using a fraction of an already calculated length (r_1 approach).

Use of an revised definition for ψ_y in the Lepage et al. equation leads to similar scatter as the r_2 approach.

2.6 Conclusions

1. ACI 318-19 [3] equations for compression lap splice length in §25.5.5 can produce calculated lengths that are substantially longer than the length of a Class B tension lap splice (§25.5.2). This is counter to expectations since compression lap splices benefit from end bearing and tension lap splices do not.
2. ACI 318-19 equations for compression lap splice length in §25.5.5 were not a good fit to the database of 89 test results, with a mean T/C of 2.58 and a coefficient of variation (*CV*) of 0.60 (although it must be emphasized that all specimens with $T/C > 2.0$ violated the ACI

318-19 minimum lap splice length). A reason for these outcomes is that §25.5.5 does not account for relevant variables including confinement and concrete compressive strength.

3. Compression lap splice length requirements in §25.5.5 can be improved and simplified by removing Eq. (a) from §25.5.5 and applying Eq. (b) to all design bar stress ranges (Eq. (b) is currently limited to bar stresses greater than 60 ksi). Equation (b) alone has a mean T/C of 1.58 and a CV of 0.16 when compared with the database, although it still omits key variables and can produce design lengths that are longer than the tension development length. Equations proposed by Cairns [13] and Chun, Lee, and Oh [9,12] were also shown to produce more accurate and precise fits to the available data.

4. Six tension development length equations were considered, and all provided a more accurate and precise fit to the dataset than ACI 318-19 §25.5.5. Use of tension development length equations for compression lap splice design would produce more consistent conservatism relative to the database, eliminate the need to calculate both tension and compression development lengths, and prevent design cases where calculated lengths are longer in compression than in tension. A drawback of this approach is that calculated compression lengths would also be longer than currently required for many common design cases.

5. Three methods were considered for making compression lap splice length a function of tension development length without causing excessive conservatism:

    a. Length multiplier, r_1: Compression lap splice length can be defined as r_1 times the tension development length, where $r_1 < 1$. To illustrate the concept, values of r_1 were derived for six tension development length equations to achieve a minimum T/C of 1.0, although other definitions of acceptable reliability might be appropriate.

b. Stress multiplier, r_2: Compression lap splice length can be calculated using tension development length equations, but for a stress of $r_2 f_y$, where $r_2 < 1$. The stress reduction is because some portion of bar force is transferred through end bearing and not bond. To illustrate the concept, values of r_2 were derived for six tension development length equations to achieve a minimum T/C of 1.0, although other definitions of acceptable reliability might be appropriate.

c. Optimized ψ_y: The tension development length equation from Lepage, Yasso and Darwin [16] contains a ψ_y value that was rederived to better fit the compression lap splice database and achieve a minimum T/C of 1.0, although other definitions of acceptable reliability might be appropriate.

2.7 Notation

A_b	=	cross-sectional area of spliced bar (in.^{2})
A_s	=	cross-sectional area of spliced bar in fib 2010 Model Code [15] (mm^2)
A_{st}	=	cross-sectional area of one leg of a confining bar, according to fib 2010 Model Code [15] (mm^2)
A_{tr}	=	total cross-sectional area of all transverse reinforcement within spacing s that crosses the potential plane of splitting through the reinforcement being developed (in.^{2})
c_b	=	lesser of: (a) the distance from center of a bar or wire to nearest concrete surface, and (b) one-half the center-to-center spacing of bars or wires developed (in.)
c_{max}	=	maximum(c_b ; c_s) (in.)
c_{min}	=	smaller of minimum concrete cover or ½ of the clear spacing between bars (in.)

c_s = minimum [c_{so} ; c_{si} + 0.25 in.] (in.)

c_{si} = ½ of the bar clear spacing (in.)

c_{so} = side concrete cover for reinforcing bar (in.)

d_b = nominal diameter or bar being spliced (in.)

$f_{1c,mod}$ = measured concrete compressive strength per Reineck [11] in reference to a 12x6 in. cylinder (ksi)

f'_c = specified concrete compressive strength (psi)

f_b = total bond strength according to Frosch, Fleet, and Glucksman [19] (ksi)

f_{bd} = design bond strength in fib 2010 Model Code [15] (MPa)

$f_{bd,0}$ = basic bond strength in fib 2010 Model Code [15] (MPa)

f_{ck} = characteristic value of compressive concrete strength in fib 2010 Model Code [15] (MPa)

F_h = 60 $f_{bd} A_s$ in fib 2010 Model Code [15] (N)

f_y = specified yield stress for non-prestressed steel reinforcement, psi

f_{yd} = design yield stress of reinforcing steel in tension in fib 2010 Model Code [15]

f_{yk} = steel reinforcement characteristic strength in fib 2010 Model Code [15] (MPa)

f_s = tensile stress in steel reinforcement (psi)

$f_{s,calc}$ = tensile stress in steel reinforcement that has been derived from provisions and calculated with measured specimen and material properties (psi)

$f_{s,test}$ = measured stress in steel reinforcement (psi)

k_d = effectiveness factor dependent on the reinforcement detail for the design bond strength in fib 2010 Model Code [15]

$K_{tr,318}$ = $40A_{tr}$ / sn transverse reinforcement index according to ACI 318-19 (in.)

$K_{tr,408}$ = $(0.52\, t_r\, t_d\, A_{tr}/sn)\sqrt{f'_c}$, transverse reinforcement index according to ACI 408R-

03 [1] (in.)

K_{tr}' = $(t_d A_{tr} \sqrt{f_c'})/2sn$, transverse reinforcement index according to Darwin et al. [17] (in.)

$K_{tr,fib}$ = $n_t A_{st}/(n_b \varnothing s_t)$ density of transverse reinforcement, relative to the anchored or lapped bars, according to fib 2010 Model Code [15]. Originally "K_{tr}" in source.

l_b = lap length in fib 2010 Model Code [15] (mm)

ℓ_d = calculated development length (in.)

$l_{d,408}$ = development length of straight bars in tension, as required by the recommended provisions by ACI 408R-03 [1], Eq. 4-11a. Originally "l_d" in source. (in.)

ℓ_s = provided lap splice length of a specimen (in.)

ℓ_{sc} = compression splice length, as required by ACI 318-19 §25.5.2.1 (in.)

ℓ_{st} = tension lap splice length for deformed bars and deformed wires in tension, as required by ACI 318-19 §25.5.2.1 (in.)

n = number of bars being developed or lap spliced at a potential splitting plane

n_t = number of legs of confining reinforcement crossing a potential splitting failure surface at a section, according to fib 2010 Model Code [15]

N_b = number of longitudinal reinforcing bars according to Frosch, Fleet, and Glucksman [19]

N_l = number of legs of transverse reinforcement crossing the splice plane according to Frosch, Fleet, and Glucksman [19]

N_s = number of stirrups in the splice region according to Frosch, Fleet, and Glucksman [19]

p_{tr} = mean compression stress perpendicular to the potential splitting failure surface at the ultimate limit state, according to fib 2010 Model Code [15] (MPa)

R_r = relative area. Ratio of the projected rib area normal to the bar axis to the product of the nominal bar perimeter and the average center-to-center rib spacing.

s_t = longitudinal spacing of confining reinforcement, fib 2010 Model Code [15] (mm)

T/C = Test-to-calculated steel stress ratio, i.e., the ratio between $f_{s,test}$ and $f_{s,calc}$.

t_d = term representing the effect of bar size on the steel contribution to total bond force for tension development length (ACI 408R-03 [1])

t_r = term representing the effect of relative rib area on the steel contribution to total bond force for tension development length (ACI 408R-03 [1])

α_2 = factor representing the influence of passive confinement from cover in the design bond strength in fib 2010 Model Code [15]

α_3 = factor representing the influence of passive confinement from transverse reinforcement in the design bond strength in fib 2010 Model Code [15]

δ = transverse reinforcement multiplier in the 'complex' compression lap splice equation by Chun et al. [9]. (1 in transverse reinforcement is placed at ends or the value of 0 if not)

γ_s = 1.5, partial safety coefficient for bond in basic bond strength in fib 2010 Model Code [15]

η_1 = coefficient affecting basic bond strength depending on reinforcement surface (1.75 for ribbed bars, 1.4 for fusion bonded epoxy coated ribbed bars) in fib 2010 Model Code [15]

η_2 = coefficient affecting basic bond strength representing reinforcement casting position (1.4 when good bond conditions are obtained, 0.7 otherwise) in fib 2010 Model Code [15]

η_3 = coefficient affecting basic bond strength representing bar diameter (1.0 for Ø ≤

25 mm, $(Ø/25)^{0.3}$ for Ø > 25 mm) in fib 2010 Model Code [15]

η_4 = coefficient affecting basic bond strength representing steel reinforcement characteristic strength (1.2 for f_{yk} = 400 MPa, 1.0 for f_{yk} = 500 MPa, 0.85 for f_{yk} = 600 MPa, 0.75 for f_{yk} = 700 MPa, 0.68 for f_{yk} = 800 MPa, interpolation permitted) in fib 2010 Model Code [15]

Ø = Diameter of bar being lap spliced, fib 2010 Model Code [15] (mm)

ω = $0.1(c_{max}/c_{min}) + 0.9 \leq 1.25$, in the ACI 408R-03 tension development length equation [1]

ψ_g = reinforcement grade modification factor in the ACI 318-19 [1] tension development length equation, calculated here as $\psi_g = 0.55 + f_{s,calc}/40{,}000$ (definition in source: 1.0 for Grade 40 or Grade 60, 1.15 for Grade 80, 1.3 for Grade 100)

ψ_e = reinforcement coating modification factor in the ACI 318-19 [1] tension development length equation (1.5 for epoxy-coated or zinc and epoxy dual-coated reinforcement with clear cover less than $3d_b$ or clear spacing less than 6 d_b, 1.2 for epoxy-coated or zinc and epoxy dual-coated reinforcement for all other conditions, 1.0 for uncoated or zinc-coated (galvanized) reinforcement)

ψ_t = casting position modification factor in the ACI 318-19 [1] tension development length equation (1.3 if more than 12 in. of fresh concrete placed below horizontal reinforcement, 1.0 otherwise)

ψ_r = confining reinforcement modification factor for the development length of deformed bars and wires in compression in ACI 318-19 [3] §25.4.9 (0.75 for reinforcement enclosed within a spiral, a circular continuously wound tie with $d_b \geq$ ¼ in. and pitch not more than 4 in., No. 4 bar or D20 wire ties in accordance with ACI 318-19 §25.7.2 spaced no more than 4 in. on center, or hoops in

accordance with ACI 318-19 §25.7.4 spaced no more than 4 in. on center ; 1.0 otherwise)

ψ_s = size factor modification factor in the ACI 318-19 [1] tension development length equation (1.0 for No. 7 and larger bars, 0.8 for No. 6 and smaller bars and deformed wires)

ψ_{sc} = $1 + 0.084\ (K_{tr,318} / d_b)$ in the 'simplified' compression lap splice equation by Chun et al.[12]

ψ_y = reinforcement yield stress factor in the Lepage et al. [16] recommended provisions for tension development length

λ = factor accounting for lightweight concrete (1.00 for normalweight concrete, 0.75 for lightweight concrete) in ACI 318-19 [3] tension development length (§25.4.2) and compression development length (§25.4.9)

Chapter 3: Embedment Length of Headed Bars in Special Moment Frames

3.1 Introduction

Reinforcing bars terminating in a head transmit forces into concrete though two mechanisms: bond along the surface of the bar and bearing forces at the head. Compared with hooked bars, use of headed bars for development can reduce reinforcement congestion, promoting ease of construction and quality control. Headed bars can be useful in frame exterior joints, where the beam longitudinal reinforcement must be anchored into the column and the reinforcement detailing can be challenging.

Use of headed bars in reinforced concrete construction is permitted and regulated by ACI 318-19 [3]. For design of frames not designated as special moment frames (SMF), the development of headed bars in tension is prescribed by Chapter 25 of ACI 318-19. According to §25.4.4, the development length $\ell_{dt,25.4.4}$ for headed deformed bars in tension shall be:

$$\ell_{dt,25.4.4} = \max\left\{\left(\frac{f_y \psi_e \psi_p \psi_{o,head} \psi_c}{75\sqrt{f_c'}}\right) d_b^{1.5};\ 8d_b;\ 6\text{ in.}\right\} \qquad \text{Eq. (22)}$$

where ψ_e, ψ_p, $\psi_{o,head}$, and ψ_c are modification factors associated with epoxy coating, parallel tie reinforcement, headed bar location, and concrete strength, respectively.

Requirements for development of hooked, headed, and straight reinforcement in joints of SMFs are articulated in §18.8.2.2:

> "*Longitudinal reinforcement terminated in a joint shall extend to the far face of the joint core and shall be developed in tension in accordance with 18.8.5 and in compression in accordance with 25.4.9.*" - ACI 318-19 [3] §18.8.2.2

For developing headed bars in tension, §18.8.5.2 requires using Eq. (22) from §25.4.4 after replacing f_y with 1.25 f_y. This requirement is consistent with the general provision in §18.8.2.1 for SMFs:

"*Forces in longitudinal beam reinforcement at the joint face shall be calculated assuming that the stress in the flexural tensile reinforcement is 1.25f_y*" - ACI 318-19 §18.8.2.1

Equation (22) thus becomes Eq. (23) for developing headed bars in SMF joints:

$$\ell_{dt,18.8.5.2} = \max\left\{\left(\frac{1.25 f_y \psi_e \psi_p \psi_{o,head} \psi_c}{75\sqrt{f_c'}}\right) d_b^{1.5};\ 8d_b;\ 6\text{ in.}\right\} \qquad \text{Eq. (23)}$$

The language in §18.8.2.2 that requires consideration of both tension and compression development has been present in successive versions of the ACI Building Code since ACI 318-83. Even though earthquakes are expected to subject beam reinforcement terminating in a joint to both tension and compression force demands, the language of §18.8.2.2 is not clear about whether it is sufficient for a headed bar to satisfy only §18.8.5 or must satisfy both §18.8.5 and §25.4.9. It could be interpreted that the reference to §25.4.9 is only for straight bars in compression since §25.4.9 has no guidance for how it should be applied to headed or hooked bars. This was clarified with new commentary in ACI 318-14:

"*For bars in compression, the development length corresponds to the straight portion of a hooked or headed bar measured from the critical section to the onset of the bend for hooked bars and from the critical section to the head for headed bars.*" - ACI 318-14 [20] §R18.8.2.2

Prior to ACI 318-14, an engineer might have assumed that a headed bar satisfying §18.8.5 was adequately developed because tension development is often more critical than compression

development. The new commentary in §R18.8.2.2 of ACI 318-14 makes clear that engineers must design headed bars so they comply with both §18.8.5 and §25.4.9.

The compression development length required for joints of SMFs by §18.8.2.2, in accordance with §25.4.9, is the longer of the lengths obtained from Eq. (24):

$$\ell_{dc,25.4.9} = \max\left\{ \frac{f_y \psi_r}{50\sqrt{f'_c}} d_b \; ; \; 0.0003 f_y \psi_r d_b \right\} \qquad \text{Eq. (24)}$$

where ψ_r is a confining reinforcement modification factor and $\sqrt{f'_c} \leq 10$ ksi .

The implications of designing headed bars for compression development (§25.4.9) are illustrated in Figure 19. Figure 19 shows the ratio between the required headed bar compression development length, $\ell_{dc,25.4.9}$ (ACI 318-19 §25.4.9), and the required headed bar tension development length, $\ell_{dt,18.8.5.2}$ (ACI 318-19 §18.8.5.2, which is 1.25 times the length obtained from §25.4.4), versus specified concrete compressive strength. Separate lines in the figure show the trends obtained for different bar sizes. A steel yield stress of 60 ksi was assumed for all cases. Unitary values were assumed for the epoxy coating, parallel tie reinforcement, and bar location modification factors ($\psi_e = \psi_p = \psi_{o,head} = 1.0$) for calculating tension development length, while a value of 0.75 was assumed for the confining reinforcement modification factor for calculating compression development length ($\psi_r = 0.75$). These assumptions are valid for uncoated headed bars terminating inside a well-confined joint.

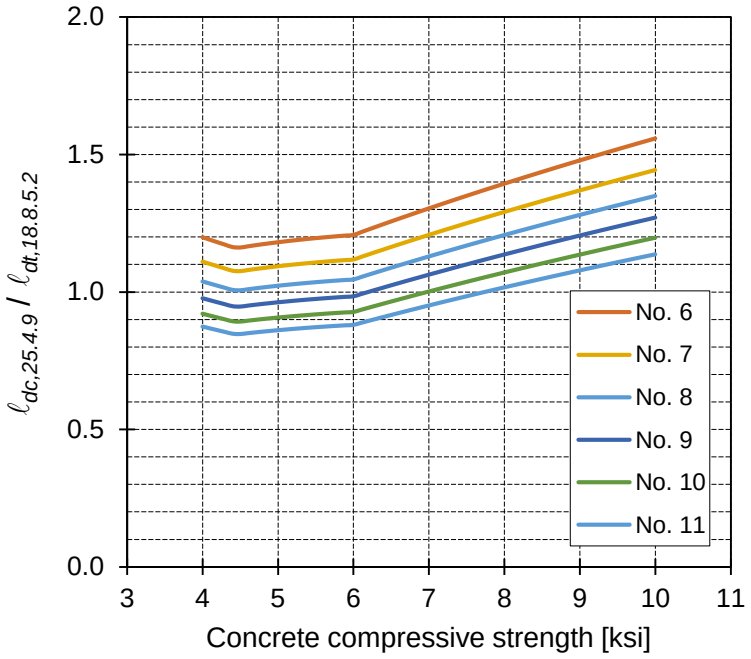

Figure 19 – Ratio of compression to tension development lengths for headed bars (§25.4.9 versus §18.8.5) versus specified concrete compressive strength

Figure 19 shows that, for $\psi_e = \psi_p = \psi_{o,head} = 1.0$ and $\psi_r = 0.75$, the required compression development length is longer than the required tension development length for No. 8 and smaller headed bars, regardless of the concrete compressive strength. The same is true for No. 9, No. 10, and No. 11 headed bars when the concrete compressive strength is greater than 6 , 7, and 8 ksi, respectively. In joints that do not satisfy the conditions necessary to obtain $\psi_p = 1$ (i.e. $A_{th} \geq 0.4A_{hs}$), $\ell_{dt,18.8.5.2}$ is likely to be longer than $\ell_{dc,25.4.9}$ because $\psi_p = 1.6$.

This chapter explores whether the compression development length should indeed frequently govern the embedment length of headed bars in joints of special moment frames. This is done by examining results from tests of exterior beam-column joints with headed beam reinforcement under reversed cyclic displacements.

3.2 Database Description

A database of test results was used to evaluate headed bar development. The database (Appendix E) includes results from 35 exterior cast-in-place reinforced concrete beam-column joint specimens subjected to reversed cyclic loading. Figure 20 shows a schematic of a representative specimen.

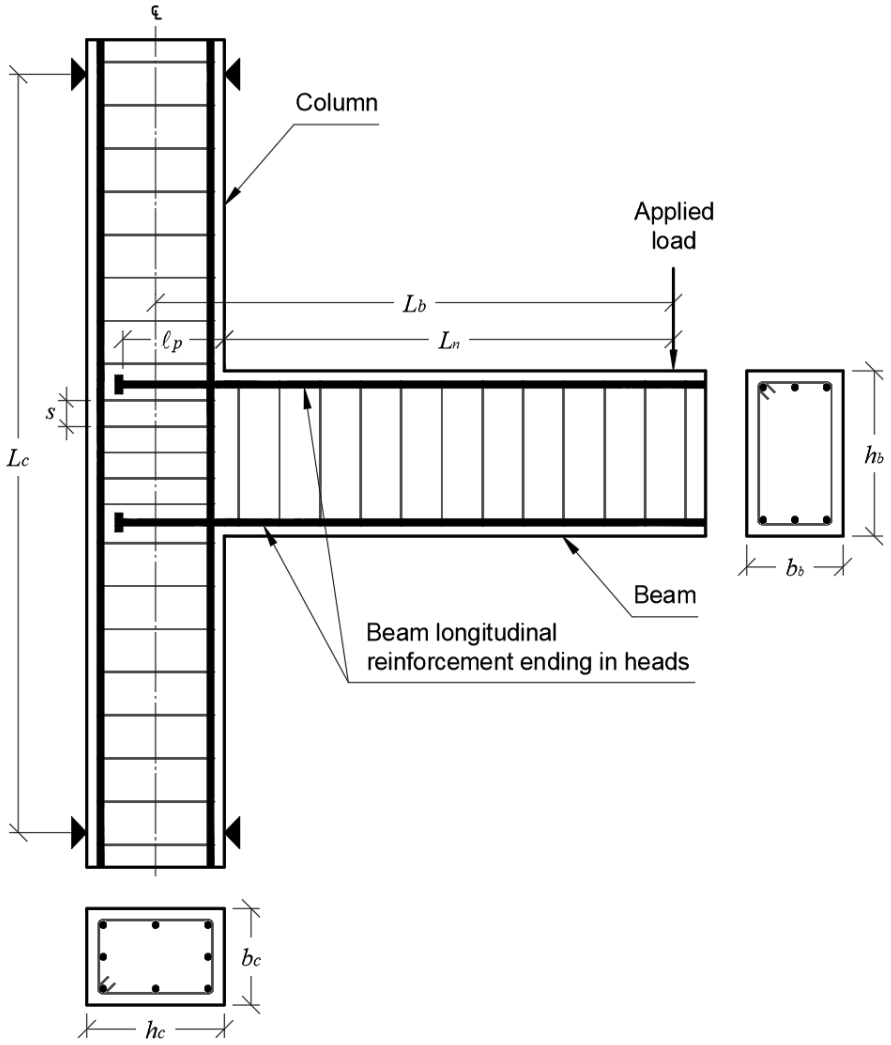

Figure 20 – Schematic of specimens in database (elevation and cross-sections)

Results were obtained from Adachi and Kiyoshi [21]; Bashandy [22]; Chun et al. [23]; Ishida et al. [24]; Kang, Ha, and Choi [25]; Kato [26]; Lee and Yu [27]; Matsushima et al. [28];

Murakami, Fuji, and Kubota [29]; Takeuchi et al. [30]; Tazaki, Kusuhara, and Shiohara [31]; Wallace et al. [32]; and Yoshida, Ishibashi, and Nakamura [33]. The specimens in the database in Appendix E were selected from databases published by Kang et al. [5] and Ghimire et al. [6]. The 35 specimens were selected for meeting the following criteria: specimens were included in both the Kang et al. [5] and Ghimire et al. [6] databases, the connection had a continuous column and at least one beam with headed bars terminating in the joint, and beam longitudinal reinforcement yield stress was not more than 85 ksi.

All specimens contained transverse reinforcement within the joint consisting of either column ties (21, or 60% of, specimens) or hoops (14, or 40% of, specimens) enclosing the column longitudinal reinforcement. The use of ties (with 90-degree hooks instead of 135-degree hooks) makes clear that not all joints in the database met the requirements for joint confinement in SMFs. The specimens had measured concrete compressive strengths of 3.5 to 10.3 ksi, No. 5 to No. 11 beam longitudinal bars, and measured beam longitudinal reinforcement yield stresses of 53 to 85 ksi. The distributions of measured concrete compressive strength, headed bar diameter, and measured steel yield stress are shown in Figures 21, 22, and 23, respectively. The provided embedment lengths of the headed bars, ℓ_p, defined as the distance from the face of the column to the bearing face of the head, as shown in Figure 20, ranged between 6.0 and 17.3 times the headed bar diameter and had the distribution shown in Figure 24.

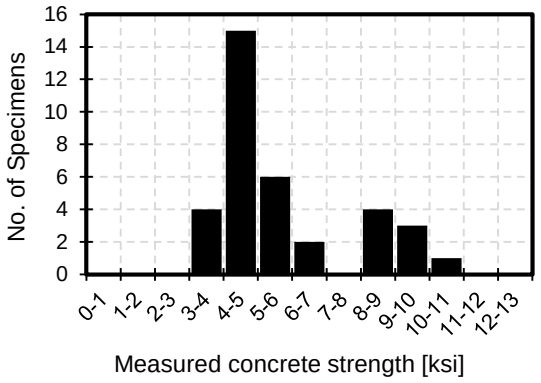

Figure 21 – Histogram of measured concrete compressive strength

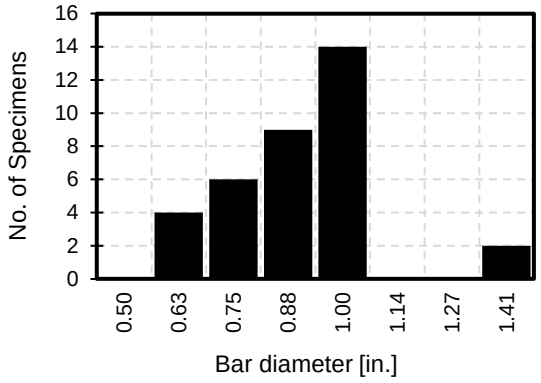

Figure 22 – Histogram of headed bar diameter (each bin includes specimens within ±1/16 in.)

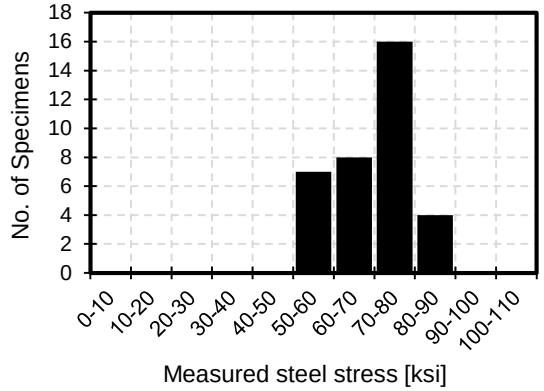

Figure 23 – Histogram of measured headed bar steel yield stress

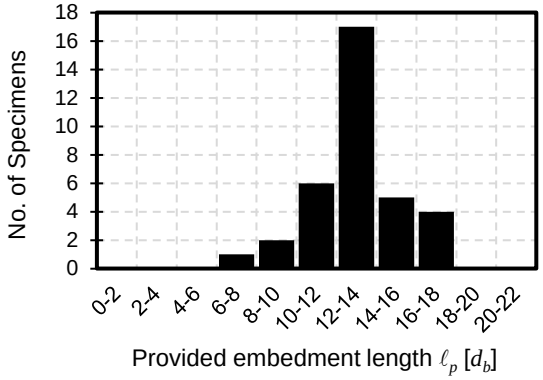

Figure 24 – Histogram of provided headed bar embedment length (column face to bearing face of head)

The specimens were all subjected to a series of fully reversed cyclic displacements of increasing magnitude. The strengths of the specimens were all limited by beam longitudinal bar yielding. No specimen in the database exhibited failure by anchorage or shear, but rather by deterioration of the joint or the beam near the joint throughout the reversed loading cycles.

Specimen drift was defined as the vertical displacement of the beam end during testing divided by the beam length measured to the centroid of the column (L_b in Figure 20). The drift ratio capacities in the database were reported by Ghimire et al. [6] based on the following definition: $\delta_{0.8peak}$ is "the drift ratio at drop to 80% [of] peak load (post peak)" based on an envelope

of the force-drift ratio results that links the peaks of the loading cycles. The reported $\delta_{0.8peak}$ values are the average of values obtained in each loading direction.

The distribution of drift ratio capacities is shown in Figure 25. Drift ratio capacities over 3% are taken to indicate acceptable seismic behavior. All specimens in the database had drift ratio capacities exceeding 3% and therefore exhibited acceptable behavior.

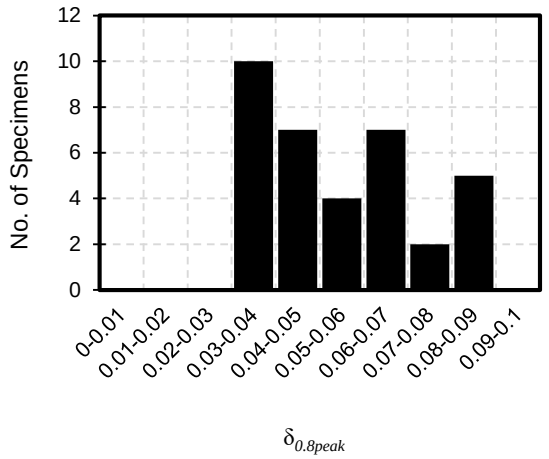

Figure 25 – Histogram of $\delta_{0.8peak}$

The nominal beam flexural strength was calculated at the face of the column using Eq. (25):

$$M_n = f_y A_{hs} (d - a/2) \qquad \text{Eq. (25)}$$

The contribution of compression reinforcement to flexural strength was neglected. In every case the beam section neglecting compression reinforcement was under-reinforced (steel strain greater than or equal to the yield strain estimated as f_y / E_s).

The maximum bending moment in the beams, M_{peak}, was calculated as the force applied to the beam tip times the clear shear span of the beam (distance from the point load to the column

face). M_{peak} ranged from 950 to 5800 kip-in., while the nominal flexural strength, M_n, ranged from 820 to 4600 kip-in. The resulting peak-to-nominal strength ratios, M_{peak}/M_n, were from 0.92 to 1.27 (Figure 26). Most specimens therefore exhibited beam strengths exceeding their nominal flexural strength based on measured material properties. The relatively high $\delta_{0.8peak}$ and M_{peak}/M_n values suggest that beam longitudinal bars yielded in every test, likely producing anchorage force demands at the face of the joint at least equal to the product of bar yield stress and cross-sectional area.

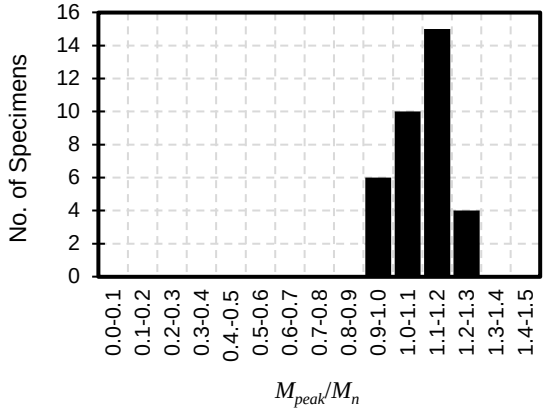

Figure 26 – Histogram of M_{peak}/M_n

The nominal joint shear strength, V_n, was calculated in accordance with ACI 318-19 §18.8.4 using Eq. (26).

$$V_n = R_n \lambda \sqrt{f_c'} A_j \qquad \text{Eq. (26)}$$

where R_n is a coefficient representing whether a transverse beam is present and had a value of either 12 or 15 for the specimens in the database. The effective joint area A_j, shown schematically in Figure 27, consists of the product of the joint depth in the plane parallel to the reinforcement generating shear (the height of the column section for these specimens) and the effective joint width, defined as the lesser of b_c , (b_b+h_c), and (b_c+2x).

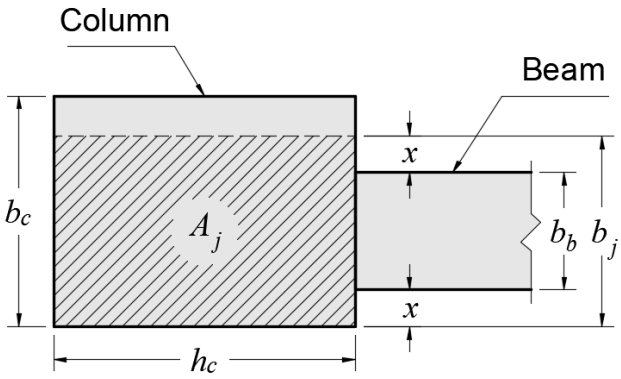

Figure 27 – Definition of effective joint area (plan view), adapted from ACI 318-19 [3] Fig. R15.4.2

Joint shear demand, V_p, was estimated with Eq. (27). Equation 27 is equivalent to the equation used in Ghimire et al. [6] except that the second term, which represents the column shear outside of the joint, is multiplied by L_b/L_n. This is necessary because M_{peak} is calculated at the column face.

$$V_p = \left(\frac{M_{peak}}{M_n} \right) nA_b f_y - \frac{M_{peak}}{L_c} \frac{L_b}{L_n} \qquad \text{Eq. (27)}$$

The value of V_p ranged from 60 to 350 kip while V_n ranged from 100 to 580 kip. The resulting V_p/V_n ranged from 0.26 to 1.27 (Figure 28). For most specimens, the shear demand was less than the nominal shear strength. Even specimens with the highest V_p/V_n did not exhibit shear failures before reaching 3% drift ratio.

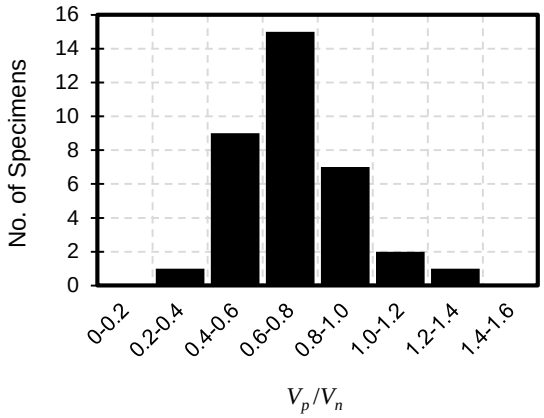

Figure 28– Histogram of V_p/V_n

Two main failure modes were identified by Kang et al. [5] for specimens in the database: beam flexure and joint failure after yielding of the beam reinforcement. A beam flexure failure mode indicates a loss of strength after several post-yield cycles due to damage within the beam clear span, which might include longitudinal bar fracture or buckling, concrete crushing, or shear strength decay. Relatively large drift capacities are expected for this failure mode in well-detailed doubly-reinforced beams with low shear stresses. In contrast, specimens with joint failures after yielding of beam reinforcement exhibited damage to concrete within the joint that limited the connection deformation capacity. Of the nine specimens that exhibited joint failure after yielding of the beam reinforcement, three had $V_p/V_n > 1$ and six had joint transverse reinforcement ratios that were less than 75% of that recommended in ACI 352 [34] according to Kang et al. [5].

Figures 29, 30, and 31 show $\delta_{0.8peak}$, M_{peak}/M_n and V_p/V_n versus ℓ_p/d_b, respectively. Closed circles and open triangles correspond to beam failure and joint failure after yielding of the beam reinforcement. Figure 29 shows that specimens where a beam flexural failure was reported exhibited larger drift capacities than those with joint failures after yielding of beam reinforcement, as expected. All but one of the specimens with a beam flexural failure had drift ratio capacities not

less than 0.04, whereas specimens with a joint failure after yielding of beam reinforcement all had drift ratio capacities of 0.03 to 0.04. No correlation is observed between $\delta_{0.8peak}$ and ℓ_p/d_b.

Figure 30 shows that the specimens with the greater peak moments, with respect to their nominal flexural strength, tended to be those with a relatively longer headed bar embedment length, although the trend is not very strong. It also appears that specimens with joint failure after beam yielding tended to have, on average, somewhat lower M_{peak}/M_n. Figure 31 shows that every specimen with $V_p/V_n > 1.0$ exhibited joint failure after yielding of beam reinforcement, but no other trends are evident. As expected, there is no correlation between V_p/V_n and ℓ_p/d_b.

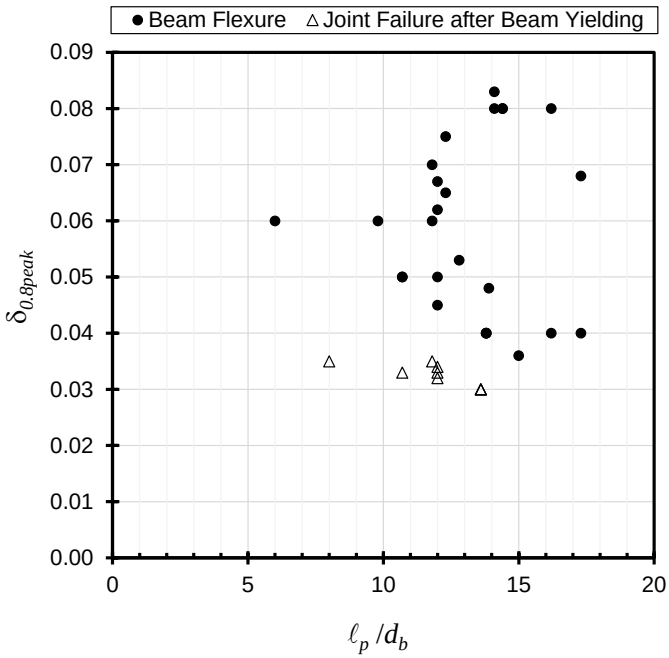

Figure 29 – $\delta_{0.8peak}$ versus ℓ_p(ACI 318-19)/d_b

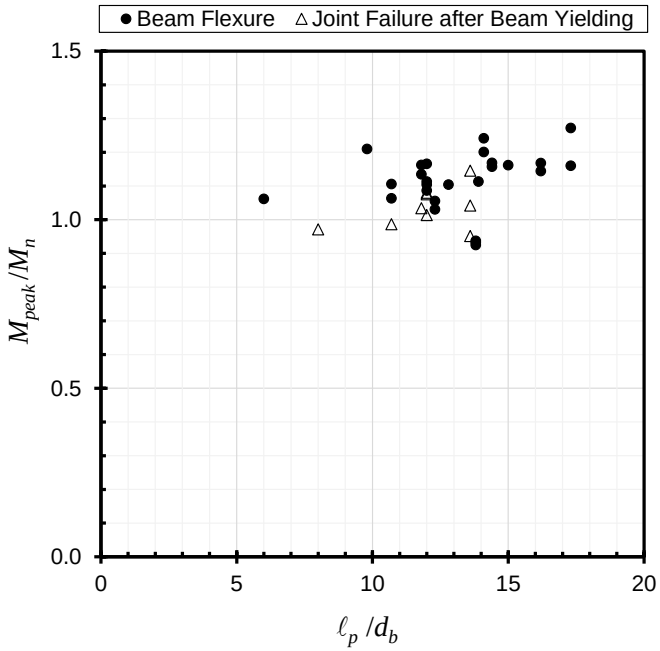

Figure 30 – M_{peak}/M_n versus ℓ_p(ACI 318-19)/d_b

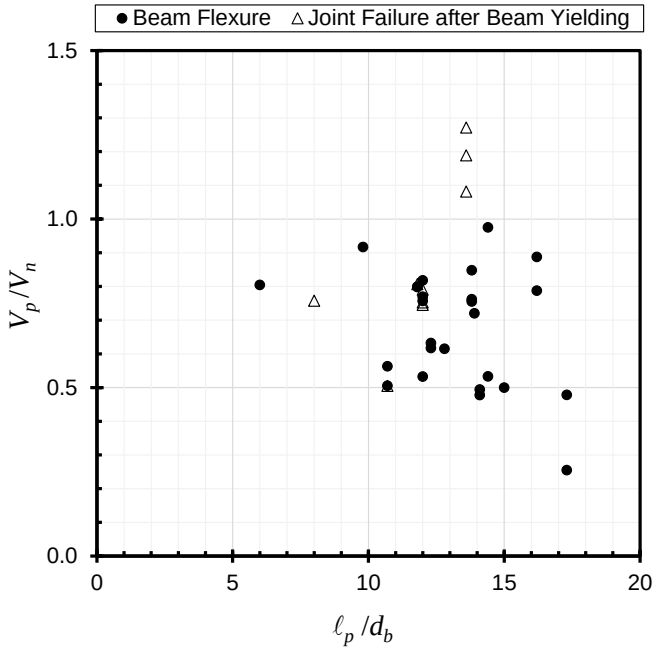

Figure 31 – V_p/V_n versus ℓ_p(ACI 318-19)/d_b

3.3 Evaluation of Database Against Current Provisions

The embedment lengths provided for specimens in the database were compared against $\ell_{dt,18.8.5.2}$ and $\ell_{dc,25.4.9}$ to evaluate the appropriateness of the requirement in §18.8.2.2 that headed bars in SMF joints satisfy the compression development length requirements of §25.4.9. Measured material properties were used in all cases.

To calculate the compression development length, $\ell_{dc,25.4.9}$, some interpretation was necessary to define the confining reinforcement modification factor, ψ_r. This factor leads to a reduction of the required compression development length when the transverse reinforcement consists of:

- A spiral,
- A circular continuously wound tie with $d_b \geq$ ¼ in. and pitch not more than 4 in.,
- No. 4 bar or D20 wire ties in accordance with ACI 318-19 §25.7.2 spaced no more than 4 in. on center, or
- Hoops in accordance with ACI 318-19 §25.7.4 spaced no more than 4 in. on center.

None of the specimens in the database, which were less than full scale, satisfy any of the conditions necessary for ψ_r = 0.75. However, it is arguably not appropriate to apply these conditions, which are intended for full-scale columns, to the smaller-scale specimens in the database. To identify specimens with transverse reinforcement similar to that required to obtain ψ_r = 0.75 in full-scale columns, a joint transverse reinforcement ratio was calculated for each specimen with Eq. (28):

$$\rho_t = \frac{A_{tr,1} N_{legs}}{s b_c} \qquad \text{Eq. (28)}$$

Specimens were assumed to qualify for $\psi_r = 0.75$ when $\rho_t \geq 0.5\%$, which is the transverse reinforcement ratio in a square column with 20 in. sides and two legs of No. 4 ties spaced at 4 in. (and thus qualifying for $\psi_r = 0.75$). The threshold 0.5% value was selected to represent the transverse reinforcement ratio required in a full-scale column to qualify for $\psi_r = 0.75$.

3.3.1 Results

Figure 32 shows the headed bar embedment lengths versus the required compression development length, $\ell_{dc,25.4.9}$, for all 35 specimens. This plot shows that the required compression development length, $\ell_{dc,25.4.9}$, was always longer than the provided embedment length. In 4 cases (11%) ℓ_p / $\ell_{dc,25.4.9}$ exceeded 2, and in one case it exceeded 3. Nonetheless, all the specimens performed adequately under reversed cyclic loading without exhibiting anchorage failures. Figure 32 shows that providing an embedment length longer than $\ell_{dc,25.4.9}$ is not necessary to prevent bond/anchorage failures and obtain good connection behavior.

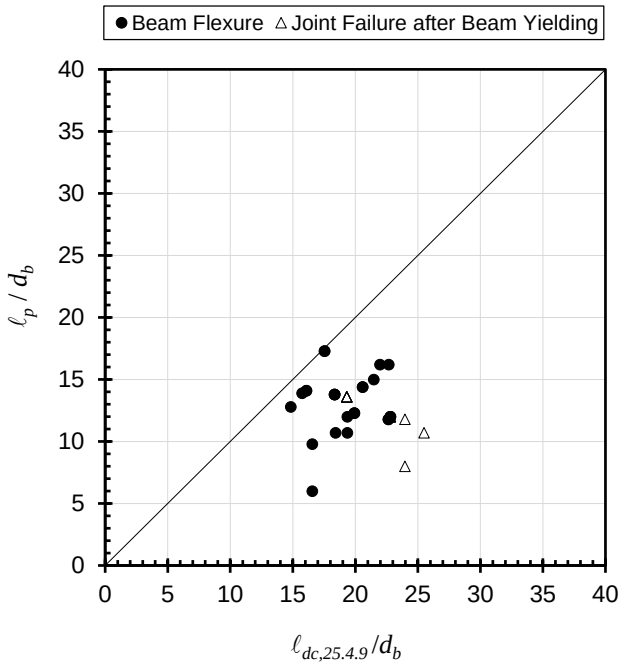

Figure 32 – ℓ_p/d_b versus $\ell_{dc,25.4.9}/d_b$

Similarly, Figure 33 shows headed bar embedment lengths versus the required tension development lengths, $\ell_{dt,18.8.5.2}$. Even though all 35 specimens exhibited good overall behavior with $\delta_{0.8peak} \geq 3\%$ and beam longitudinal bar yielding, only two of the 35 specimens had $\ell_p \geq \ell_{dt,18.8.5.2}$. It therefore appears that satisfying $\ell_p \geq \ell_{dt,18.8.5.2}$ is also not necessary to prevent bond/anchorage failures and obtain good overall connection behavior. Furthermore, Figure 33 has more scatter than Figure 32, which indicates that $\ell_{dt,18.8.5.2}$ can be excessively conservative in some design conditions. In 14 (39%) cases, ℓ_p / $\ell_{dt,18.8.5.2}$ was more than 2, including one specimens with ℓ_p / $\ell_{dt,18.8.5.2}$ of 4.4.

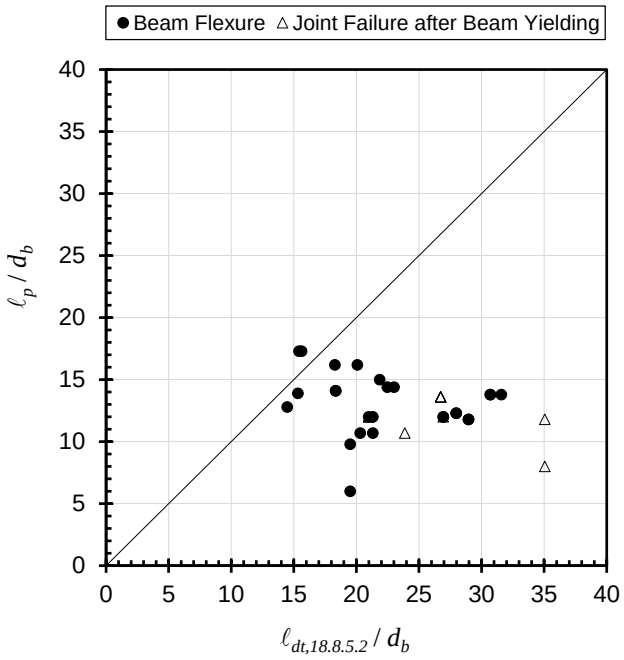

Figure 33 – ℓ_p/d_b versus $\ell_{dt,18.8.5.2}/d_b$

These results show that satisfactory connection behavior, characterized by beam longitudinal bar yielding and drift ratio capacities exceeding 3%, can be obtained without satisfying the requirements of either §25.4.9 or §18.8.5.2. It is acknowledged that design provisions should incorporate some conservatism, but the scatter and extent of conservatism shown in Figures 32 and 33 are considerable.

3.4 Evaluation of Database Against Other Equations

Both §25.4.9 and §18.8.5.2 appear to be considerably, perhaps excessively, conservative for headed bar development in special moment frame joints. This observation prompts consideration of other equations that might better fit the dataset. Four equations are considered.

3.4.1 Equations Considered

i) Development of headed bars in tension (ACI 318-14 §25.4.4)

ACI 318-14 [20] had different provisions for headed bar development than ACI 318-19. Equation (29) is the development length equation for headed deformed bars in tension from §25.4.4 of ACI 318-14:

$$\ell_{dt,318\text{–}14} = \max\left\{\left(\frac{0.016\, f_y \psi_e}{\sqrt{f_c'}}\right) d_b;\ 8d_b;\ 6\text{ in.}\right\} \qquad \text{Eq. (29)}$$

Unlike ACI 318-19, ACI 318-14 capped the values of both the concrete compressive strength and the reinforcing steel yield stress to 6,000 psi and 60,000 psi, respectively. In the database, these limits are exceeded in 10 and 28 of the 35 specimens, respectively. These caps, however, were due to a lack of test data at the time of publication, so, for the purpose of this analysis, both limits are disregarded.

ii) Development length of hooked bars in tension in SMF joints (ACI 318-19 §18.8.5.1).

Section 18.8.5.1 of ACI 318-19 has a development length equation for hooked bars in tension, shown here as Eq. (30):

$$\ell_{dh} = \max\left\{\frac{f_y d_b}{65\lambda\sqrt{f_c'}};\ 8d_b;\ 6\text{ in.}\right\} \qquad \text{Eq. (30)}$$

This equation is intended for use with hooked bars and is based on the hooked bar development length provisions in §25.4 of ACI 318-14 and several earlier codes. It is considered

here for headed bars because experience and test data do not support requiring substantially different development lengths for hooked and headed bars.

iii) Ghimire et al. [6] descriptive equation

Ghimire et al. [6] concluded that the anchorage strength of headed bars in beam-column joints under reversed cyclic loading can be estimated using descriptive equations derived from monotonic tests. For the case of headed bars with confining reinforcement, Ghimire et al. proposed the following descriptive equation:

$$T_h = \left(781 f_{cm}^{\ 0.24} \ell_{eh}^{\ 1.03} d_b^{\ 0.35} + 48800 \frac{A_{tt}}{n} d_b^{\ 0.88} \right) \left(0.0622 \frac{c_{ch}}{d_b} + 0.543 \right) \qquad \text{Eq. (31)}$$

$$\text{with } 0.0622 c_{ch}/d_b + 0.543 \le 1.0 \text{ and } A_{tt}/n \le 0.3 A_b$$

The embedment length associated with developing the yield stress of the headed bars, denoted ℓ_{ehy}, can be solved for from Eq. (31) by replacing the anchorage strength T_h by the product of the measured value of the steel yield stress f_y and the cross-sectional area of the (individual) headed bar A_b.

$$\ell_{ehy} = \left[\left(\frac{f_y A_b}{0.0622 \frac{c_{ch}}{d_b} + 0.543} - 48800 \frac{A_{tt}}{n} d_b^{\ 0.88} \right) \frac{1}{781 f_{cm}^{\ 0.24} d_b^{\ 0.35}} \right]^{1.03} \qquad \text{Eq. (32)}$$

$$\text{with } 0.0622 c_{ch}/d_b + 0.543 \le 1.0 \text{ and } A_{tt}/n \le 0.3 A_b$$

iv) ACI 408R-03 Tension development length with 0.7 reduction factor

The analyses of compression lap splices in Chapter 2 suggest that compression lap splice length can be calculated as a fraction of the tension development length. The fraction differs depending on which tension development equation is used. Here compression development is

taken as 0.7 times the length obtained from the ACI 408R-03 tension development length equation (Eq. (33)). If headed bars in special moment frame joints should be designed for compression development, then the embedment lengths provided in the beam-column connection database should generally exceed the length calculated with Eq. (33).

$$l_{dc,408} = 0.7 l_{d,408} = 0.7 \frac{\left(\frac{f_y}{\phi \, f_c'^{1/4}} - 2400\omega \right) \alpha\beta\lambda}{76.3 \left(\frac{c\omega + K_{tr,408}}{d_b} \right)} d_b \qquad \text{Eq. (33)}$$

where α, β, and λ are all unitary for this database, and with:

$$\omega = 0.1 \frac{c_{max}}{c_{min}} + 0.9 \le 1.25 \; ; \; t_r = 9.6 \, R_r + 0.28 \le 1.72 \; ; \; t_d = 0.03 \, d_b + 0.22$$

$$K_{tr,408} = \frac{6.26 t_r t_d A_{tr}}{sn} f_c'^{1/2} \; ; \; f_c'^{1/4} \le 11.0 \; ; \; f_y \le 80 \text{ ksi} \; ; \; \phi = 0.82$$

A relative rib area, R_r, of 0.0727 was assumed for all specimens based on recommendations in ACI 408R-03.

Application of Eq. (33) to headed bars in joints requires some interpretation because identification of potential splitting planes is not as obvious in a column-beam joint as is may be for longitudinal bars in a column or beam; the definition of splitting plane does not readily apply where breakout anchorage failures occur. To bracket the range of possible outcomes, two cases are considered in these analyses: $K_{tr,408} = 0$, which represents a lack of confining reinforcement, and $(c\omega + K_{tr,408})/d_b = 4$, the upper bound recommended in ACI 408R-03. These two cases bracket the possible required tension development length and, lacking a precise quantification of confinement, both are evaluated for each specimen.

3.4.2 Results

Figures 34 through 39 are analogous to Figures 32 and 33. Each figure shows the development length obtained from a design equation (Eqs. 22, 29, 30, 32, and 33) plotted versus the provided embedment length. These equations include the tension development length for headed bars in non-earthquake-resistant construction, $\ell_{dt,25.4.4}$ (Eq. (22)); the ACI 318-14 tension development length for headed bars, $\ell_{dt,318\text{-}14}$, with no caps on concrete or steel strengths (Eq. 29); the ACI 318-19 tension development length for hooked bars in special moment frames, ℓ_{dh}, (Eq. 30); the embedment length derived from the anchorage strength descriptive equation from Ghimire et al. [6], ℓ_{eyh}, (Eq. 32); and 0.7 times the ACI 408R-03 tension development length, l_d, (Eq. 33) with either $K_{tr,408} = 0$ (Case I) or $(c\omega+K_{tr,408})/d_b = 4.0$ (Case II).

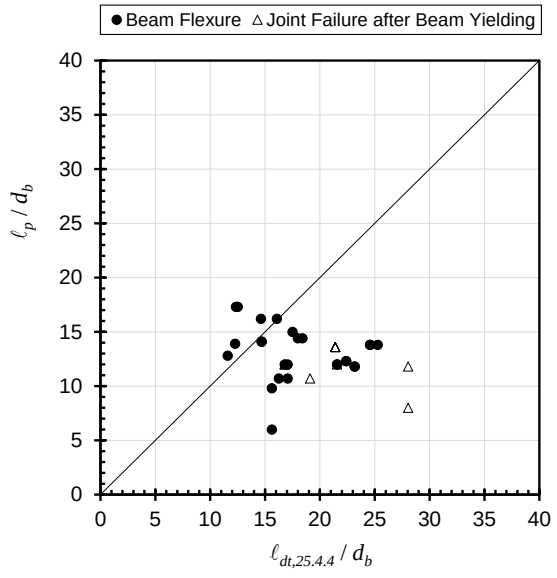

Figure 34 – ℓ_p/d_b versus $\ell_{dt,25.4.4}/d_b$

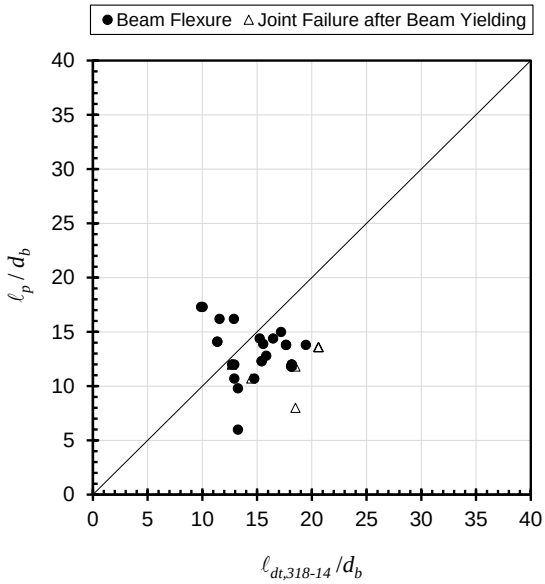

Figure 35 – ℓ_p/d_b versus ℓ_{dt} (ACI 318-14 §25.4.4 with no caps)/d_b

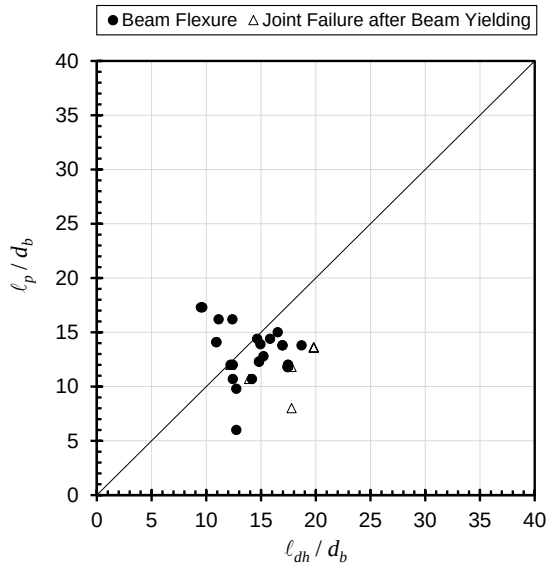

Figure 36 – ℓ_p/d_b versus ℓ_{dh} (ACI 318-19 §18.8.5.1)/d_b

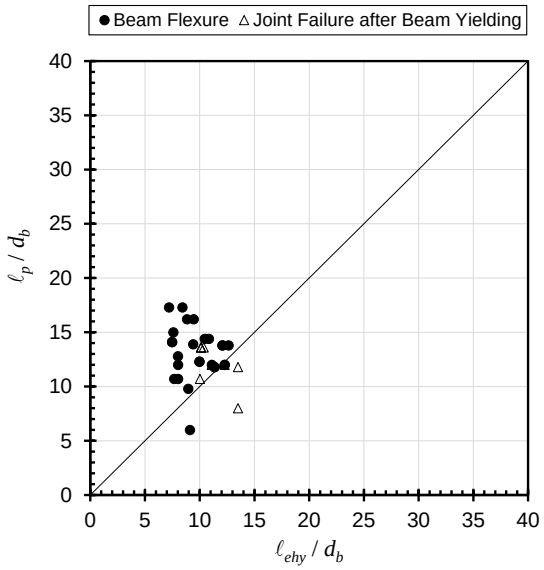

Figure 37 – ℓ_p/d_b versus ℓ_{eyh} (Ghimire et al.)/d_b

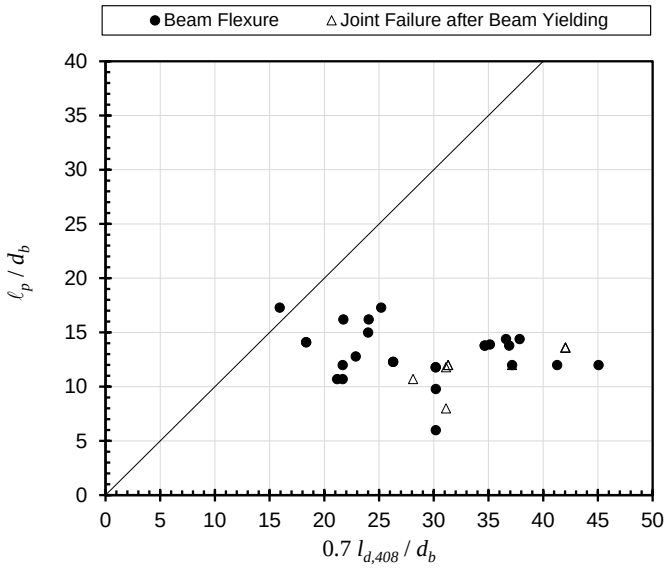

Figure 38 – ℓ_p/d_b versus 0.7l_d (ACI 408R-03 Case I: $K_{tr,408}$ = 0)/d_b

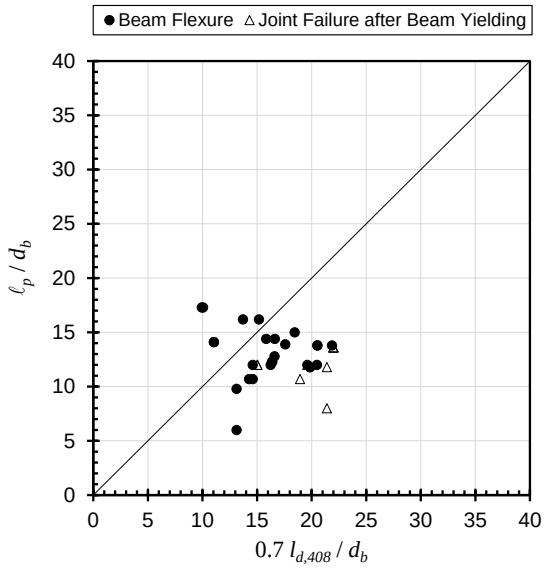

Figure 39 – ℓ_p/d_b versus $0.7l_d$ (ACI 408R-03 Case II: $(c\omega+K_{tr,408})/d_b = 4.0)/d_b$

Since none of the 35 specimens exhibited anchorage failures, it is reasonable to expect that the provided embedment length typically exceeded or was close to the required development lengths. That was not the case in Figures 32 and 33 , which demonstrated that ACI 318-19 §25.4.9 and §18.8.5.2 are both very conservative. Figures 34 through 39 show that all the equations considered in this section, except for $0.7\ell_d$ Case I in Figure 38, perform better than $\ell_{dt,18.8.5.2}$ from ACI 318-19. In some specimens the provided embedment length exceeded the required lengths calculated as $\ell_{dt,25.4.4}$, ℓ_{dh}, ℓ_{eyh} and $0.7l_d$ Case II, which is to be expected in specimens that do not exhibit anchorage failures during reversed cycle loading testing.

The behaviors of $\ell_{dt,318\text{-}14}$, ℓ_{dh}, and $0.7\ell_d$ Case II (Figures 35, 36, and 39) are all very similar: some specimens had embedment lengths longer than required while most had embedment lengths that were only somewhat shorter than required. These trends are reasonable for specimens that did not exhibit bond/anchorage failures when compared against design equations with some inherent

conservatism. Although further analyses are necessary, these results imply that $\ell_{dt,318\text{-}14}$, $\ell_{dh,18.8.5.1}$, and $0.7\ell_d$ Case II might be more appropriate for design of SMF joints than ACI 318-19 provisions.

The trends in Figure 37 for ℓ_{eyh} stand out among the equations considered, with almost all specimens having a longer provided length than what is obtained from the equation. This equation is derived from a so-called descriptive equation, which, unlike design equations, has no built-in safety factors. It should therefore be expected that specimens with no evidence of anchorage failures likely have headed bar embedment lengths longer than ℓ_{eyh}.

Table 2 provides another way to compare the different length requirements. The value of each cell represents the mean ratio between the length in the row and the length in the column in question for specimens in the database. An expanded version of the table with values for all lengths against each other can be found in Appendix F.

Table 2 - Average length ratios: length in row / length in column

	ℓ_p	ℓ_{ehy}
ℓ_p	1	1.32
$\ell_{dt,318\text{-}14}$, no caps [Eq. (29)]	1.15	1.55
$\ell_{dt,25.4.4}$ [Eq. (22)]	1.38	1.87
$\ell_{dt,18.8.5.2}$ [Eq. (23)]	1.73	2.34
$\ell_{dc,25.4.9}$ [Eq. (24)]	1.54	2.02
ℓ_{ehy} [Eq. (32)]	0.76	1
ℓ_{dh} [Eq. (30)]	1.10	1.45
$0.7l_{d,408}$, Case II [Eq. (33)]	1.25	1.65

The middle column of Table 2 shows that all the different length requirements, except for ℓ_{ehy}, surpass, on average, the embedment length that was provided in the specimens, with different levels of conservatism. The tension development length required by the current ACI Building Code provisions, $\ell_{dt,18.8.5.2}$, is by far the most conservative of the equations considered. For the database in question, §18.8.5.2 of ACI 318-19 requires, on average, 73% more embedment length than was provided, even though the specimens did not exhibit anchorage failures. The next most conservative is the compression development length requirement, $\ell_{dc,25.4.9}$ from §25.4.9 of ACI 318-19, which would require, on average, 54% more embedment length than provided in specimens that did not exhibit anchorage failures. In contrast, ℓ_{ehy} was, on average, only 76% of the provided lengths, which is to be expected for a descriptive equation compared against specimens that did not exhibit anchorage failures.

The last column of Table 2 provides ratios of calculated lengths versus ℓ_{ehy} obtained from the descriptive equation in Eq. (31). If ℓ_{ehy} is taken as the length necessary to develop headed bars in SMF joints without a safety factor, ℓ_p / ℓ_{ehy} should generally exceed 1.0 in specimens that did not exhibit bond/anchorage failures. Table 2 shows $\ell_p / \ell_{ehy} = 1.32$ for this dataset. Furthermore, if ℓ_{ehy} is taken as the length necessary to develop headed bars in SMF joints without a safety factor, the last column of Table 2 shows the extent of the conservatism embedded in various equations

considered. Both $\ell_{dt,318\text{-}14}$ and $\ell_{dh,18.8.5.1}$ are approximately 50% longer than ℓ_{ehy}, whereas both $\ell_{dt,18.8.5.2}$ and $\ell_{dc,25.4.9}$ are, on average, more than twice as long as ℓ_{ehy}.

3.5 Conclusions

1. Satisfying the compression development length requirements of §25.4.9 is not a necessary condition to obtain adequate joint behavior under cyclic loads. None of the 35 beam-column connection specimens considered satisfied §25.4.9, even though all had drift ratio capacities not less than 3% and no reported evidence of anchorage distress. Furthermore, §25.4.9 produced lengths that were, on average, double the lengths obtained from the Ghimire, Darwin, and Lepage [16] descriptive equation for headed bar anchorage strength. ACI 318-19 §18.8.2.2 should not require that headed bars satisfy §25.4.9.
2. Analyses suggest that satisfying the tension development length requirements of §18.8.5.2, which refer to §25.4.4, is also not a necessary condition to obtain adequate joint behavior under cyclic loads. Stated differently, §25.4.4 and thus §18.8.5.2 may be overly conservative for joint design. Only two of the 35 beam-column connection specimens considered satisfied §18.8.5.2, even though all had drift ratio capacities not less than 3% and no reported evidence of anchorage distress. Furthermore, §18.8.5.2 produced lengths that were, on average, 2.3 times the lengths obtained from the Ghimire, Darwin, and Lepage [6] descriptive equation for headed bar anchorage strength.
3. The equation for headed bar development length from §25.4.4 of ACI 318-14 (without caps on bar grade or concrete compressive strength) and the equation for hooked bar development length in §18.8.5.1 of ACI 318-19 appear more appropriate for design of specimens like those

in the database. Each was a more reasonable fit to the database and still conservate relative to the Ghimire, Darwin, and Lepage [6] descriptive equation for headed bar anchorage strength.

3.6 Notation

a	=	depth of rectangular compression stress block in beam flexure (in.)
A_b	=	cross-sectional area of an individual headed bar (in.^{2})
A_{hs}	=	total cross-sectional area of headed bars (in.^{2})
A_j	=	effective cross-sectional area of a joint in a plane parallel to plane of beam reinforcement generating shear in the joint, per ACI 318-19 [3] §R15.4.2 = $b_j \times h_c$ (in.^{2})
$A_{tr,1}$	=	cross-sectional area of a tie leg (in.^{2})
A_{tt}	=	total cross-sectional area of effective confining reinforcement parallel to the headed bars (in.^{2})
b_b	=	width of beam (in.)
b_c	=	width of column (in.)
b_j	=	effective joint width, see Figure 27 (in.)
c_{max}	=	maximum(c_b ; c_s) (in.)
c_{min}	=	smaller of minimum concrete cover or ½ of the clear spacing between bars (in.)
c_s	=	minimum(c_{so} ; c_{si} + 0.25 in) (in.)
c_{si}	=	½ of the bar clear spacing (in.)
c_{so}	=	side concrete cover for reinforcing bar (in.)
d	=	distance between centroid of beam longitudinal reinforcing bars and extreme compression fiber of beam section (in.)
d_b	=	nominal diameter of a headed bar (in.)
E_s	=	modulus of elasticity of steel: 29.000 ksi

f_c'	=	measured concrete compressive strength (psi)
f_y	=	measured yield stress of reinforcing steel in tension (ksi)
h_b	=	height of beam (in.)
h_c	=	height of column (in.)
$K_{tr,408}$	=	transverse reinforcement index according to ACI 408R-03 [1]
n	=	number of headed bars in tension
L_b	=	beam span measured to the center of the column (in.)
L_c	=	length of column between inflection points (in.)
L_n	=	clear beam span (in.)
ℓ_c	=	compression development length of straight bars or wires, as required by ACI 318-19 [3] §25.4.9 (in.)
ℓ_p	=	provided embedment length of headed bars in a specimen, measured from the critical section at the face of column (in.)
ℓ_d	=	development length of straight bars in tension as required by ACI 318-19 [3] §25.4.2 (in.)
$l_{d,408}$	=	development length of straight bars in tension, as required by the recommended provisions by ACI 408R-03, Eq. 4-11a (in.). Originally "l_d" in source.
ℓ_{dh}	=	development length of a hooked bar in tension, as required by ACI 318-19 [3] §18.8.5.1 for SMF joints (in.)
$\ell_{dt,18.8.5.2}$	=	development length of headed bar in tension ACI 318-19 [3] §18.8.5.2 for SMF joints (in.). Originally "ℓ_{dt}" in source.
$\ell_{dt,25.4.4}$	=	development length of headed bar in tension ACI 318-19 [3] §25.4.4 (in.). Originally "ℓ_{dt}" in source.

$\ell_{dt,318\text{-}14}$	=	development length of headed bar in tension ACI 318-14 [20] §25.4.4 (in.). Originally "ℓ_{dt}" in source.
ℓ_{ehy}	=	embedment length of a headed bar necessary to develop its yield strength, derived from the anchorage strength descriptive equation by Ghimire et al. [6]
M_n	=	nominal bending moment capacity of the beam cross section at the face of the column (kip-in.)
M_{peak}	=	the maximum beam moment at the face of the column based on measured forces (kip-in.)
N_{legs}	=	number of legs within a layer of column ties or hoops
R_n	=	coefficient representing whether a transverse beam is present in the calculation of the nominal joint shear V_n, according to ACI 318-19 [3] §15.4.2
s	=	spacing of column hoops or ties (in.)
t_d	=	term representing the effect of bar size on the steel contribution to total bond force
t_r	=	term representing the effect of relative rib area on the steel contribution to total bond force
V_n	=	nominal joint shear strength according to ACI 318-19 [3] §18.8.4 (kip)
V_p	=	horizontal joint shear demand at mid depth of the beam (kip)
T_h	=	anchorage strength of a headed bar, calculated using the descriptive equation by Ghimire et al. [6]
$\delta_{0.8peak}$	=	the drift ratio when, after reaching the peak load, the load drops to 80% of the peak load
ε_s	=	strain of steel reinforcement

λ	=	lightweight concrete modification factor for the development length of deformed bars and wires in compression (ACI 318-19 [3] §25.4.9) and the development length of hooked bars in tension (ACI 318-19 [3] §25.4.3)
ρ_t	=	ratio of area of distributed transverse reinforcement to gross concrete area perpendicular to that reinforcement
$\rho_{t,req}$	=	minimum required ratio of area of distributed transverse reinforcement to gross concrete area perpendicular to that reinforcement (ACI 352R-02 [34])
ψ_c	=	concrete strength modification factor for the development length of headed bars in tension (ACI 318-19 [3] §25.4.4)
ψ_e	=	epoxy coating modification factor for the development length of headed bars in tension (ACI 318-19 [3] §25.4.4 and ACI 318-14 §25.4.4)
$\psi_{o,head}$	=	location modification factor for the development length of headed bars in tension (ACI 318-19 [3] §25.4.4). Originally "ψ_o" in source.
$\psi_{o,hook}$	=	location modification factor for the development length of hooked bars in tension (ACI 318-19 [3] §25.4.3)
ψ_p	=	parallel tie reinforcement modification factor for the development length of headed bars in tension (ACI 318-19 [3] §25.4.4)
ψ_r	=	confining reinforcement modification factor for the development length of deformed bars and wires in compression (ACI 318-19 [3] §25.4.9)

Chapter 4: Embedment Length of Hooked Bars in Special Moment Frames

4.1 Introduction

Reinforcing bars terminating in a hook transmit forces into concrete through bond along the straight and curved portions of the bar and through bearing of the curved portion against concrete. Hooked bars are often used in frame exterior joints, where the beam longitudinal reinforcement must be anchored into the column.

Use of hooked bars in reinforced concrete construction is permitted and regulated by ACI 318-19 [3]. For design of frames not designated as special moment frames (SMF), the development of hooked bars in tension is prescribed by Chapter 25 of ACI 318-19. According to §25.4.3, the development length $\ell_{dh,25.4.3}$ for hooked deformed bars in tension shall be:

$$\ell_{dh,25.4.3} = \max\left\{ \frac{f_y \psi_e \psi_r \psi_o \psi_c}{55\lambda\sqrt{f_c'}} d_b^{1.5} \; ; \; 8d_b \; ; \; 6\text{in.} \right\} \qquad \text{Eq. (34)}$$

where λ, ψ_e, ψ_r, ψ_o, and ψ_c are modification factors associated with lightweight concrete, epoxy coating, confining reinforcement, hooked bar location, and concrete strength, respectively.

Requirements for development of hooked, headed, and straight reinforcement in joints of SMFs are articulated in §18.8.2.2:

> "*Longitudinal reinforcement terminated in a joint shall extend to the far face of the joint core and shall be developed in tension in accordance with 18.8.5 and in compression in accordance with 25.4.9.*" - ACI 318-19 [3] §18.8.2.2

For developing hooked bars in tension in SMFs, ACI 318-19 §18.8.5.1 requires providing the length given by Eq. (35):

$$\ell_{dh,18.8.5.1} = \max\left\{ \frac{f_y d_b}{65\lambda\sqrt{f_c'}} \; ; \; \ell_{dh,18.8.5.1,\min} \right\} \qquad \text{Eq. (35)}$$

where $\ell_{dh,18.8.5.1,min}$ is the greater of $8d_b$ and 6 in. for normal-weight concrete and the greater of 10 d_b and 7½ in. for lightweight concrete.

The language in §18.8.2.2 that requires consideration of both tension and compression development has been present in successive versions of the ACI Building Code since ACI 318-83. Even though earthquakes are expected to subject beam reinforcement terminating in a joint to both tension and compression force demands, the language of §18.8.2.2 is not clear about whether it is sufficient for a hooked bar to satisfy only §18.8.5 or must satisfy both §18.8.5 and §25.4.9. It could be interpreted that the reference to §25.4.9 is only for straight bars in compression since §25.4.9 has no guidance for how it should be applied to headed or hooked bars. This was clarified with new commentary in ACI 318-14:

> "*For bars in compression, the development length corresponds to the straight portion of a hooked or headed bar measured from the critical section to the onset of the bend for hooked bars and from the critical section to the head for headed bars.*" - ACI 318-14 [20] §R18.8.2.2

This definition is illustrated in Figure 40.

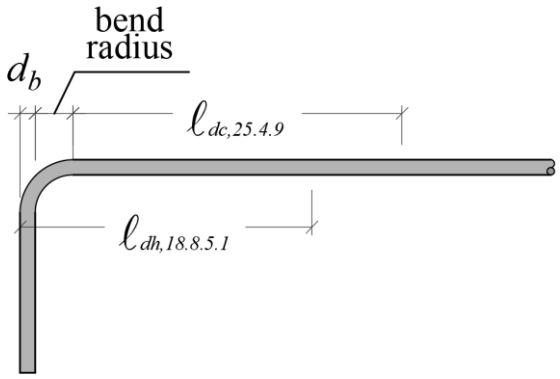

Figure 40 – ACI 318-19 definitions for $\ell_{dc,25.4.9}$ and $\ell_{dh,18.8.5.1}$ in hooked bars

Prior to ACI 318-14, an engineer might have assumed that a hooked bar satisfying §18.8.5 was adequately developed without checking §25.4.9 because tension development is often more critical than compression development, and there is no experimental evidence of hooks adequately anchored in tension failing when subjected to compression. Nevertheless, the new commentary in §R18.8.2.2 of ACI 318-14 makes clear that engineers must design hooked bars so they comply with both §18.8.5 and §25.4.9.

The compression development length required for joints of SMFs by §18.8.2.2, in accordance with §25.4.9, is the longer of the values obtained from the expressions in Eq. (36):

$$\ell_{dc,25.4.9} = \max\left\{ \frac{f_y \psi_r}{50\sqrt{f'_c}} d_b \ ; \ 0.0003 f_y \psi_r d_b \right\} \qquad \text{Eq. (36)}$$

where ψ_r is a confining reinforcement modification factor and $\sqrt{f'_c} \leq 10$ ksi .

The implications of designing hooked bars for compression development (§25.4.9) are shown in Figure 41. Figure 41 shows the ratio between the required hooked bar compression length ($\ell_{dc,25.4.9}$ + bend radius + d_b) and the required hooked bar tension development length, $\ell_{dh,18.8.5.1}$, versus specified concrete compressive strength. For the bar sizes considered, two curves are obtained: one for No. 6 to No. 8 bars and another for No. 9 to No. 11 bars.

Normal-weight concrete (λ= 1.0) and a steel yield stress of 60 ksi were assumed for all cases. A value of 0.75 was assumed for the confining reinforcement modification factor for calculating compression development length (ψ_r = 0.75). These assumptions are valid for uncoated hooked bars terminating inside a well-confined joint. The bend radius was either 3d_b (No. 3 through No. 8 bars) or 4 d_b (No. 9 through No. 11 bars), as required in ACI 318-19 §25.3.1.

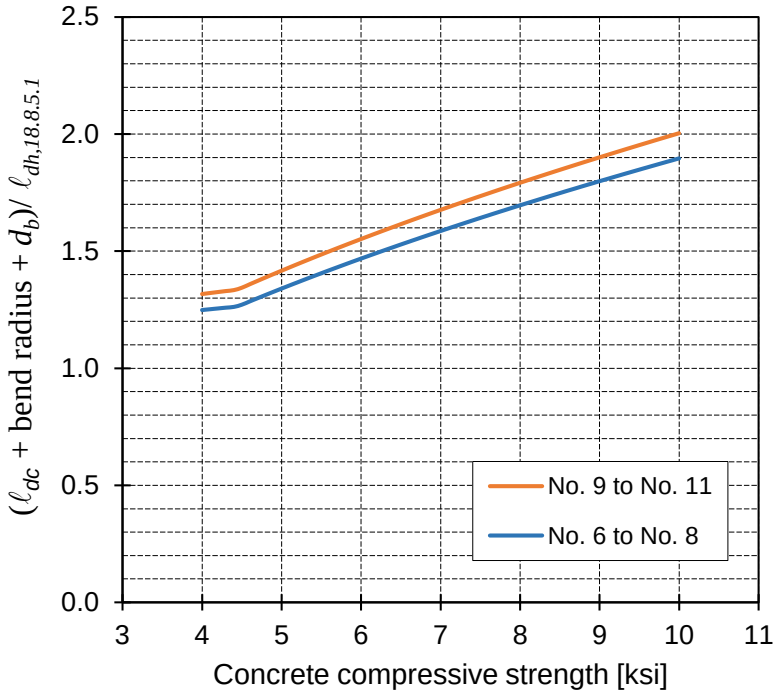

Figure 41 – ACI 318-19 provisions for hooked bars: (ℓ_{dc} + bend radius + d_b)/ℓ_{dh} versus concrete compressive strength

Figure 41 shows that, for λ = 1.0 and ψ_r = 0.75, the length required to satisfy the compression development length is longer than the required tension development length for hooked bars of sizes typically used in practice, regardless of the concrete compressive strength.

The effect of ACI 318-19 §18.8.2.2 is considerably more pronounced for hooked bars than for headed bars (Chapter 3, Figure 19). The compression development length requirement is, in all cases, at least 25% longer than the tension development requirement for any of the bar sizes considered (No. 6 through No. 11) and the range of concrete compressive strengths considered (4 ksi through 10 ksi).

This chapter explores whether the compression development length should indeed govern the embedment length of hooked bars in joints of special moment frames. This is done by

examining results from tests of exterior beam-column joints with hooked beam reinforcement under reversed cyclic displacements.

4.2 Database Description

A database of test results was used to evaluate hooked bar development. The database (Appendix G) includes results from seven studies and consists of 27 exterior cast-in-place reinforced concrete beam-column joint specimens subjected to reversed cyclic loading.

Results were obtained from Hanson [35], Uzumeri [36], Scribner and Wight [37], Ehsani and Alameddine [38], Kurose et al. [39], and Hwang et al [40]. The 27 specimens were selected for meeting the following criteria: (1) specimens were cast-in-place reinforced concrete beam-column connections, (2) columns were continuous through the joint and had a minimum cross-sectional dimension of 11 inches, (3) connections were subjected to reversed cyclic displacement demands, (4) beam longitudinal reinforcing bars ended in overlapping 90° hooks placed with the hooks turned towards mid depth of the joint, (5) hooked beam bars diameter was at least 0.94 in. and no mixed bar sizes were used within the top or bottom layers of beam reinforcement, (6) joints had at least two column hoops, and (7) no intermediate-depth web longitudinal reinforcement was present in the beams (i.e. beams had top and bottom longitudinal bars only). Figure 42 shows a schematic of a representative specimen.

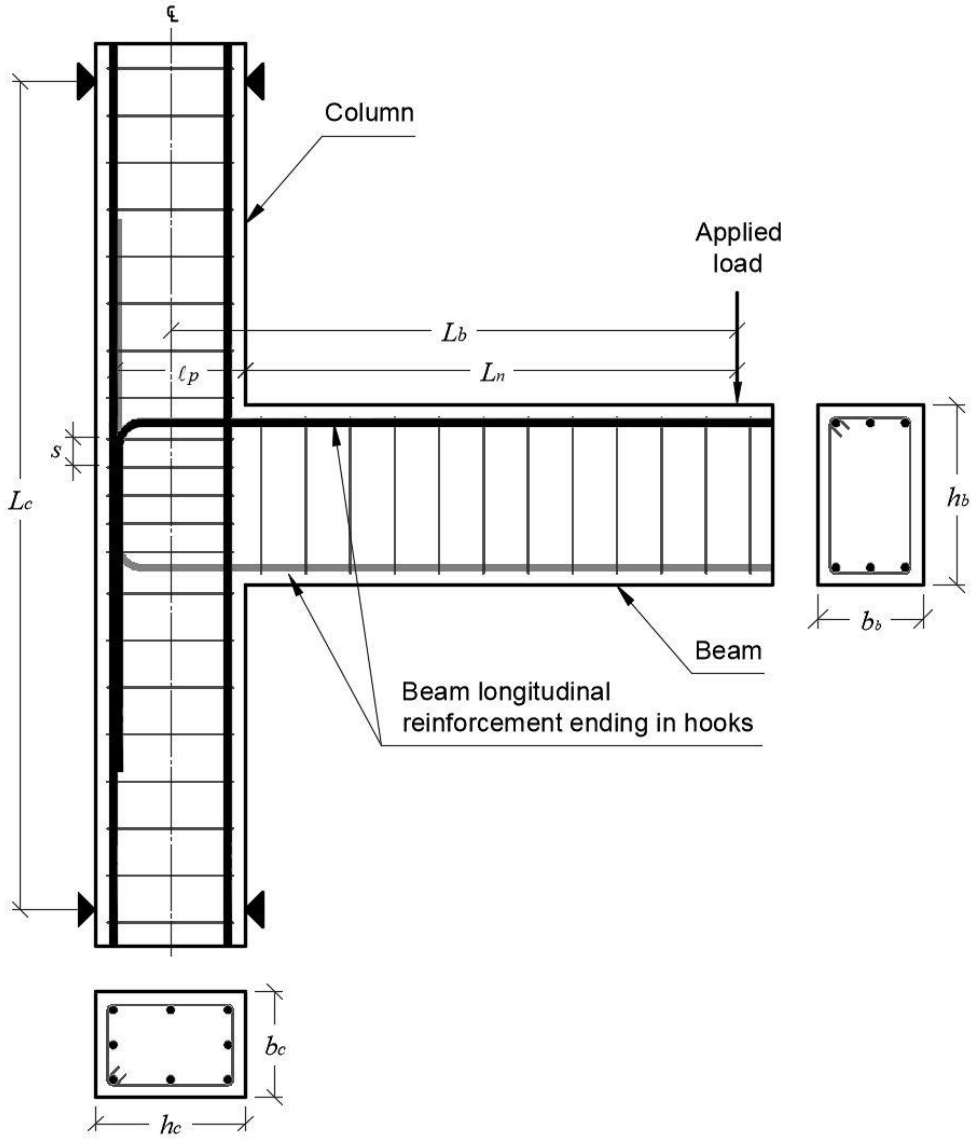

Figure 42 – Schematic of specimens in database (elevation and cross-sections)

Specimens with relatively large bars were selected for two reasons. Firstly, large bars (No. 8 and 9) are representative of bar sizes used in practice, and secondly, differences between Eq. (34) and Eq. (35) (which represent ACI 318-19 §25.4.3 for non-SMF design and §18.8.5.1 for SMF design) are likely to be most substantial for large bars because the exponent on d_b differs. The exponent on d_b is 1.5 in Eq. (34) and 1.0 in Eq. (35).

Every specimen contained transverse reinforcement within the joint consisting of column hoops, although not all connections would satisfy the joint transverse reinforcement requirements of ACI 318-19 [3] for SMF joints.

The specimens had measured concrete compressive strengths of 3.8 to 13.6 ksi. Hooked bars had diameters that approximately coincided with U.S. No. 8 and No. 9 bars sizes and measured yield stresses of 50.6 to 75.5 ksi. The distributions of measured concrete compressive strength, hooked bar diameter, and measured steel yield stress are shown in Figure 44, 45, and 46, respectively. The provided embedment lengths of the hooked bars, defined as shown in Figure 43, were 10.6 to 16 times the diameter of the hooked bar with the distribution shown in Figure 47.

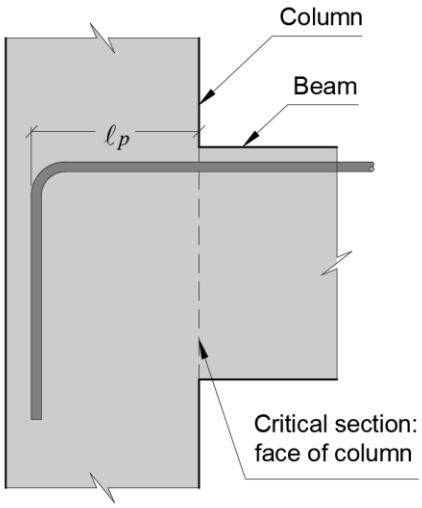

Figure 43 – Definition of the embedment length in specimens, ℓ_p, consistent with ACI 318-19 definition of development length

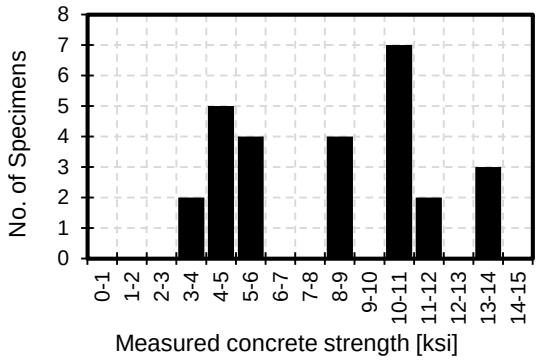

Figure 44 – Histogram of measured concrete compressive strength

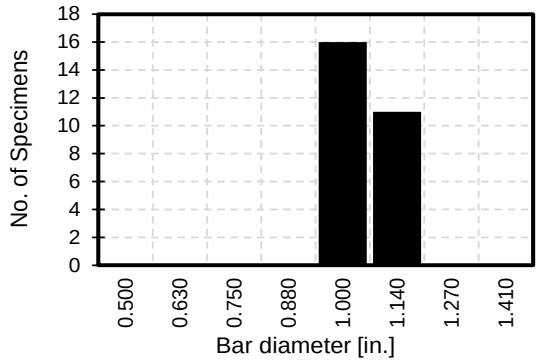

Figure 45 – Histogram of hooked bar diameter (each bin includes specimens within ±1/16 in.)

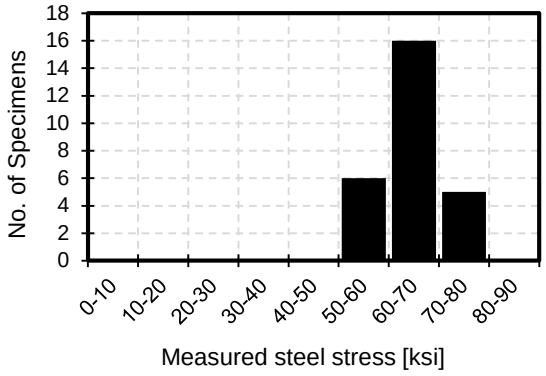

Figure 46 – Histogram of measured hooked bar steel yield stress

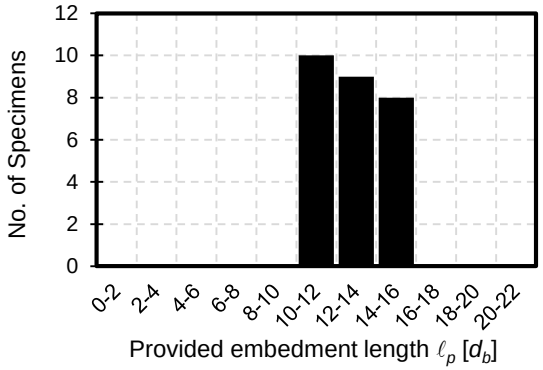

Figure 47 – Histogram of provided hooked bar embedment length (column face to tail of hook)

The specimens were all subjected to a series of fully reversed cyclic displacements of increasing magnitude. No specimen in the database exhibited failure by anchorage or shear, but rather by deterioration of the joint or the beam near the joint throughout the reversed loading cycles.

Specimen drift was defined as the vertical displacement of the beam end during testing divided by the beam length measured to the centroid of the column (L_b in Figure 42). The drift ratio capacities in the database correspond to the drift at which strength decayed to 0.8 times the peak strength in each loading direction based on an envelope drawn to the peak of each load cycle. Rather than reporting precise $\delta_{0.8,peak}$ values, the database indicates for each specimen either (a)

whether $\delta_{0.8,peak}$ was at least 3%, or (b) that insufficient information was available to assess $\delta_{0.8,peak}$. All specimens with published force-displacement results had $\delta_{0.8,peak}$ of at least 3%.

The nominal beam flexural strength was calculated at the column face using Eq. (25):

$$M_n = f_y A_{hs} (d - a/2) \qquad \text{Eq. (25)}$$

The contribution of compression reinforcement to flexural strength was neglected. In every case the beam section neglecting compression reinforcement was under-reinforced (steel strain greater than or equal to the yield strain estimated as f_y / E_s).

The maximum bending moment in the beams, M_{peak}, was calculated as the force applied to the beam tip times the clear shear span of the beam (distance from the point load to the column face). M_{peak} ranged from 2500 to 4200 kip-in., while the nominal flexural strength, M_n, ranged from 1800 to 5100 kip-in. The resulting peak-to-nominal strength ratios, M_{peak}/M_n, were from 0.57 to 1.34 (Figure 48).

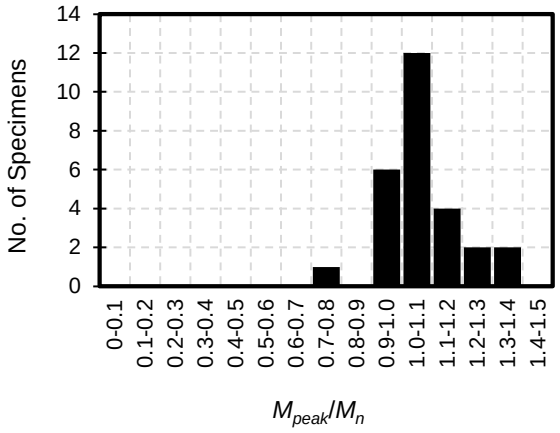

Figure 48 – Histogram of M_{peak}/M_n

The nominal joint shear strength, V_n, was calculated in accordance with ACI 318-19 §18.8.4 using Eq. (26).

$$V_n = R_n \lambda \sqrt{f_c'} A_j \qquad \text{Eq. (26)}$$

where R_n is a coefficient representing whether a transverse beam is present and had a value of 12 for all specimens in the database, except for that from Kurose et al. [39], where the confinement provided by transverse beams resulted in R_n = 15. The effective joint area A_j, shown schematically in Figure 49, consists of the product of the joint depth in the plane parallel to the reinforcement generating shear (the height of the column section for these specimens) and the effective joint width, defined as the lesser of b_c , (b_b+h_c), and (b_c+2x).

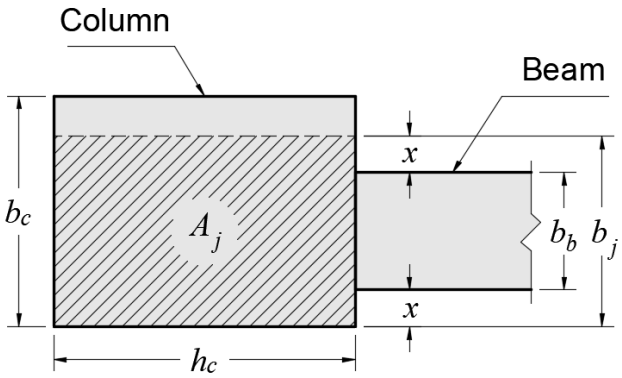

Figure 49 – Definition of effective joint area (plan view), adapted from ACI 318-19 [3] Fig. R15.4.2

Joint shear demand, V_p, was estimated with Eq. (27). Equation (27) is equivalent to the equation used in Ghimire et al. [6] for similar tests with headed bars, except that the second term, which represents the column shear outside of the joint, is multiplied by L_b/L_n. This is necessary because M_{peak} is calculated at the face of the column.

$$V_p = \left(\frac{M_{peak}}{M_n} \right) n A_b f_y - \frac{M_{peak}}{L_c} \frac{L_b}{L_n} \qquad \text{Eq. (27)}$$

The value of V_p ranged from 130 to 240 kip while V_n ranged from 130 to 330 kip. The resulting V_p/V_n ranged from 0.71 to 1.48 (Figure 50). For most specimens, the shear demand was less than the nominal joint shear strength.

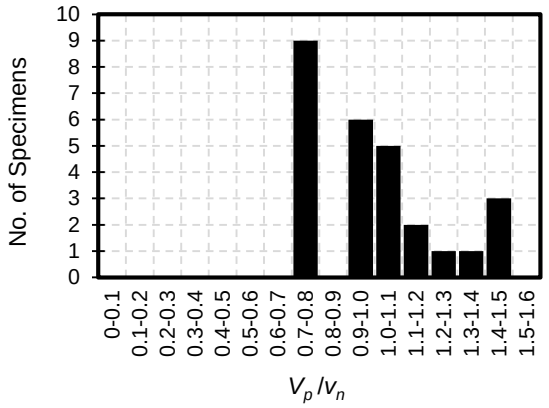

Figure 50– Histogram of V_p/V_n

Figures 51 and 52 show M_{peak}/M_n and V_p/V_n versus ℓ_p/d_b, respectively. Closed circles correspond to specimens whose drift capacity surpassed 3%, which coincidentally is every specimen for which drift data were reported. Open circles indicate specimens for which drift was not reported.

Figure 51 shows that in specimens with $\delta_{0.8peak} \geq 3\%$, the peak moments were generally greater than the nominal flexural strength. All specimens considered, there might be a tendency for specimens with relatively longer hooked bar embedment lengths to exhibit greater peak moments, but this trend is not clear in specimens with $\delta_{0.8peak} \geq 3\%$.

As expected, there is no correlation between V_p/V_n and ℓ_p/d_b in Figure 52.

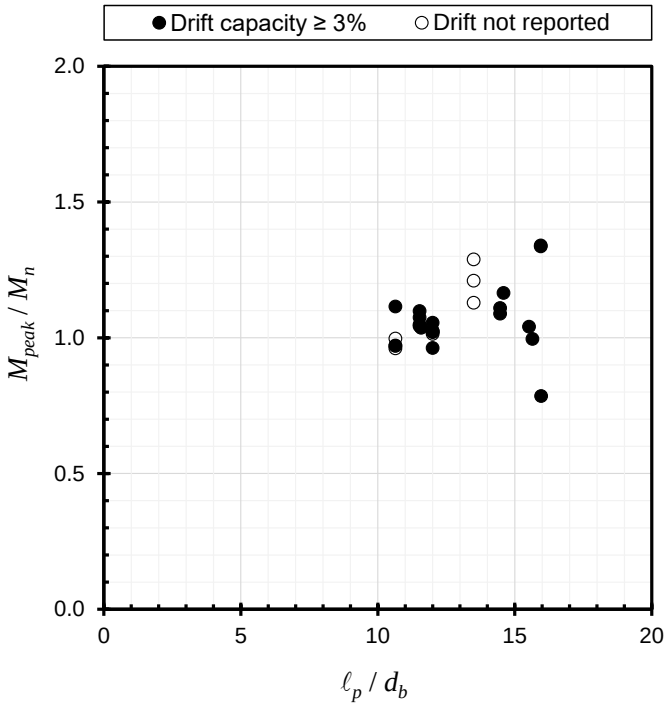

Figure 51 – M_{peak}/M_n versus ℓ_p(ACI 318-19)/d_b

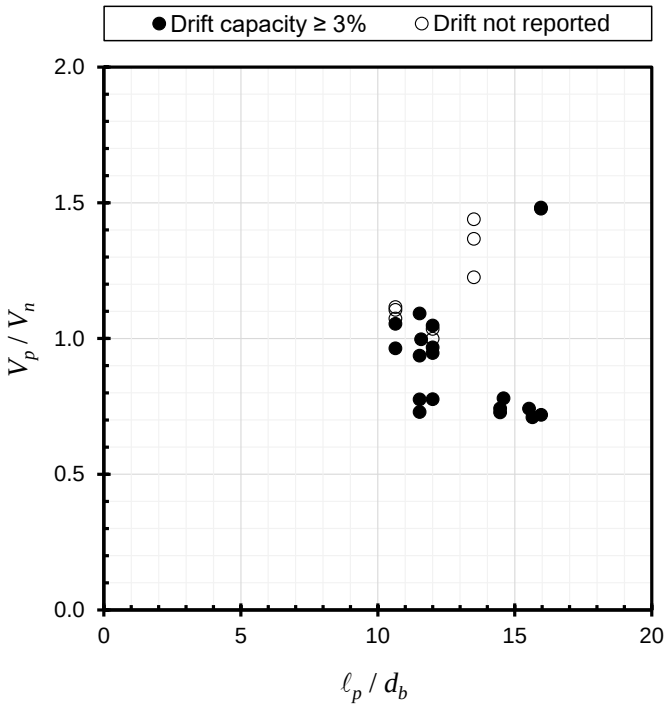

Figure 52 – V_p/V_n versus ℓ_p(ACI 318-19)/d_b

4.3 Evaluation of database against current provisions

The embedment lengths provided for specimens in the database were compared against $\ell_{dt,18.8.5.1}$ and $\ell_{dc,25.4.9}$ to evaluate the appropriateness of the requirement in §18.8.2.2 that hooked bars in SMF joints satisfy the compression development length requirements. Measured material properties were used in all cases.

To calculate the compression development length, $\ell_{dc,25.4.9}$, some interpretation was necessary to define the confining reinforcement modification factor, ψ_r. This factor leads to a reduction of the required compression development length when the transverse reinforcement consists of:

- A spiral,
- A circular continuously wound tie with $d_b \geq$ ¼ in. and pitch not more than 4 in.,
- No. 4 bar or D20 wire ties in accordance with ACI 318-19 [3] §25.7.2 spaced no more than 4 in. on center, or
- Hoops in accordance with ACI 318-19 §25.7.4 spaced no more than 4 in. on center.

25, or 93%, of the 27 specimens had hoops that qualified for $\psi_r = 0.75$.

4.3.1 Results

Figure 53 shows the hooked bar embedment lengths versus the required compression length, ($\ell_{dc,25.4.9}$ + bend radius + d_b), for all 27 specimens. This plot shows that the required length due to compression development length, ($\ell_{dc,25.4.9}$ + bend radius + d_b), was always longer than the provided embedment length. For specimens with $\delta_{0.8peak} \geq 3\%$, the required length was up to 85%

longer than the provided length, and yet the specimens performed adequately under reversed cyclic loading, without exhibiting anchorage failures. Figure 53 therefore shows that providing an embedment length longer than ($\ell_{dc,25.4.9}$ + bend radius + d_b) is not necessary to prevent bond/anchorage failures and obtain good connection behavior.

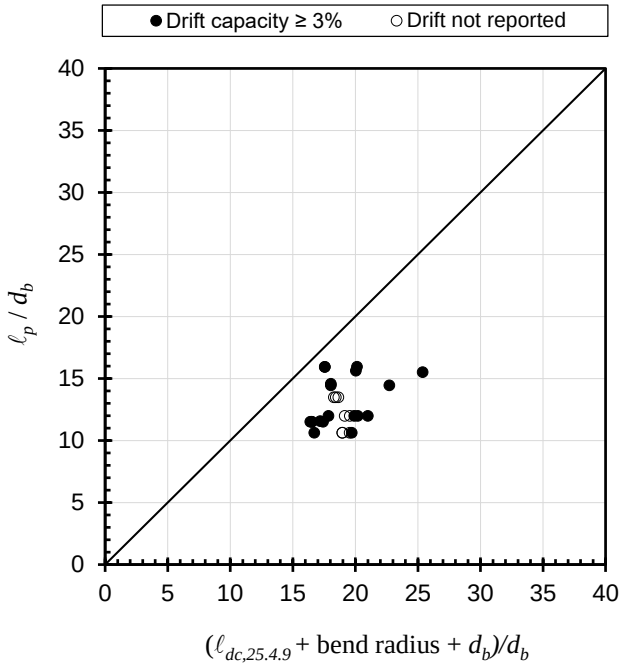

Figure 53 – ℓ_p/d_b versus ($\ell_{dc,25.4.9}$ + bend radius + d_b)

Figure 54 shows hooked bar embedment lengths versus the required tension development lengths, $\ell_{dt,18.8.5.1}$. Almost all the specimens that attained $\delta_{0.8peak} \geq 3\%$ had an embedment length ℓ_p longer that the required tension development length $\ell_{dt,18.8.5.1}$, which should be expected for specimens that did not exhibit anchorage failures. The current tension development length provision for SMF joints, $\ell_{dt,18.8.5.1}$, therefore appears appropriate for design of hooked bar

development in joints like those in the database. This was not the case for headed bars (Chapter 3), for which it was shown that both the tension and the compression development requirements from ACI 318-19 §18.8.2.2 are substantially conservative.

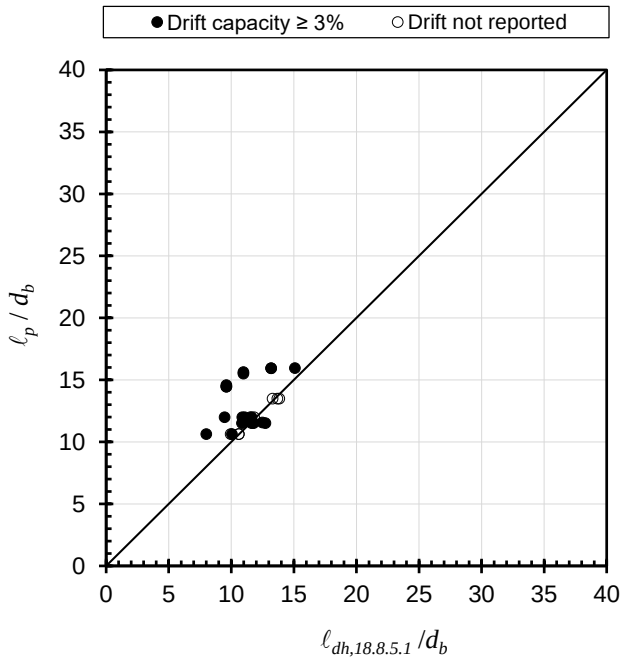

Figure 54 – ℓ_p/d_b versus $\ell_{dt,18.8.5.1}/d_b$

These results show that satisfactory connection behavior, characterized by drift ratio capacities exceeding 3%, can be obtained without satisfying the requirements of §25.4.9. It is acknowledged that design provisions should incorporate some conservatism, but the scatter and extent of conservatism shown in Figure 53, with required/provided differences of up to 85%, is considerable. The results also suggest that §18.8.5.1 may be appropriate for design of connections like those in the database.

4.4 Evaluation of database against other equations

The compression development length requirements in ACI 318-19 §25.4.9 appear to be considerably, perhaps excessively, conservative for hooked bar development in special moment frame joints. This observation prompts consideration of other equations that might better fit the dataset. Four equations are considered.

4.4.1 Equations Considered

i) Development of hooked bars in tension (ACI 318-14 §25.4.3)

ACI 318-14 [20] had different provisions for hooked bar development than ACI 318-19. Equation (37) is the development length equation for hooked deformed bars in tension from §25.4.3 of ACI 318-14:

$$\ell_{dh,318-14} = \max\left\{ \frac{f_y \psi_e \psi_c \psi_r}{50\lambda\sqrt{f_c'}} \; ; \; 8d_b \; ; \; 6 \text{ in.} \right\} \qquad \text{Eq. (37)}$$

ii) Development of hooked bars in tension (ACI 318-19 §25.4.3)

As stated earlier, Chapter 25 of ACI 318-19 [3] prescribes Eq. (38) for the development length of hooked bars in tension design of frames not designated as special moment frames:

$$\ell_{dh,25.4.3} = \max\left\{ \frac{f_y \psi_e \psi_r \psi_o \psi_c}{50\lambda\sqrt{f_c'}} d_b \; ; \; 8d_b \; ; \; 6\text{in.} \right\} \qquad \text{Eq. (38)}$$

iii) Ajaam et al. [41] descriptive equation

Ajaam et al. [41] reported that the hooked bar provisions in ACI 318-14 assigned inaccurate importance to some variables:

"[…] the current Code provisions overestimate the contribution of the concrete compressive strength and the bar size [to] the anchorage strength of hooked bars." – Ajaam et al. [41]

They proposed the following descriptive equations for the anchorage strength of a single hooked bar, depending on the relative distance to other hooked bars and the presence of transverse reinforcement:

- For widely spaced hooked bars ($c_{ch} \geq 6d_b$):

$$T_h = 294 f_{cm}^{0.295} \ell_{eh}^{1.0845} d_b^{0.47} + 55050 \left(\frac{A_{tt}}{n} \right)^{1.0175} d_b^{0.73}$$

- For closely spaced hooked bars ($c_{ch} < 6d_b$) without transverse reinforcement:

$$T_h = \left(294 f_{cm}^{0.295} \ell_{eh}^{1.0845} d_b^{0.47} \right) \left(0.0974 \frac{c_{ch}}{d_b} + 0.3911 \right)$$

$$\text{with } \left(0.0974 c_{ch}/d_b + 0.3911 \right) \leq 1.0$$

- For closely spaced hooked bars ($c_{ch} < 6d_b$) with transverse reinforcement:

$$T_h = \left(294 f_{cm}^{0.295} \ell_{eh}^{1.0845} d_b^{0.47} + 55050 \left(\frac{A_{tt}}{n} \right)^{1.0175} d_b^{0.73} \right) \left(0.0516 \frac{c_{ch}}{d_b} + 0.6572 \right)$$

$$\text{with} \left(0.0516 c_{ch}/d_b + 0.6572 \right) \leq 1.0$$

Eq. (39)

The embedment length associated with developing the yield stress of the hooked bars, denoted ℓ_{ehy}, can be solved for from Eq. (39) by replacing the anchorage strength T_h by the product

of the measured value of the steel yield stress f_y and the cross-sectional area of the (individual) hooked bar A_b.

- For widely spaced hooked bars ($c_{ch} \geq 6d_b$):

$$\ell_{ehy} = \left[\frac{f_y A_b - 55050\left(\frac{A_{tt}}{n}\right)^{1.0175} d_b^{0.73}}{294 f_{cm}^{0.24} d_b^{0.47}} \right]^{\frac{1}{1.0845}}$$

- For closely spaced hooked bars ($c_{ch} < 6d_b$) without confining reinforcement:

$$\ell_{ehy} = \left[\frac{f_y A_b}{\left(0.0974 \frac{c_{ch}}{d_b} + 0.3911\right)\left(294 f_{cm}^{0.295} d_b^{0.47}\right)} \right]^{\frac{1}{1.0845}} \quad \text{Eq. (40)}$$

$$\text{with } \left(0.0974 c_{ch}/d_b + 0.3911\right) \leq 1.0$$

- For closely spaced hooked bars ($c_{ch} < 6d_b$) with confining reinforcement:

$$\ell_{ehy} = \left[\left(\frac{f_y A_b}{0.0516 \frac{c_{ch}}{d_b} + 0.6572} - 55050\left(\frac{A_{tt}}{n}\right)^{1.0175} d_b^{0.73} \right) \frac{1}{294 f_{cm}^{0.24} d_b^{0.47}} \right]^{\frac{1}{1.0845}}$$

$$\text{with} \left(0.0516 c_{ch}/d_b + 0.6572\right) \leq 1.0$$

iv) ACI 408R-03 [1] Tension Development length with 0.7 reduction factor

The analyses of compression lap splices in Chapter 2 suggest that compression lap splice length can be calculated as a fraction of the tension development length. The fraction differs depending on which tension development equation is used. Here compression development is

taken as 0.7 times the length obtained from the ACI 408R-03 [1] tension development length equation (Eq. (41)). If hooked bars in special moment frame joints should be designed for compression development, then Eq. (41) should be a reasonably good fit with the embedment provided in the beam-column connection database.

$$l_{dc,408} = 0.7 l_{d,408} = 0.7 \frac{\left(\frac{f_y}{\phi\, f_c'^{1/4}} - 2400\omega \right) \alpha\beta\lambda}{76.3 \left(\frac{c\omega + K_{tr,408}}{d_b} \right)} d_b \qquad \text{Eq. (41)}$$

where α, β, and λ are all unitary for this database, and with:

$$\omega = 0.1 \frac{c_{\max}}{c_{\min}} + 0.9 \le 1.25 \; ; \; t_r = 9.6\, R_r + 0.28 \le 1.72 \; ; \; t_d = 0.03\, d_b + 0.22$$

$$K_{tr,408} = \frac{6.26 t_r t_d A_{tr}}{sn} f_c'^{1/2} \; ; \; f_c'^{1/4} \le 11.0 \; ; \; f_y \le 80 \text{ ksi} \; ; \; \phi = 0.82$$

A relative rib area, R_r, of 0.0727 was assumed for all specimens based on recommendations in ACI 408R-03.

Application of Eq. (41) to hooked bars in joints requires some interpretation. For instance, identification of potential splitting planes is not as obvious in a column-beam joint as is may be for longitudinal bars in a column or beam; the definition of splitting plane does not readily apply where breakout anchorage failures occur. To bracket the range of possible outcomes, two cases are considered in these analyses: $K_{tr,408} = 0$, which represents a lack of confining reinforcement, and $(c\omega + K_{tr,408})/d_b = 4$, the upper bound recommended in ACI 408R-03. These two cases bracket the possible required tension development length and, lacking a precise quantification of confinement, both are evaluated for each specimen.

4.4.2 Results

Figures 55 through 59 are analogous to Figures 53 and 54. Each figure shows the development length obtained from a design equation (Eqs. (37), (38), (40), and (41)) plotted versus the provided embedment length. These equations include the ACI 318-14 tension development length for hooked bars, $\ell_{dt,318\text{-}14}$ (Eq. (37)); the tension development length for hooked bars in non-earthquake-resistant construction, $\ell_{dt,25.4.3}$ (Eq. (34)); the embedment length derived from the anchorage strength descriptive equations from Ajaam et al. [41], ℓ_{eyh}, (Eq. (40)); and 0.7 times the ACI 408R-03 tension development length, l_d , (Eq. (41)) plus bend radius and bar diameter with either $K_{tr,408} = 0$ (Case I) or $(c\omega+K_{tr,408})/d_b = 4.0$ (Case II).

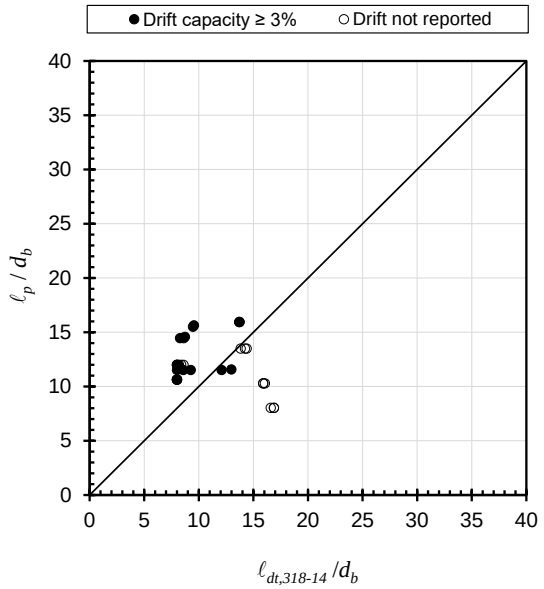

Figure 55 – ℓ_p/d_b versus $\ell_{dt,318\text{-}14}/d_b$

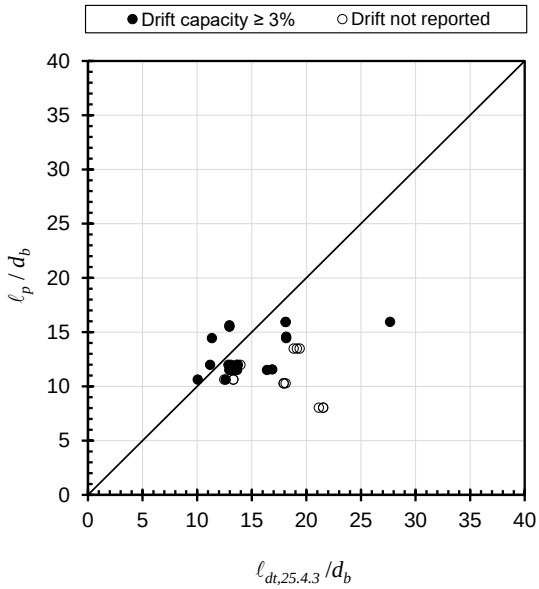

Figure 56 – ℓ_p/d_b versus $\ell_{dt,25.4.3}/d_b$

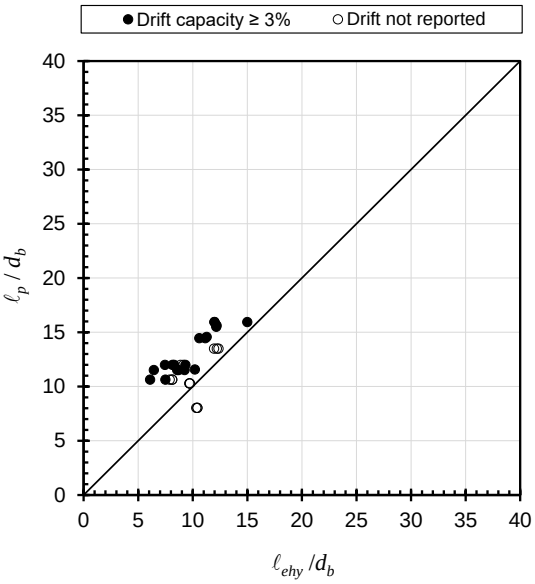

Figure 57 – ℓ_p/d_b versus ℓ_{eyh} (Ajaam et al.)/d_b

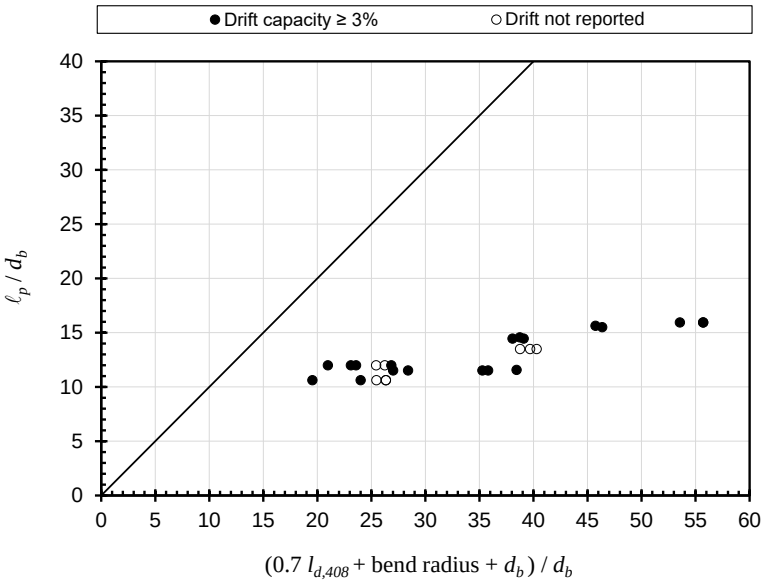

Figure 58 – ℓ_p/d_b versus (0.7l_d [ACI 408R-03 Case I: $K_{tr,408}$ = 0] + bend radius + d_b)/d_b

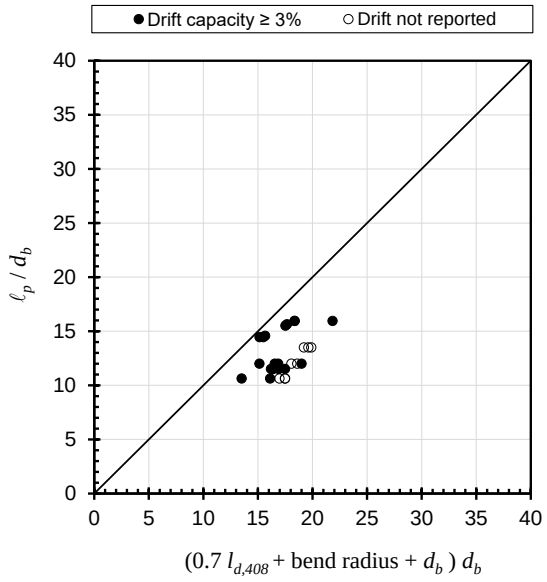

Figure 59 – ℓ_p/d_b versus (0.7l_d [ACI 408R-03 Case II: $(c\omega+K_{tr,408})/d_b$] + bend radius + d_b)= 4.0)/d_b

Since none of the 19 specimens with $\delta_{0.8peak} \geq 3\%$ were reported to have exhibited anchorage failures, it is reasonable to expect that the provided embedment length in those specimens typically exceeded or was close to the required development lengths. That was not the case in Figure 53, which suggests that satisfying ACI 318-19 §25.4.9 is not necessary to obtain adequate joint behavior without evidence of anchorage distress. Except for $0.7\ell_d$ Case I in Figure 19, all of the other equations – including $\ell_{dt,18.8.5.1}$ – perform reasonably well, with specimens with $\delta_{0.8peak} \geq 3\%$ generally having provided embedment lengths that were longer than the calculated value.

The trends in Figure 57 for ℓ_{eyh} stand out among the equations considered, with all specimens having a longer provided length than what is obtained from the equation. This equation is derived from a so-called descriptive equation, which, unlike design equations, has no built-in

safety factors. It should therefore be expected that specimens with no evidence of anchorage failures likely have hooked bar embedment lengths longer than ℓ_{eyh}.

Table 3 provides another way to compare the different length requirements. The value of each cell represents the mean ratio between the length in the row and the length in the column in question. An expanded version of the table with values for all lengths against each other can be found in Appendix H.

Table 3 - Average length ratios: length in row / length in column (all 27 specimens)

	ℓ_p	ℓ_{ehy}
ℓ_p	1	1.34
$\ell_{dh,318\text{-}14}$ [Eq. (39)]	0.75	1.02
$\ell_{dh,25.4.3}$ [Eq. (33)]	1.14	1.56
$\ell_{dc,25.4.9}$ [Eq. (35)] + bend radius + d_b	1.47	2.01
ℓ_{ehy} [Eq. (41)]	0.75	1
$\ell_{dh,18.8.5.1}$ [Eq. (34)]	0.88	1.16
0.7 $l_{d,408}$ Case I [Eq. (42)] + bend radius + d_b	2.53	3.38
0.7 $l_{d,408}$ Case II [Eq. (42)] + bend radius + d_b	1.35	1.78

The middle column of Table 3 shows that $\ell_{dh,25.4.3}$, ($\ell_{dc,25.4.9}$ + bend radius + d_b) and 0.7 $l_{d,408}$ Cases I and II (0.7 $l_{d,408}$ + bend radius + d_b), surpass, on average, the embedment length that was provided in the specimens, with different levels of conservatism. For the database in question, providing the required compression development length by means of ($\ell_{dc,25.4.9}$ + bend radius + d_b) requires, on average, 47% more embedment length than was provided, even though the specimens did not exhibit anchorage distress.

In contrast, the tension development length required by the current ACI Building Code provisions, $\ell_{dh,18.8.5.1}$, and ℓ_{ehy} were, on average, 88% and 75% of the provided embedment lengths

in this database. On average, the specimens therefore satisfied the requirements of Section 18.8.5.1 and exceeded ℓ_{ehy}, which should be expected of specimens that did not exhibit anchorage distress.

The last column of Table 3 provides ratios of calculated lengths versus ℓ_{ehy} obtained from the descriptive equations in Eq. (40). If ℓ_{ehy} is taken as the length necessary to develop hooked bars in SMF joints without a safety factor, ℓ_p / ℓ_{ehy} should generally exceed 1.0 in specimens that did not exhibit bond/anchorage failures. Table 3 shows $\ell_p / \ell_{ehy} = 1.34$ for this dataset. Furthermore, if ℓ_{ehy} is taken as the length necessary to develop hooked bars in SMF joints without a safety factor, the last column of Table 3 shows the extent of the conservatism embedded in various equations considered. ACI 318-19's $\ell_{dh,25.4.3}$ is on average 56% longer than ℓ_{ehy}, while the previous version of the equation, $\ell_{dh,318\text{-}14}$ is on average only 2% longer than ℓ_{ehy}. Table 3 shows that while $\ell_{dh,18.8.5.1}$ requires on average 16% more length than ℓ_{ehy}, ($\ell_{dc,25.4.9}$ + bend radius + d_b) requires more than twice the length of ℓ_{ehy}. This again illustrates how overly conservative the compression development requirement is for hooked bars in SMF joints.

The same analysis can be done for just the specimens with $\delta_{0.8peak} \geq 3\%$. Table 4 is analogous to Table 3 but includes just 19 out of 27 specimens. Again, the compression development length equation is an outlier.

Table 4 - Average length ratios: length in row / length in column (specimens with $\delta_{0.8peak} \geq 3\%$: 19 specimens)

	ℓ_p	ℓ_{ehy}
ℓ_p	1	1.37
$\ell_{dh,318\text{-}14}$ [Eq. (8)]	0.72	1.02
$\ell_{dh,25.4.3}$ [Eq. (1)]	1.10	1.55
$\ell_{dc,25.4.9}$ [Eq. (3)] + bend radius + d_b	1.43	2.01
ℓ_{ehy} [Eq. (10)]	0.73	1
$\ell_{dh,18.8.5.1}$ [Eq. (2)]	0.84	1.14
0.7 $l_{d,408}$ Case I [Eq. (11)] + bend radius + d_b	2.54	3.50
0.7 $l_{d,408}$ Case II [Eq. (11)] + bend radius + d_b	1.28	1.73

4.5 Conclusions

Analyses of the database suggest that the compression development requirement in §18.8.2.2 of ACI 318-19 [3] is excessively conservative for hooked bars in SMF joints. Even though none of the 27 specimens exhibited anchorage failures, none of the specimens satisfied the compression development length requirements in §25.4.9. Furthermore, the requirements in §25.4.9 more than double the lengths obtained from the Ajaam et al. [41] descriptive equation for hooked bar anchorage strength. Satisfying Chapter 25 is therefore not necessary to prevent anchorage failure or obtain adequate behavior in SMF joints.

The analyses suggest that the tension development length requirements in §18.8.5.1 of ACI 318-19 are appropriate for design of specimens like those in the database.

4.6 Notation

a	=	depth of rectangular compression stress block in beam flexure (in.)
A_b	=	cross-sectional area of an individual hooked bar (in.^{2})
A_{hs}	=	total cross-sectional area of hooked bars (in.^{2})
A_j	=	effective cross-sectional area of a joint in a plane parallel to plane of beam reinforcement generating shear in the joint, per ACI 318-19 [3] §R15.4.2 = $b_j \times h_c$ (in.^{2})
$A_{tr,1}$	=	cross-sectional area of a tie leg (in.^{2})
A_{tt}	=	total cross-sectional area of effective confining reinforcement parallel to the hooked bars (in.^{2})
b_b	=	beam width (in.)
b_c	=	column width (in.)
b_j	=	effective joint width (Figure 49) (in.)
c_{max}	=	maximum(c_b ; c_s) (in.)
c_{min}	=	smaller of minimum concrete cover or ½ of the clear spacing between bars (in.)
c_s	=	minimum (c_{so} ; c_{si} + 0.25 in) (in.)
c_{si}	=	½ of the bar clear spacing (in.)
c_{so}	=	side concrete cover for reinforcing bar (in.)
d	=	distance between centroid of beam longitudinal reinforcing bars and extreme compression fiber of beam section (in.)
d_b	=	nominal diameter of a hooked bar (in.)
E_s	=	modulus of elasticity of steel: 29.000 ksi
f_c'	=	measured concrete compressive strength (psi)
f_y	=	measured yield stress of reinforcing steel in tension (ksi)
h_b	=	beam height (in.)

h_c = column height (in.)

$K_{tr,408}$ = transverse reinforcement index according to ACI 408R-03 [1]

n = number of hooked bars in tension

L_b = beam span measured to the center of the column (in.)

L_c = length of column between inflection points (in.)

L_n = clear span of beam (in.)

ℓ_c = compression development length of straight bars or wires, as required by ACI 318-19 [3] §25.4.9 (in.)

ℓ_p = provided embedment length of hooked bars in a specimen, measured from the critical section (face of column), according to the definition of ACI 318-19 [3]

$l_{d,408}$ = development length of straight bars in tension, as required by the recommended provisions by ACI 408R-03 [1], Eq. 4-11a (in.). Originally "l_d" in source.

$\ell_{dh,18.8.5.1}$ = development length of hooked bar in tension ACI 318-19 §18.8.5.1 (in.). Originally "ℓ_{dh}" in source.

$\ell_{dh,18.8.5.1,min}$ = minimum development length of hooked bar in tension according to ACI 318-19 [3] §18.8.5.1 (in.). The greater of $8d_b$ and 6 in. for normal-weight concrete and the greater of $10d_b$ and 7½ in.

$\ell_{dh,25.4.3}$ = development length of hooked bar in tension ACI 318-19 [3] §25.4.3 (in.). Originally "ℓ_{dh}" in source.

$\ell_{dh,318\text{-}14}$ = development length of hooked bar in tension ACI 318-14 [20] §25.4.3 (in.). Originally "ℓ_{dh}" in source.

ℓ_{ehy} = embedment length of a hooked bar associated required to develop its yield

		strength, derived from the anchorage strength descriptive equation by Ajaam et al. [41]
M_n	=	nominal bending moment capacity of the beam cross section at the face of the column, according to ACI 318-19 [3] (kip-in.)
M_{peak}	=	the peak recorded bending moment in the beam at the face of the column in the reversed cyclic loading testing history (kip-in.)
N_{legs}	=	number of legs within a layer of column ties or hoops
R_n	=	coefficient representing whether a transverse beam is present in the calculation of the nominal joint shear V_n, according to ACI 318-19 [3] §15.4.2
s	=	spacing of column hoops or ties (in.)
t_d	=	term representing the effect of bar size on the steel contribution to total bond force
t_r	=	term representing the effect of relative rib area on the steel contribution to total bond force
V_n	=	nominal joint shear strength according to ACI 318-19 [3] §18.8.4 (kip)
V_p	=	horizontal joint shear demand at mid depth of the beam (kip)
T_h	=	anchorage strength of a hooked bar, calculated using the descriptive equation by Ajaam et al. [41]
$\delta_{0.8peak}$	=	the drift ratio when, after reaching the peak load, the load drops to 80% of the peak load
ε_s	=	strain of steel reinforcement
λ	=	lightweight concrete modification factor for the development length of deformed bars and wires in compression (ACI 318-19 [3] §25.4.9) and the development length of hooked bars in tension (ACI 318-19 [3] §25.4.3)
ψ_c	=	concrete strength modification factor for the development length of hooked

bars in tension (ACI 318-19 [3] §25.4.4)

ψ_e = epoxy coating modification factor for the development length of hooked bars in tension (ACI 318-19 [3] §25.4.4 and ACI 318-14 [20] §25.4.4)

$\psi_{o,hook}$ = location modification factor for the development length of hooked bars in tension (ACI 318-19 [3] §25.4.3)

ψ_p = parallel tie reinforcement modification factor for the development length of hooked bars in tension (ACI 318-19 [3] §25.4.4)

ψ_r = confining reinforcement modification factor for the development length of deformed bars and wires in compression (ACI 318-19 §25.4.9)

Chapter 5: Summary and Conclusions

Databases of test results were used to examine ACI 318-19 requirements for three cases related to compression development: compression lap splice length, compression development of headed bars in special moment frame (SMF) joints, and compression development of hooked bars in SMF joints. For each case, the distribution of variables within the database was described and ACI 318-19 requirements were compared against test results using ratios of test/calculated (T/C) bar stress. Comparisons were also made against several alternative equations.

These analyses were motivated by two counterintuitive observations. First, ACI 318-19 equations for compression lap splice length in §25.5.5 can produce calculated lengths that are substantially longer than the length of a Class B tension lap splice (§25.5.2). This is counter to expectations since compression lap splices benefit from end bearing and tension lap splices do not. Second, ACI 318-19 §18.8.2.2 requires that headed and hooked bars in SMF joints be developed in tension in accordance with §18.8.5 and in compression in accordance with §25.4.9. Counter to expectations, the compression requirements in §25.4.9 often produce longer development lengths than required in §18.8.5 for common combinations of variables even though tension development is generally thought to be more critical in joints.

On the basis of the analyses, the following were concluded:

Chapter 2: Compression Lap Splice Length

1. ACI 318-19 equations for compression lap splice length in §25.5.5 were not a good fit to the database of 89 test results, with a mean T/C of 2.58 and a coefficient of variation (CV) of 0.60 (although it must be emphasized that all specimens with $T/C > 2.0$ violated the ACI

318-19 minimum lap splice length). A reason for these outcomes is that §25.5.5 does not account for relevant variables including confinement and concrete compressive strength.

2. Compression lap splice length requirements in §25.5.5 can be improved and simplified by removing Eq. (a) from §25.5.5 and applying Eq. (b) to all design bar stress ranges (Eq. (b) is currently limited to bar stresses greater than 60 ksi). Equation (b) alone has a mean T/C of 1.58 and a CV of 0.16 when compared with the database, although it still omits key variables and can produce design lengths that are longer than the tension development length. Equations proposed by Cairns [13] and Chun, Lee, and Oh [9,12] were also shown to produce more accurate and precise fits to the available data.
3. Six tension development length equations were considered, and all provided a more accurate and precise fit to the dataset than ACI 318-19 §25.5.5. Use of tension development length equations for compression lap splice design would produce more consistent conservatism relative to the database, eliminate the need to calculate both tension and compression development lengths, and prevent design cases where calculated lengths are longer in compression than in tension. A drawback of this approach is that calculated compression lengths would also be longer than currently required for many common design cases.
4. Three methods were considered for making compression lap splice length a function of tension development length without causing excessive conservatism:
    a. Length multiplier, r_1: Compression lap splice length can be defined as r_1 times the tension development length, where $r_1 < 1$. To illustrate the concept, values of r_1 were derived for six tension development length equations to achieve a minimum T/C of 1.0, although other definitions of acceptable reliability might be appropriate.

b. Stress multiplier, r_2: Compression lap splice length can be calculated using tension development length equations, but for a stress of $r_2 f_y$, where $r_2 < 1$. The stress reduction is because some portion of bar force is transferred through end bearing and not bond. To illustrate the concept, values of r_2 were derived for six tension development length equations to achieve a minimum T/C of 1.0, although other definitions of acceptable reliability might be appropriate.

c. Optimized ψ_y: The tension development length equation from Lepage, Yasso and Darwin [16] contains a ψ_y value that was rederived to better fit the compression lap splice database and achieve a minimum T/C of 1.0, although other definitions of acceptable reliability might be appropriate.

Chapter 3: Compression Development of Headed Bars in SMF Joints

1. Satisfying the compression development length requirements of §25.4.9 is not a necessary condition to obtain adequate joint behavior under cyclic loads. None of the 35 beam-column connection specimens considered satisfied §25.4.9, even though all had drift ratio capacities not less than 3% and no reported evidence of anchorage distress. Furthermore, §25.4.9 produced lengths that were, on average, double the lengths obtained from the Ghimire, Darwin, and Lepage [16] descriptive equation for headed bar anchorage strength. ACI 318-19 §18.8.2.2 should not require that headed bars satisfy §25.4.9.
2. Analyses suggest that satisfying the tension development length requirements of §18.8.5.2, which refer to §25.4.4, is also not a necessary condition to obtain adequate joint behavior under cyclic loads. Stated differently, §25.4.4 and thus §18.8.5.2 may be overly conservative for joint design. Only two of the 35 beam-column connection specimens

considered satisfied §18.8.5.2, even though all had drift ratio capacities not less than 3% and no reported evidence of anchorage distress. Furthermore, §18.8.5.2 produced lengths that were, on average, 2.3 times the lengths obtained from the Ghimire, Darwin, and Lepage [6] descriptive equation for headed bar anchorage strength.

3. The equation for headed bar development length from §25.4.4 of ACI 318-14 (without caps on bar grade or concrete compressive strength) and the equation for hooked bar development length in §18.8.5.1 of ACI 318-19 appear more appropriate for design of specimens like those in the database. Each was a more reasonable fit to the database and still conservative relative to the Ghimire, Darwin, and Lepage [6] descriptive equation for headed bar anchorage strength.

Chapter 4: Compression Development of Hooked Bars in SMF Joints

1. Satisfying the compression development length requirements of §25.4.9 is not a necessary condition to obtain adequate joint behavior under cyclic loads. Of the 19 beam-column connection specimens that achieved drift capacities above 3% without evidence of anchorage distress, none satisfied §25.4.9. Furthermore, §25.4.9 produced lengths that were, on average, double the lengths obtained from the Ajaam, Darwin, and O'Reilly [41] descriptive equation for hooked bar anchorage strength. ACI 318-19 §18.8.2.2 should not require that hooked bars satisfy §25.4.9.
2. Results suggest that the tension development length requirements in ACI 318-19 §18.8.5.1 may be adequate for design of hooked bar development in beam-column joints. 15, or 79%, of the 19 specimens with drift capacities above 3% and no evidence of anchorage distress satisfied §18.8.5.1. Furthermore, §18.8.5.1 produced lengths that were, on average, 16%

longer than those obtained from the Ajaam, Darwin, and O'Reilly [41] descriptive equation for hooked bar anchorage strength.

3. The ACI 318-19 §25.4.3 equation for hooked bar development length, which is intended for design of hooked bars outside intermediate and special moment frame joints, may also be overly conservative. 5, or 19%, of the 27 specimens satisfied §25.4.3, which required lengths that were, on average, more than 56% longer than those obtained from the Ajaam, Darwin, and O'Reilly [41] descriptive equation for hooked bar anchorage strength.

Chapter 6: References

1. ACI Committee 408 (2003). *Bond and Development of Straight Reinforcing Bars in Tension (ACI 408R-03),* American Concrete Institute, 49 pp.
2. fib (2014). *Bond and anchorage of embedded reinforcement: Background to the fib Model Code for Concrete Structures 2010,* fib Bulletin No. 72, 170 pp.
3. ACI Committee 318 (2019). *Building Code Requirements for Structural Concrete (ACI 318-19) and Commentary (ACI 318R-19),* American Concrete Institute, Farmington Hills, MI, 628 pp.
4. ACI Committee 408 (2021). *Compression Lap Splice Database*, American Concrete Institute, Farmington Hills, MI. [Available from ACI Store at concrete.org]
5. Kang, T. H.-K., Shin, M., Mitra, N., and Bonacci, J. F., (2009). "Seismic Design of Reinforced Concrete Beam-Column Joints with Headed Bars." *ACI Structural Journal*, Vol. 106: pp. 868-877.
6. Ghimire, K. P., Darwin, D., and Lepage, A., (2021). "Headed Bars in Beam-Column Joints Subjected to Reversed Cyclic Loading." *ACI Structural Journal* Vol. 118: pp. 27-33.
7. Pfister, J. F., and Mattock, A. H., (1963). “High Strength Bars as Concrete Reinforcement, Part 5. Lapped Splices in Concentrically Loaded Columns,” *Journal of the Portland Cement Association Research and Development Laboratories*, Development Department, 5(2), 27-40.
8. Chun, S. C., Lee, S. H., and Oh, B., (2010). “Compression Lap Splice in Unconfined Concrete of 40 and 60 MPa (5800 and 8700 psi) Compressive Strengths,” *ACI Structural Journal*, 107(2), 170-178.

9. Chun, S. C., Lee, S. H., and Oh, B., (2010). “Compression Lap Splice in Confined Concrete of 40 and 60 MPa (5800 and 8700 psi) Compressive Strengths,” *ACI Structural Journal*, 107(4), 476-485.
10. Chun, S. C., Lee, S. H., and Oh, B., (2011). “Compression Splices in High-Strength Concrete of 100 MPa (14,500 psi) and Less,” *ACI Structural Journal*, 108(6), 715-724.
11. Reineck, K. H., Kuchma, D. A., Kim, K. S., and Marx, S., (2003). “Shear Database for Reinforced Concrete Members without Shear Reinforcement,” *ACI Structural Journal*, 100(2), 240-249.
12. Chun, S. C., Lee, S. H., and Oh, B., (2010). “Simplified Design Equation of Lap Splice Length in Compression,” *International Journal of Concrete Structures and Materials*, 4(1), 63-68.
13. Cairns, J. W., (1985). “Strength of Compression Splices: A Reevaluation of Test Data,” *ACI Structural Journal*, 82(4), pp. 510-516.
14. Cairns, J. W. and Arthur, P. D., (1979). “Strength of Lapped Splices in Reinforced Concrete Columns.”, *ACI Journal*, pp. 277-296
15. fib MC2010, (2013). *fib Model Code for Concrete Structures 2010*, Ernst & Sohn, 434 pp.
16. Lepage, A., Yasso, S., and Darwin, D., (2020). *Recommended Provisions and Commentary on Development Length for High-Strength Reinforcement in Tension*, Structural Engineering and Engineering Materials, SL Report 20-2.
17. Darwin, D., Lutz, L. A., and Zuo, J., (2005). “Recommended Provisions and Commentary on Development and Lap Splice Lengths for Deformed Reinforcing Bars in Tension,” *ACI Structural Journal*, 102(6), 892-900.

18. Canbay, E., and Frosch, R. J., (2006). “Design of Lap-Spliced Bars: Is Simplification Possible?”, *ACI Structural Journal*, 103(3), 444-451.
19. Frosch, R., Fleet, E., and Glucksman, R., (2020). *Development and Splice Lengths for High-Strength Reinforcement Volume I: General Bar Development*, Lyles School of Civil Engineering, Purdue University, 358 pp.
20. ACI Committee 318 (2014). *Building Code Requirements for Structural Concrete (ACI 318-14) and Commentary (ACI 318R-14),* American Concrete Institute, Farmington Hills, MI, 520 pp.
21. Adachi, M., and Kiyoshi, M., (2007). "The Effect of Orthogonal Beams on Ultimate Strength or R/C Exterior Beam-Column Joint using Mechanical Anchorages." *Proceeding of the Architectural Institute of Japan*, Tokyo, Japan, pp. 633-634.
22. Bashandy, T. R., (1996). *Application of Headed Bars in Concrete Members*, PhD dissertation, University of Texas at Austin, Austin, TX, 303 pp.
23. Chun, S. C., Lee, S. H., Kang, T. H.-K., Oh, B., and Wallace, J. W., (2007). "Mechanical Anchorage in Exterior Beam-Column Joints Subjected to Cyclic Loading", *ACI Structural Journal*, Vol. 104. 12 pp.
24. Ishida, Y., Fujiwara, A., Adachi, T., Matsui, T., and Kuramoto, H., (2007). "Structural Performance of Exterior Beam-Column Joint with Wide Width Beam Using Headed Bars - Part 1: Outline of test and failure Modes and Part 2: Test Result and Discussion." *Proceedings of the Architectural Institute of Japan*. Tokyo, Japan. pp. 657-660.
25. Kang, T. H.-K., Ha, S.-S., and Choi, D.-U., (2008). "Seismic Assessment of Beam-to-Column Interaction Utilizing Headed Bars." *Proceedings of the 14th World Conference on Earthquake Engineering*. Beijing, China. 8 pp.

26. Kato, T., (2005). "Mechanical Anchorage Using Anchor Plate for Beam/Column Joints of R/C Frames - Part 2: Pull-Out Behavior and Structural Behavior of T-Shaped Frame Using Frictional Anchor Plate." *Proceedings of the Architectural Institute of Japan*. Tokyo, Japan. 277-278.

27. Lee, H.-J., and Yu, S.-Y., (2009). "Cyclic Response of Exterior Beam-Column Joints with Different Anchorage Methods." *ACI Structural Journal*, Vol. 106: pp. 329-339.

28. Matsushima, M., Kuramoto, H., Meada, M., Kenta, S., and Ozone, S., (2000). "Test on Corner Beam-Column Joint under Tri-Axial Loadings - Outline for Test: Study on Structural Performance of Mechanical Anchorage (No. 10); Discussion of Test Results: Study on Structural Performance of Mechanical Anchorage (No. 11)." *Proceedings of the Architectural Institute of Japan*. Tokyo, Japan. pp. 861-864.

29. Murakami, M., Fuji, T., and Kubota, T., (1998). "Failure Behavior of External Beam-Column Joints with Mechanical Anchorage in Subassemblage Frames." *Concrete Research and Technology*, Vol. 9 (1).

30. Takeuchi, H., Hattori, S., Nakamura, K., Hosoya, H., and Ichikawa, M., (2001). "Development of Mechanical Anchorage using Circular Anchor Plate - Part 3: Outline of Exterior Beam-Joint Test and Experimental Results and Part 4: Experimental Results and Discussion of Exterior Beam-Column Joint Test." *Proceedings of the Architectural Institute of Japan*. Tokyo, Japan. pp. 111-114.

31. Tazaki, W., Kusuhara, F., and Shiohara, H., (2007). "Tests of R/C Beam-Column Joints with Irregular Details on Anchorage of Beam Longitudinal Bars (Part 1: Outline of Tests and Part 2: Test Results and Discussions)." *Proceedings of the Architectural Institute of Japan*. Tokyo, Japan. pp. 653-660.

32. Wallace, J. W., McConnell, S. W., Gupta, P., and Cote, P. A., (1998). "Use of Headed Reinforcement in Beam-Column Joints Subjected to Earthquake Loads." *ACI Structural Journal*, Vol. 95: pp. 590-602.

33. Yoshida, J., Ishibashi, K., and Nakamura, K., (2000). "Experimental Study on Mechanical Anchorage Using Bolt and Nut in Exterior Beam-Column Joint - Part 1: Specimens and Outline of Experiment and Part 2: Analysis of Experiment." *Proceedings of the Architectural Institute of Japan*. Tokyo, Japan. pp. 635-638.

34. ACI Committee 352 (2010). *Recommendations for Design of Beam-Column Connections in Monolithic Reinforced Concrete Structures (ACI 352R-02)*, American Concrete Institute, Farmington Hills, MI, 42 pp.

35. Hanson, N. W., (1971). "Seismic Resistance of Concrete Frames with Grade 60 Reinforcement." *ASCE Journal of the Structural Division*, Vol. 97, pp. 1685-1700.

36. Uzumeri, S. M., (1977). "Strength and Ductility of Cast-in-Place Beam-Column Joints". *Reinforced Concrete Structures in Seismic Zones*, ACI Symposium Publication, Vol. 52, pp. 293-350

37. Scribner, C. F., and Wight, J. K., (1978). *Delaying Shear Strength Decay in Reinforced Concrete Flexural Members under Large Load Reversals*. Report UMEE 78R2. The University of Michigan. 246 pp.

38. Ehsani, M. R., and Alameddine, F., (1991). "Design Recommendations of Type 2 High-Strength Reinforced Concrete Connections." *ACI Structural Journal*. 88-S30. 15 pp.

39. Kurose, Y., Guimaraes, G. N., Zuhua, L. M., Kreger, M. E., Jirsa, J. O., (1991). "Evaluation of Slab-Beam-Column Connections Subjected to Bidirectional Loading". ACI Symposium Publication, Vol. 123, pp. 39-67.

40. Hwang, S.-J, Lee, H.-J., Liao, T.-F., Wang, K.-C, and Tsai, H.-H., (2005). “Role of Hoops on Shear Strength of Reinforced Concrete Beam-Column Joints” *ACI Structural Journal*.

41. Ajaam, A., Darwin, D., and O´Reilly, M., (2017). *Anchorage Strength of Reinforcing Bars with Standard Hooks*,. Structural Engineering and Engineering Materials. SM Report No. 125. 372 pp.

Appendix A: Summary of Lap Splice Database

[1]	[2]	[3]	[4]	[5]	[6]	[7]	[8]
Authors	I.D	Concrete test specimen	f_{cm} (psi)	$f_{1c,mod}$ (ksi)	f_y (ksi)	f_{su} (ksi)	f_{yt} (ksi)
Pfister and Mattock [7]	4B	6x12 in.	3715	3.72	86.0	-	58.5
	5B	6x12 in.	4140	4.14	86.0	-	58.5
	6B	6x12 in.	3950	3.95	86.0	-	58.5
	5B1	6x12 in.	4190	4.19	80.0	-	58.5
	6B1	6x12 in.	3640	3.64	80.0	-	58.5
	$4A^+$	6x12 in.	3530	3.53	88.0	-	62.0
	$5A^+$	6x12 in.	3530	3.53	88.0	-	62.0
	$6A^+$	6x12 in.	3510	3.51	88.0	-	62.0
	$7A^+$	6x12 in.	3510	3.51	88.0	-	62.0
Chun, Lee, and Oh [8]	C40D22-S.75-L10-HO	3.9x7.9 in.	7085	6.86	74.5	89.6	-
	C40D22-S.75-L10-HO-1	3.9x7.9 in.	7085	6.86	74.5	89.6	-
	C40D22-S.75-L15	3.9x7.9 in.	7085	6.86	74.5	89.6	-
	C40D22-S.75-L15-1	3.9x7.9 in.	7085	6.86	74.5	89.6	-
	C40D22-S1.25-L10-H0-1	3.9x7.9 in.	7085	6.86	74.5	89.6	-
	C40D22-S1.25-L15-HO	3.9x7.9 in.	7085	6.86	74.5	89.6	-
	C40D22-S1.25-L15-HO-1	3.9x7.9 in.	7085	6.86	74.5	89.6	-
	C40D22-S1.25-L20-HO-1	3.9x7.9 in.	7085	6.86	74.5	89.6	-
	C40D22-S1.5-L10-H0	3.9x7.9 in.	7085	6.86	74.5	89.6	-
	C40D22-S1.5-L10-H0-1	3.9x7.9 in.	7085	6.86	74.5	89.6	-
	C40D22-S1.5-L15-H0	3.9x7.9 in.	7085	6.86	74.5	89.6	-
	C40D22-S1.5-L15-H0-1	3.9x7.9 in.	7085	6.86	74.5	89.6	-
	C60D22-S.75-L10-HO	3.9x7.9 in.	10181	9.86	74.5	89.6	-
	C60D22-S.75-L10-HO-1	3.9x7.9 in.	10152	9.83	74.5	89.6	-
	C60D22-S1.25-L10-H0	3.9x7.9 in.	10174	9.85	74.5	89.6	-
	C60D22-S1.25-L10-H0-1	3.9x7.9 in.	10142	9.82	74.5	89.6	-
	C60D22-S1.25-L15-HO-1	3.9x7.9 in.	10142	9.82	74.5	89.6	-
	C60D22-S1.5-L10-H0	3.9x7.9 in.	9938	9.62	74.5	89.6	-
	C60D22-S1.5-L10-H0-1	3.9x7.9 in.	10131	9.81	74.5	89.6	-
	C60D22-S1.5-L15-1	3.9x7.9 in.	10360	10.03	74.5	89.6	-
	C40D29-S.75-L10-HO-1	3.9x7.9 in.	9358	9.06	68.4	87.3	-
	C40D29-S.75-L15-1	3.9x7.9 in.	9337	9.04	68.4	87.3	-
	C40D29-S.75-L20	3.9x7.9 in.	8185	7.93	68.4	87.3	-
	C60D29-S.75-L10-HO	3.9x7.9 in.	10425	10.10	68.4	87.3	-
	C60D29-S.75-L10-HO-1	3.9x7.9 in.	10686	10.35	68.4	87.3	-
	C60D29-S1.25-L10-H0	3.9x7.9 in.	10654	10.32	68.4	87.3	-
Chun, Lee, and Oh [9]	C40D22-S.75-L10-HE	3.9x7.9 in.	7085	6.86	74.5	89.6	60
	C40D22-S.75-L10-HE-1	3.9x7.9 in.	7085	6.86	74.5	89.6	60
	C40D22-S.75-L10-HW	3.9x7.9 in.	7085	6.86	74.5	89.6	60
	C40D22-S.75-L10-HW-1	3.9x7.9 in.	7085	6.86	74.5	89.6	60
	C40D22-S1.25-L10-HE	3.9x7.9 in.	7085	6.86	74.5	89.6	60
	C40D22-S1.25-L10-HE-1	3.9x7.9 in.	7085	6.86	74.5	89.6	60
	C40D22-S1.25-L10-HW	3.9x7.9 in.	7085	6.86	74.5	89.6	60
	C40D22-S1.25-L10-HW-1	3.9x7.9 in.	7085	6.86	74.5	89.6	60
	C40D22-S1.5-L10-HE	3.9x7.9 in.	7085	6.86	74.5	89.6	60
	C40D22-S1.5-L10-HE-1	3.9x7.9 in.	7085	6.86	74.5	89.6	60

[1]	[2]	[3]	[4]	[5]	[6]	[7]	[8]
Authors	I.D	Concrete test specimen	f_{cm} (psi)	$f_{1c,mod}$ (ksi)	f_y (ksi)	f_{su} (ksi)	f_{yt} (ksi)
Chun, Lee, and Oh [9] (cont'd)	C40D22-S1.5-L10-HW	3.9x7.9 in.	7085	6.86	74.5	89.6	60
	C40D22-S1.5-L10-HW-1	3.9x7.9 in.	7085	6.86	74.5	89.6	60
	C60D22-S.75-L10-HE	3.9x7.9 in.	10177	9.86	74.5	89.6	60
	C60D22-S.75-L10-HE-1	3.9x7.9 in.	10152	9.83	74.5	89.6	60
	C60D22-S1.25-L10-HE	3.9x7.9 in.	10170	9.85	74.5	89.6	60
	C60D22-S1.25-L10-HE-1	3.9x7.9 in.	10145	9.83	74.5	89.6	60
	C40D29-S.75-L10-HE	3.9x7.9 in.	7892	7.64	68.4	87.3	60
	C40D29-S.75-L10-HW-1	3.9x7.9 in.	9358	9.06	68.4	87.3	60
	C60D29-S.75-L10-HE-1	3.9x7.9 in.	10686	10.35	68.4	87.3	60
Chun, Lee, and Oh [10]	C80D22-L4	3.9x7.9 in.	12096	11.71	67.8	87.5	-
	C80D22-L4-1	3.9x7.9 in.	12259	11.87	67.8	87.5	-
	C80D22-L4-2	3.9x7.9 in.	11592	11.23	67.8	87.5	-
	C80D22-L4-3	3.9x7.9 in.	11709	11.34	67.8	87.5	-
	C80D22-L7	3.9x7.9 in.	12111	11.73	67.8	87.5	-
	C80D22-L7-1	3.9x7.9 in.	12340	11.95	67.8	87.5	-
	C80D22-L7-2	3.9x7.9 in.	11511	11.15	67.8	87.5	-
	C80D22-L7-3	3.9x7.9 in.	11606	11.24	67.8	87.5	-
	C80D22-L10	3.9x7.9 in.	12259	11.87	67.8	87.5	-
	C80D22-L10-1	3.9x7.9 in.	12247	11.86	67.8	87.5	-
	C80D22-L10-3	3.9x7.9 in.	11645	11.28	67.8	87.5	-
	C80D29-L4	3.9x7.9 in.	12542	12.15	71.3	90.2	-
	C80D29-L4-1	3.9x7.9 in.	12876	12.47	71.3	90.2	-
	C80D29-L4-2	3.9x7.9 in.	11888	11.51	71.3	90.2	-
	C80D29-L4-3	3.9x7.9 in.	11865	11.49	71.3	90.2	-
	C80D29-L7	3.9x7.9 in.	12502	12.11	71.3	90.2	-
	C80D29-L7-2	3.9x7.9 in.	11770	11.40	71.3	90.2	-
	C80D29-L7-3	3.9x7.9 in.	11818	11.44	71.3	90.2	-
	C80D29-L10	3.9x7.9 in.	12917	12.51	71.3	90.2	-
	C80D29-L10-2	3.9x7.9 in.	11794	11.42	71.3	90.2	-
	C100D29-L4-1	3.9x7.9 in.	14660	14.20	66.5	87.6	-
	C80D22-L4-HW	3.9x7.9 in.	12352	11.96	67.8	87.5	60
	C80D22-L4-HW-1	3.9x7.9 in.	12318	11.93	67.8	87.5	60
	C80D22-L4-HW-2	3.9x7.9 in.	11454	11.09	67.8	87.5	60
	C80D22-L4-HW-3	3.9x7.9 in.	11696	11.33	67.8	87.5	60
	C80D22-L7-HW-1	3.9x7.9 in.	12329	11.94	67.8	87.5	60
	C80D22-L7-HW-2	3.9x7.9 in.	11592	11.23	67.8	87.5	60
	C80D29-L4-HW	3.9x7.9 in.	12818	12.41	71.3	90.2	60
	C80D29-L4-HW-1	3.9x7.9 in.	12471	12.08	71.3	90.2	60
	C80D29-L4-HW-2	3.9x7.9 in.	12312	11.92	71.3	90.2	60
	C80D29-L4-HW-3	3.9x7.9 in.	12219	11.83	71.3	90.2	60
	C80D29-L7-HW	3.9x7.9 in.	12892	12.49	71.3	90.2	60
	C80D29-L7-HW-3	3.9x7.9 in.	12321	11.93	71.3	90.2	60
	C100D29-L4-HW	3.9x7.9 in.	14394	13.94	66.5	87.6	60
	C100D29-L4-HW-1	3.9x7.9 in.	14550	14.09	66.5	87.6	60

[1]	[2]	[9]	[10]	[11]	[12]	[13]	[14]	[15]	[16]
Authors	I.D	Section	b (in.)	h (in.)	b/h	d_b (in.)	A_b (in.^{2})	Symm. Reinf.	l_s (in.)
Pfister and Mattock [7]	4B	R	12.0	10.0	1.20	1.00	0.79	yes	10.0
	5B	R	12.0	10.0	1.20	1.00	0.79	yes	20.0
	6B	R	12.0	10.0	1.20	1.00	0.79	yes	30.0
	5B1	R	12.0	10.0	1.20	1.00	0.79	yes	20.0
	6B1	R	12.0	10.0	1.20	1.00	0.79	yes	30.0
	4A$^+$	C	12.0	-	1.00	1.00	0.79	yes	5.00
	5A$^+$	C	12.0	-	1.00	1.00	0.79	yes	10.0
	6A$^+$	C	12.0	-	1.00	1.00	0.79	yes	20.0
	7A$^+$	C	12.0	-	1.00	1.00	0.79	yes	30.0
Chun, Lee, and Oh [8]	C40D22-S.75-L10-HO	R	7.4	10.5	1.41	0.88	0.60	yes	8.7
	C40D22-S.75-L10-HO-1	R	7.4	10.5	1.41	0.88	0.60	yes	8.7
	C40D22-S.75-L15	R	7.4	10.5	1.41	0.88	0.60	yes	13.0
	C40D22-S.75-L15-1	R	7.4	10.5	1.41	0.88	0.60	yes	13.0
	C40D22-S1.25-L10-H0-1	R	8.3	10.5	1.26	0.88	0.60	yes	8.7
	C40D22-S1.25-L15-HO	R	8.3	10.5	1.26	0.88	0.60	yes	13.0
	C40D22-S1.25-L15-HO-1	R	8.3	10.5	1.26	0.88	0.60	yes	13.0
	C40D22-S1.25-L20-HO-1	R	8.3	10.5	1.26	0.88	0.60	yes	17.3
	C40D22-S1.5-L10-H0	R	8.8	10.5	1.20	0.88	0.60	yes	8.7
	C40D22-S1.5-L10-H0-1	R	8.8	10.5	1.20	0.88	0.60	yes	8.7
	C40D22-S1.5-L15-H0	R	8.8	10.5	1.20	0.88	0.60	yes	13.0
	C40D22-S1.5-L15-H0-1	R	8.8	10.5	1.20	0.88	0.60	yes	13.0
	C60D22-S.75-L10-HO	R	7.4	10.5	1.41	0.88	0.60	yes	8.7
	C60D22-S.75-L10-HO-1	R	7.4	10.5	1.41	0.88	0.60	yes	8.7
	C60D22-S1.25-L10-H0	R	8.3	10.5	1.26	0.88	0.60	yes	8.7
	C60D22-S1.25-L10-H0-1	R	8.3	10.5	1.26	0.88	0.60	yes	8.7
	C60D22-S1.25-L15-HO-1	R	8.3	10.5	1.26	0.88	0.60	yes	13.0
	C60D22-S1.5-L10-H0	R	8.8	10.5	1.20	0.88	0.60	yes	8.7
	C60D22-S1.5-L10-H0-1	R	8.8	10.5	1.20	0.88	0.60	yes	8.7
	C60D22-S1.5-L15-1	R	8.8	10.5	1.20	0.88	0.60	yes	13.0
	C40D29-S.75-L10-HO-1	R	9.6	9.0	1.06	1.13	1.00	no	11.4
	C40D29-S.75-L15-1	R	9.6	9.0	1.06	1.13	1.00	no	17.1
	C40D29-S.75-L20	R	9.6	9.0	1.06	1.13	1.00	no	22.8
	C60D29-S.75-L10-HO	R	9.6	9.0	1.06	1.13	1.00	no	11.4
	C60D29-S.75-L10-HO-1	R	9.6	9.0	1.06	1.13	1.00	no	11.4
	C60D29-S1.25-L10-H0	R	10.7	9.0	1.19	1.13	1.00	no	11.4
Chun, Lee, and Oh [9]	C40D22-S.75-L10-HE	R	7.4	10.5	1.41	0.88	0.60	yes	8.7
	C40D22-S.75-L10-HE-1	R	7.4	10.5	1.41	0.88	0.60	yes	8.7
	C40D22-S.75-L10-HW	R	7.4	10.5	1.41	0.88	0.60	yes	8.7
	C40D22-S.75-L10-HW-1	R	7.4	10.5	1.41	0.88	0.60	yes	8.7
	C40D22-S1.25-L10-HE	R	8.3	10.5	1.26	0.88	0.60	yes	8.7
	C40D22-S1.25-L10-HE-1	R	8.3	10.5	1.26	0.88	0.60	yes	8.7
	C40D22-S1.25-L10-HW	R	8.3	10.5	1.26	0.88	0.60	yes	8.7
	C40D22-S1.25-L10-HW-1	R	8.3	10.5	1.26	0.88	0.60	yes	8.7
	C40D22-S1.5-L10-HE	R	8.8	10.5	1.20	0.88	0.60	yes	8.7
	C40D22-S1.5-L10-HE-1	R	8.8	10.5	1.20	0.88	0.60	yes	8.7

Section: R= rectangular; C =circular. “Symm. Reinf.” = Symmetric Reinforcement.

[1]	[2]	[9]	[10]	[11]	[12]	[13]	[14]	[15]	[16]
Authors	I.D	Section	b (in.)	h (in.)	b/h	d_b (in.)	A_b (in.^{2})	Symm. Reinf.	l_s (in.)
Chun, Lee, and Oh [9] (cont'd)	C40D22-S1.5-L10-HW	R	8.8	10.5	1.20	0.88	0.60	yes	8.7
	C40D22-S1.5-L10-HW-1	R	8.8	10.5	1.20	0.88	0.60	yes	8.7
	C60D22-S.75-L10-HE	R	7.4	10.5	1.41	0.88	0.60	yes	8.7
	C60D22-S.75-L10-HE-1	R	7.4	10.5	1.41	0.88	0.60	yes	8.7
	C60D22-S1.25-L10-HE	R	8.3	10.5	1.26	0.88	0.60	yes	8.7
	C60D22-S1.25-L10-HE-1	R	8.3	10.5	1.26	0.88	0.60	yes	8.7
	C40D29-S.75-L10-HE	R	9.6	9.0	1.06	1.13	1.00	no	11.4
	C40D29-S.75-L10-HW-1	R	9.6	9.0	1.06	1.13	1.00	no	11.4
	C60D29-S.75-L10-HE-1	R	9.6	9.0	1.06	1.13	1.00	no	11.4
Chun, Lee, and Oh [10]	C80D22-L4	R	7.4	10.5	1.41	0.88	0.60	yes	3.5
	C80D22-L4-1	R	7.4	10.5	1.41	0.88	0.60	yes	3.5
	C80D22-L4-2	R	7.4	10.5	1.41	0.88	0.60	yes	3.5
	C80D22-L4-3	R	7.4	10.5	1.41	0.88	0.60	yes	3.5
	C80D22-L7	R	7.4	10.5	1.41	0.88	0.60	yes	6.1
	C80D22-L7-1	R	7.4	10.5	1.41	0.88	0.60	yes	6.1
	C80D22-L7-2	R	7.4	10.5	1.41	0.88	0.60	yes	6.1
	C80D22-L7-3	R	7.4	10.5	1.41	0.88	0.60	yes	6.1
	C80D22-L10	R	7.4	10.5	1.41	0.88	0.60	yes	8.7
	C80D22-L10-1	R	7.4	10.5	1.41	0.88	0.60	yes	8.7
	C80D22-L10-3	R	7.4	10.5	1.41	0.88	0.60	yes	8.7
	C80D29-L4	R	9.6	13.5	1.41	1.13	1.00	yes	4.6
	C80D29-L4-1	R	9.6	13.5	1.41	1.13	1.00	yes	4.6
	C80D29-L4-2	R	9.6	13.5	1.41	1.13	1.00	yes	4.6
	C80D29-L4-3	R	9.6	13.5	1.41	1.13	1.00	yes	4.6
	C80D29-L7	R	9.6	13.5	1.41	1.13	1.00	yes	8.0
	C80D29-L7-2	R	9.6	13.5	1.41	1.13	1.00	yes	8.0
	C80D29-L7-3	R	9.6	13.5	1.41	1.13	1.00	yes	8.0
	C80D29-L10	R	9.6	13.5	1.41	1.13	1.00	yes	11.4
	C80D29-L10-2	R	9.6	13.5	1.41	1.13	1.00	yes	11.4
	C100D29-L4-1	R	9.6	13.5	1.41	1.13	1.00	yes	4.6
	C80D22-L4-HW	R	7.4	10.5	1.41	0.88	0.60	yes	3.5
	C80D22-L4-HW-1	R	7.4	10.5	1.41	0.88	0.60	yes	3.5
	C80D22-L4-HW-2	R	7.4	10.5	1.41	0.88	0.60	yes	3.5
	C80D22-L4-HW-3	R	7.4	10.5	1.41	0.88	0.60	yes	3.5
	C80D22-L7-HW-1	R	7.4	10.5	1.41	0.88	0.60	yes	6.1
	C80D22-L7-HW-2	R	7.4	10.5	1.41	0.88	0.60	yes	6.1
	C80D29-L4-HW	R	9.6	13.5	1.41	1.13	1.00	yes	4.6
	C80D29-L4-HW-1	R	9.6	13.5	1.41	1.13	1.00	yes	4.6
	C80D29-L4-HW-2	R	9.6	13.5	1.41	1.13	1.00	yes	4.6
	C80D29-L4-HW-3	R	9.6	13.5	1.41	1.13	1.00	yes	4.6
	C80D29-L7-HW	R	9.6	13.5	1.41	1.13	1.00	yes	8.0
	C80D29-L7-HW-3	R	9.6	13.5	1.41	1.13	1.00	yes	8.0
	C100D29-L4-HW	R	9.6	13.5	1.41	1.13	1.00	yes	4.6
	C100D29-L4-HW-1	R	9.6	13.5	1.41	1.13	1.00	yes	4.6

Section: R= rectangular; C =circular. “Symm. Reinf.” = Symmetric Reinforcement.

[1]	[2]	[3]	[4]	[5]	[6]	[7]	[8]	[9]	[10]	[11]
Authors	I.D	l_s/d_b	N_b	n	R_r	d_{tr} (in.)	A_t (in.^{2})	c_{so} (in.)	c_{si} (in.)	c_b (in.)
Pfister and Mattock [7]	4B	10.0	6	3	0.073	0.25	0.05	1.75	0.63	1.75
	5B	20.0	6	3	0.073	0.25	0.05	1.75	0.63	1.75
	6B	30.0	6	3	0.073	0.25	0.05	1.75	0.63	1.75
	5B1	20.0	6	3	0.073	0.25	0.05	1.75	0.63	1.75
	6B1	30.0	6	3	0.073	0.25	0.05	1.75	0.63	1.75
	$4A^+$	5.00	6	1	0.073	0.25	0.05	1.25	1.18	1.25
	$5A^+$	10.0	6	1	0.073	0.25	0.05	1.25	1.18	1.25
	$6A^+$	20.0	6	1	0.073	0.25	0.05	1.25	1.18	1.25
	$7A^+$	30.0	6	1	0.073	0.25	0.05	1.25	1.18	1.25
Chun, Lee, and Oh [8]	C40D22-S.75-L10-HO	9.9	4	2	0.10	-	-	1.31	0.66	2.19
	C40D22-S.75-L10-HO-1	9.9	4	2	0.10	-	-	1.31	0.66	2.19
	C40D22-S.75-L15	14.8	4	2	0.10	-	-	1.31	0.66	2.19
	C40D22-S.75-L15-1	14.8	4	2	0.10	-	-	1.31	0.66	2.19
	C40D22-S1.25-L10-H0-1	9.9	4	2	0.10	-	-	1.31	1.09	2.19
	C40D22-S1.25-L15-HO	14.8	4	2	0.10	-	-	1.31	1.09	2.19
	C40D22-S1.25-L15-HO-1	14.8	4	2	0.10	-	-	1.31	1.09	2.19
	C40D22-S1.25-L20-HO-1	19.8	4	2	0.10	-	-	1.31	1.09	2.19
	C40D22-S1.5-L10-H0	9.9	4	2	0.10	-	-	1.31	1.31	2.19
	C40D22-S1.5-L10-H0-1	9.9	4	2	0.10	-	-	1.31	1.31	2.19
	C40D22-S1.5-L15-H0	14.8	4	2	0.10	-	-	1.31	1.31	2.19
	C40D22-S1.5-L15-H0-1	14.8	4	2	0.10	-	-	1.31	1.31	2.19
	C60D22-S.75-L10-HO	9.9	4	2	0.10	-	-	1.31	0.66	2.19
	C60D22-S.75-L10-HO-1	9.9	4	2	0.10	-	-	1.31	0.66	2.19
	C60D22-S1.25-L10-H0	9.9	4	2	0.10	-	-	1.31	1.09	2.19
	C60D22-S1.25-L10-H0-1	9.9	4	2	0.10	-	-	1.31	1.09	2.19
	C60D22-S1.25-L15-HO-1	14.8	4	2	0.10	-	-	1.31	1.09	2.19
	C60D22-S1.5-L10-H0	9.9	4	2	0.10	-	-	1.31	1.31	2.19
	C60D22-S1.5-L10-H0-1	9.9	4	2	0.10	-	-	1.31	1.31	2.19
	C60D22-S1.5-L15-1	14.8	4	2	0.10	-	-	1.31	1.31	2.19
	C40D29-S.75-L10-HO-1	10.1	2	2	0.10	-	-	1.69	0.85	2.82
	C40D29-S.75-L15-1	15.2	2	2	0.10	-	-	1.69	0.85	2.82
	C40D29-S.75-L20	20.2	2	2	0.10	-	-	1.69	0.85	2.82
	C60D29-S.75-L10-HO	10.1	2	2	0.10	-	-	1.69	0.85	2.82
	C60D29-S.75-L10-HO-1	10.1	2	2	0.10	-	-	1.69	0.85	2.82
	C60D29-S1.25-L10-H0	10.1	2	2	0.10	-	-	1.69	1.41	2.82
Chun, Lee, and Oh [9]	C40D22-S.75-L10-HE	9.9	4	2	0.10	0.375	0.11	1.31	0.66	2.19
	C40D22-S.75-L10-HE-1	9.9	4	2	0.10	0.375	0.11	1.31	0.66	2.19
	C40D22-S.75-L10-HW	9.9	4	2	0.10	0.375	0.11	1.31	0.66	2.19
	C40D22-S.75-L10-HW-1	9.9	4	2	0.10	0.375	0.11	1.31	0.66	2.19
	C40D22-S1.25-L10-HE	9.9	4	2	0.10	0.375	0.11	1.31	1.09	2.19
	C40D22-S1.25-L10-HE-1	9.9	4	2	0.10	0.375	0.11	1.31	1.09	2.19
	C40D22-S1.25-L10-HW	9.9	4	2	0.10	0.375	0.11	1.31	1.09	2.19
	C40D22-S1.25-L10-HW-1	9.9	4	2	0.10	0.375	0.11	1.31	1.09	2.19
	C40D22-S1.5-L10-HE	9.9	4	2	0.10	0.375	0.11	1.31	1.31	2.19
	C40D22-S1.5-L10-HE-1	9.9	4	2	0.10	0.375	0.11	1.31	1.31	2.19

[1]	[2]	[3]	[4]	[5]	[6]	[7]	[8]	[9]	[10]	[11]
Authors	I.D	l_s/d_b	N_b	n	R_r	d_{tr} (in.)	A_t (in.^{2})	c_{so} (in.)	c_{si} (in.)	c_b (in.)
Chun, Lee, and Oh [9] (cont'd)	C40D22-S1.5-L10-HW	9.9	4	2	0.10	0.375	0.11	1.31	1.31	2.19
	C40D22-S1.5-L10-HW-1	9.9	4	2	0.10	0.375	0.11	1.31	1.31	2.19
	C60D22-S.75-L10-HE	9.9	4	2	0.10	0.375	0.11	1.31	0.66	2.19
	C60D22-S.75-L10-HE-1	9.9	4	2	0.10	0.375	0.11	1.31	0.66	2.19
	C60D22-S1.25-L10-HE	9.9	4	2	0.10	0.375	0.11	1.31	1.09	2.19
	C60D22-S1.25-L10-HE-1	9.9	4	2	0.10	0.375	0.11	1.31	1.09	2.19
	C40D29-S.75-L10-HE	10.1	2	2	0.10	0.375	0.11	1.69	0.85	2.82
	C40D29-S.75-L10-HW-1	10.1	2	2	0.10	0.375	0.11	1.69	0.85	2.82
	C60D29-S.75-L10-HE-1	10.1	2	2	0.10	0.375	0.11	1.69	0.85	2.82
Chun, Lee, and Oh [10]	C80D22-L4	4.0	4	2	0.10	-	-	1.31	0.66	2.19
	C80D22-L4-1	4.0	4	2	0.10	-	-	1.31	0.66	2.19
	C80D22-L4-2	4.0	4	2	0.10	-	-	1.31	0.66	2.19
	C80D22-L4-3	4.0	4	2	0.10	-	-	1.31	0.66	2.19
	C80D22-L7	7.0	4	2	0.10	-	-	1.31	0.66	2.19
	C80D22-L7-1	7.0	4	2	0.10	-	-	1.31	0.66	2.19
	C80D22-L7-2	7.0	4	2	0.10	-	-	1.31	0.66	2.19
	C80D22-L7-3	7.0	4	2	0.10	-	-	1.31	0.66	2.19
	C80D22-L10	9.9	4	2	0.10	-	-	1.31	0.66	2.19
	C80D22-L10-1	9.9	4	2	0.10	-	-	1.31	0.66	2.19
	C80D22-L10-3	9.9	4	2	0.10	-	-	1.31	0.66	2.19
	C80D29-L4	4.1	4	2	0.10	-	-	1.69	0.85	2.82
	C80D29-L4-1	4.1	4	2	0.10	-	-	1.69	0.85	2.82
	C80D29-L4-2	4.1	4	2	0.10	-	-	1.69	0.85	2.82
	C80D29-L4-3	4.1	4	2	0.10	-	-	1.69	0.85	2.82
	C80D29-L7	7.1	4	2	0.10	-	-	1.69	0.85	2.82
	C80D29-L7-2	7.1	4	2	0.10	-	-	1.69	0.85	2.82
	C80D29-L7-3	7.1	4	2	0.10	-	-	1.69	0.85	2.82
	C80D29-L10	10.1	4	2	0.10	-	-	1.69	0.85	2.82
	C80D29-L10-2	10.1	4	2	0.10	-	-	1.69	0.85	2.82
	C100D29-L4-1	4.1	4	2	0.10	-	-	1.69	0.85	2.82
	C80D22-L4-HW	4.0	4	2	0.10	0.375	0.11	1.31	0.66	2.19
	C80D22-L4-HW-1	4.0	4	2	0.10	0.375	0.11	1.31	0.66	2.19
	C80D22-L4-HW-2	4.0	4	2	0.10	0.375	0.11	1.31	0.66	2.19
	C80D22-L4-HW-3	4.0	4	2	0.10	0.375	0.11	1.31	0.66	2.19
	C80D22-L7-HW-1	6.9	4	2	0.10	0.375	0.11	1.31	0.66	2.19
	C80D22-L7-HW-2	6.9	4	2	0.10	0.375	0.11	1.31	0.66	2.19
	C80D29-L4-HW	4.1	4	2	0.10	0.375	0.11	1.69	0.85	2.82
	C80D29-L4-HW-1	4.1	4	2	0.10	0.375	0.11	1.69	0.85	2.82
	C80D29-L4-HW-2	4.1	4	2	0.10	0.375	0.11	1.69	0.85	2.82
	C80D29-L4-HW-3	4.1	4	2	0.10	0.375	0.11	1.69	0.85	2.82
	C80D29-L7-HW	7.1	4	2	0.10	0.375	0.11	1.69	0.85	2.82
	C80D29-L7-HW-3	7.1	4	2	0.10	0.375	0.11	1.69	0.85	2.82
	C100D29-L4-HW	4.1	4	2	0.10	0.375	0.11	1.69	0.85	2.82
	C100D29-L4-HW-1	4.1	4	2	0.10	0.375	0.11	1.69	0.85	2.82

[1]	[2]	[3]	[4]	[5]	[6]	[7]	[8]	[9]
Authors	I.D	N_s (in.)	N_l (in.)	s (in.)	x (in.)	f_{sc} (ksi)	f_{brg} (ksi)	P_e (kip)
Pfister and Mattock [7]	4B	1	4	10.0	5.0	40.0	-	498
	5B	3	4	10.0	0.0	53.0	-	635
	6B	3	4	10.0	5.0	58.0	-	645
	5B1	3	4	10.0	0.0	64.5	-	659
	6B1	3	4	10.0	5.0	68.0	-	688
	$4A^+$	3	1	1.5	0.375	50.0	-	603
	$5A^+$	7	1	1.5	0.375	52.9	-	623
	$6A^+$	13	1	1.5	0.375	67.0	-	725
	$7A^+$	20	1	1.5	0.375	82.6	-	769
Chun, Lee, and Oh [8]	C40D22-S.75-L10-HO	-	-	-	-	57.9	-	540
	C40D22-S.75-L10-HO-1	-	-	-	-	59.0	18.4	637
	C40D22-S.75-L15	-	-	-	-	58.2	16.7	626
	C40D22-S.75-L15-1	-	-	-	-	54.1	14.0	604
	C40D22-S1.25-L10-H0-1	-	-	-	-	46.7	12.4	656
	C40D22-S1.25-L15-HO	-	-	-	-	57.0	18.7	654
	C40D22-S1.25-L15-HO-1	-	-	-	-	64.0	14.6	721
	C40D22-S1.25-L20-HO-1	-	-	-	-	61.4	17.1	677
	C40D22-S1.5-L10-H0	-	-	-	-	47.1	18.4	716
	C40D22-S1.5-L10-H0-1	-	-	-	-	45.6	17.0	703
	C40D22-S1.5-L15-H0	-	-	-	-	60.9	16.3	705
	C40D22-S1.5-L15-H0-1	-	-	-	-	56.8	17.8	743
	C60D22-S.75-L10-HO	-	-	-	-	70.4	18.1	755
	C60D22-S.75-L10-HO-1	-	-	-	-	68.7	21.5	762
	C60D22-S1.25-L10-H0	-	-	-	-	64.5	20.3	824
	C60D22-S1.25-L10-H0-1	-	-	-	-	71.9	21.8	866
	C60D22-S1.25-L15-HO-1	-	-	-	-	67.0	24.1	813
	C60D22-S1.5-L10-H0	-	-	-	-	61.5	16.2	881
	C60D22-S1.5-L10-H0-1	-	-	-	-	73.2	20.4	950
	C60D22-S1.5-L15-1	-	-	-	-	69.2	21.0	889
	C40D29-S.75-L10-HO-1	-	-	-	-	63.1	23.0	804
	C40D29-S.75-L15-1	-	-	-	-	63.8	20.7	806
	C40D29-S.75-L20	-	-	-	-	62.9	11.5	851
	C60D29-S.75-L10-HO	-	-	-	-	66.9	21.8	943
	C60D29-S.75-L10-HO-1	-	-	-	-	63.3	19.7	849
	C60D29-S1.25-L10-H0	-	-	-	-	56.5	18.4	910
Chun, Lee, and Oh [9]	C40D22-S.75-L10-HE	1	2	8.7	0.0	48.9	18.6	582
	C40D22-S.75-L10-HE-1	1	2	8.7	0.0	52.9	19.0	649
	C40D22-S.75-L10-HW	3	2	2.9	0.0	67.5	20.4	627
	C40D22-S.75-L10-HW-1	3	2	2.9	0.0	61.4	19.3	670
	C40D22-S1.25-L10-HE	1	2	8.7	0.0	56.0	18.9	662
	C40D22-S1.25-L10-HE-1	1	2	8.7	0.0	60.2	20.3	700
	C40D22-S1.25-L10-HW	3	2	2.9	0.0	61.3	16.5	641
	C40D22-S1.25-L10-HW-1	3	2	2.9	0.0	66.3	-	695
	C40D22-S1.5-L10-HE	1	2	8.7	0.0	49.4	16.3	723
	C40D22-S1.5-L10-HE-1	1	2	8.7	0.0	55.4	17.5	769

x = estimated distance between tie and splice end

[1]	[2]	[3]	[4]	[5]	[6]	[7]	[8]	[9]
Authors	I.D	N_s (in.)	N_l (in.)	s (in.)	x (in.)	f_{sc} (ksi)	f_{brg} (ksi)	P_e (kip)
Chun, Lee, and Oh [9] (cont'd)	C40D22-S1.5-L10-HW	3	2	2.9	0.0	55.3	17.5	723
	C40D22-S1.5-L10-HW-1	3	2	2.9	0.0	65.8	19.2	783
	C60D22-S.75-L10-HE	1	2	8.7	0.0	70.7	30.3	753
	C60D22-S.75-L10-HE-1	1	2	8.7	0.0	65.6	21.9	804
	C60D22-S1.25-L10-HE	1	2	8.7	0.0	65.9	20.9	820
	C60D22-S1.25-L10-HE-1	1	2	8.7	0.0	72.8	17.9	859
	C40D29-S.75-L10-HE	1	2	11.4	0.0	67.2	22.4	838
	C40D29-S.75-L10-HW-1	3	2	3.8	0.0	66.0	18.2	767
	C60D29-S.75-L10-HE-1	1	2	11.4	0.0	65.4	19.1	747
Chun, Lee, and Oh [10]	C80D22-L4	-	-	-	6.2	60.9	31.1	822
	C80D22-L4-1	-	-	-	6.2	42.9	19.7	797
	C80D22-L4-2	-	-	-	6.2	50.1	19.5	780
	C80D22-L4-3	-	-	-	6.2	49.0	-	767
	C80D22-L7	-	-	-	4.9	64.4	24.2	898
	C80D22-L7-1	-	-	-	4.9	59.6	19.9	847
	C80D22-L7-2	-	-	-	4.9	52.0	22.0	848
	C80D22-L7-3	-	-	-	4.9	63.5	16.9	736
	C80D22-L10	-	-	-	3.6	65.7	25.8	862
	C80D22-L10-1	-	-	-	3.6	63.8	19.6	913
	C80D22-L10-3	-	-	-	3.6	64.1	16.4	830
	C80D29-L4	-	-	-	7.9	52.6	22.4	1297
	C80D29-L4-1	-	-	-	7.9	48.4	24.3	1278
	C80D29-L4-2	-	-	-	7.9	49.3	8.9	1292
	C80D29-L4-3	-	-	-	7.9	51.4	24.9	1290
	C80D29-L7	-	-	-	6.2	61.2	22.1	1432
	C80D29-L7-2	-	-	-	6.2	58.9	26.0	1222
	C80D29-L7-3	-	-	-	6.2	58.4	24.9	1370
	C80D29-L10	-	-	-	4.5	56.7	16.2	1282
	C80D29-L10-2	-	-	-	4.5	62.5	15.7	1212
	C100D29-L4-1	-	-	-	7.9	64.4	25.1	935
	C80D22-L4-HW	1	2	3.9	1.8	56.7	20.9	857
	C80D22-L4-HW-1	1	2	3.9	1.8	57.4	23.1	877
	C80D22-L4-HW-2	1	2	3.9	1.8	59.2	16.6	811
	C80D22-L4-HW-3	1	2	3.9	1.8	59.0	19.0	806
	C80D22-L7-HW-1	2	2	3.9	0.9	54.8	17.2	949
	C80D22-L7-HW-2	2	2	3.9	0.9	66.4	18.8	837
	C80D29-L4-HW	1	2	3.9	0.3	63.3	23.9	1569
	C80D29-L4-HW-1	1	2	3.9	0.3	64.2	26.7	1270
	C80D29-L4-HW-2	1	2	3.9	0.3	59.3	26.2	1541
	C80D29-L4-HW-3	1	2	3.9	0.3	70.9	18.8	1527
	C80D29-L7-HW	2	2	3.9	1.9	60.0	20.3	1747
	C80D29-L7-HW-3	2	2	3.9	1.9	49.7	29.7	1544
	C100D29-L4-HW	1	2	3.9	0.3	66.3	28.1	1608
	C100D29-L4-HW-1	1	2	3.9	0.3	62.0	25.0	1576

x = estimated distance between tie and splice end

Appendix B: Compression Lap Splices: Relationships between Variables within Database

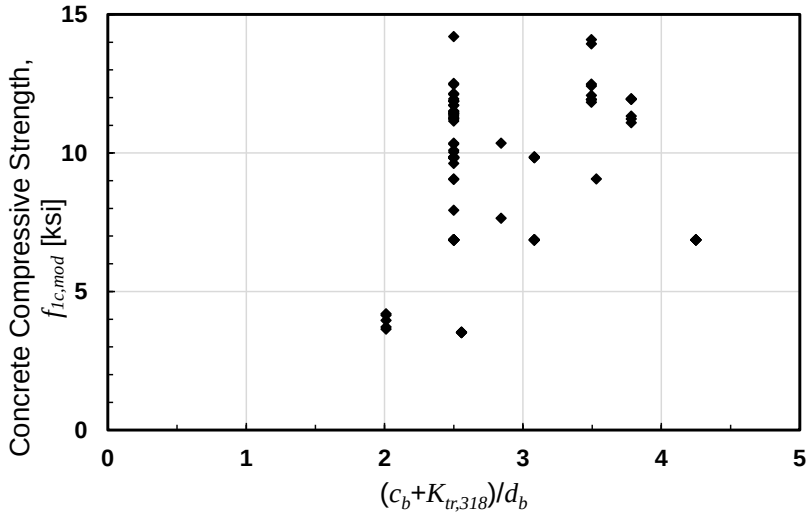

Figure 60 – Correlation between concrete compressive strength and $(c_b+K_{tr,318})/d_b$

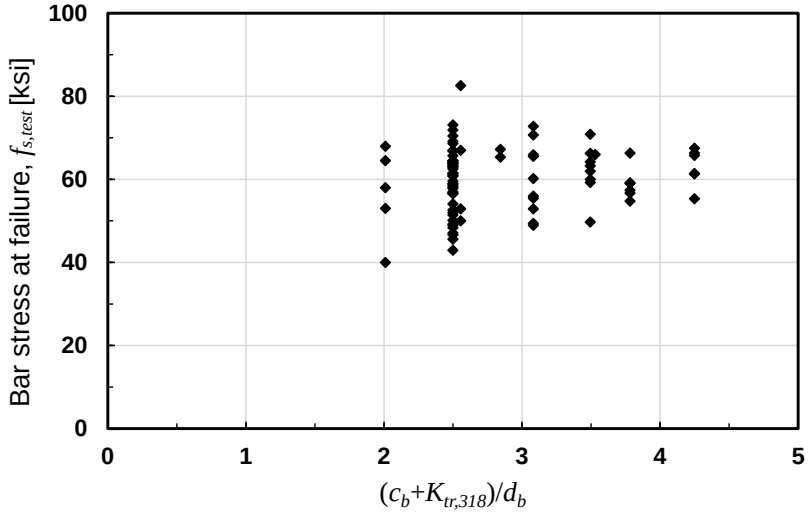

Figure 61 – Correlation between bar stress at failure and $(c_b+K_{tr,318})/d_b$

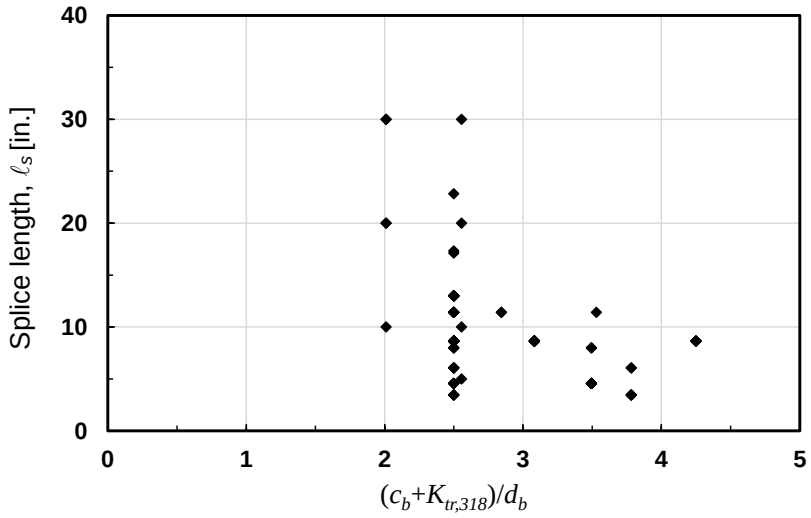

Figure 62 – Correlation between splice length and $(c_b+K_{tr,318})/d_b$

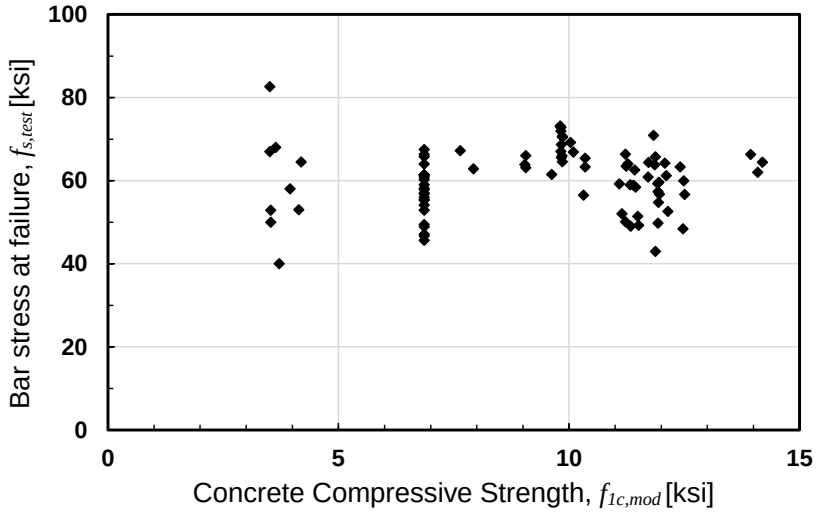

Figure 63 – Correlation between bar stress at failure and concrete compressive strength

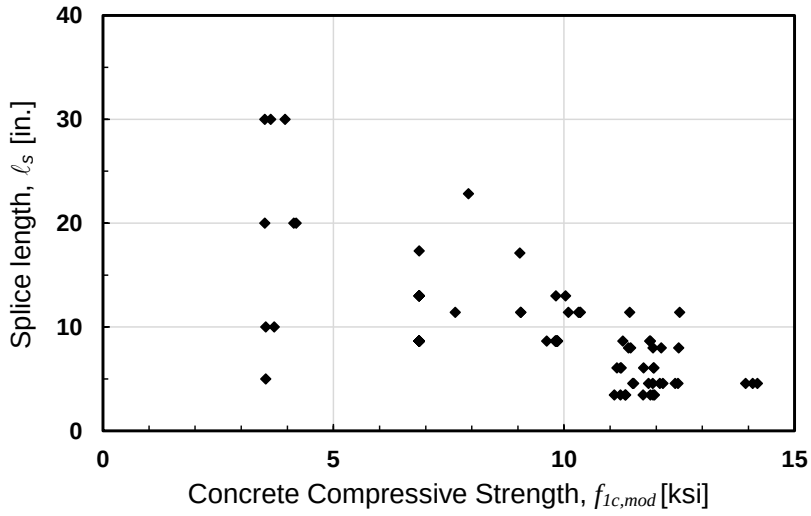

Figure 64 – Correlation between splice length and concrete compressive strength

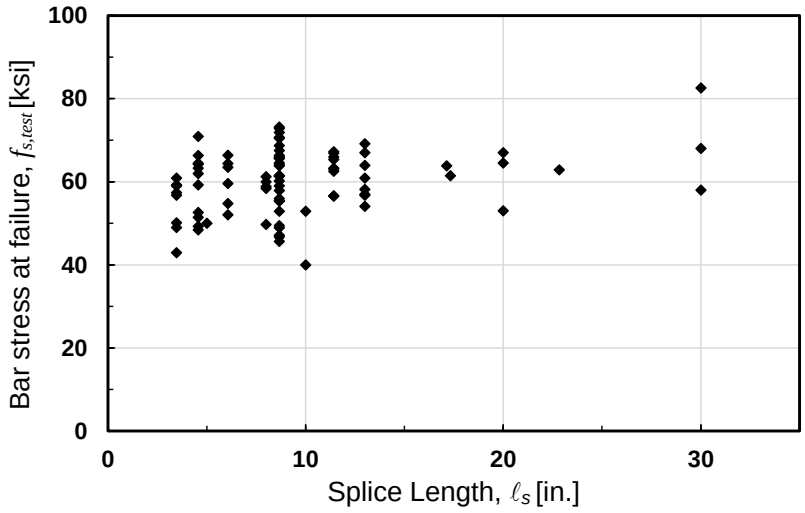

Figure 65 – Correlation between bar stress at failure and splice length

Appendix C: Compression Lap Splices: Behavior of Compression Development or Compression Lap Splice Equations

Plots show the performance of the equations against the database in terms of T/C versus: (a) $(c_b + K_{tr,318})/d_b$ (b) measured concrete compressive strength, $f_{1c,mod}$ (c) measured steel failure stress, $f_{s,test}$, and (d) provided splice length, ℓ_s.

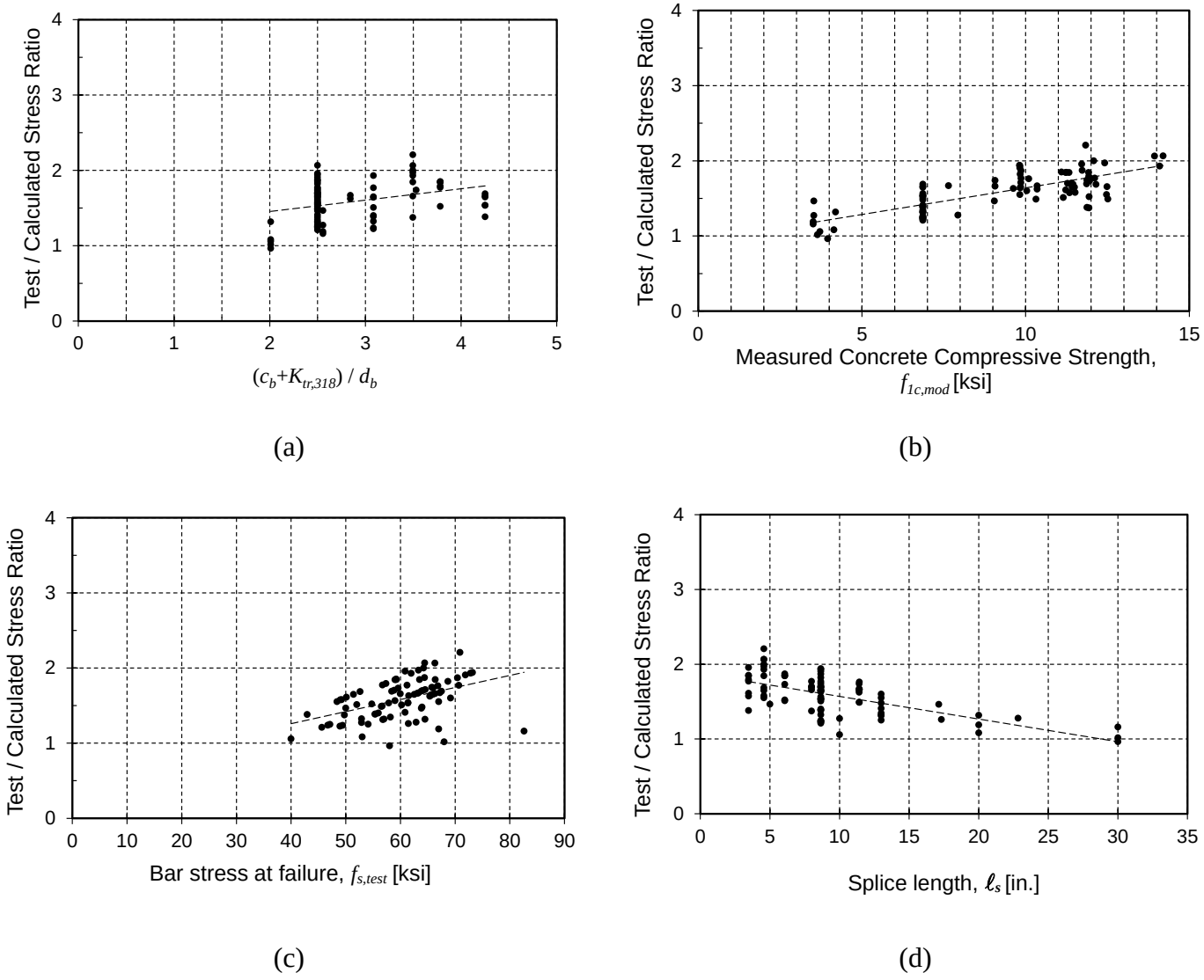

Figure 66 – ACI 318-19 [3] §25.5.5 Compression Lap Splice Eq. (b): *T*/*C* vs.: (a) $(c_b + K_{tr,318})/d_b$ (b) measured concrete compressive strength, $f_{1c,mod}$ (c) measured steel failure stress $f_{s,test}$ (d) provided splice length ℓ_s

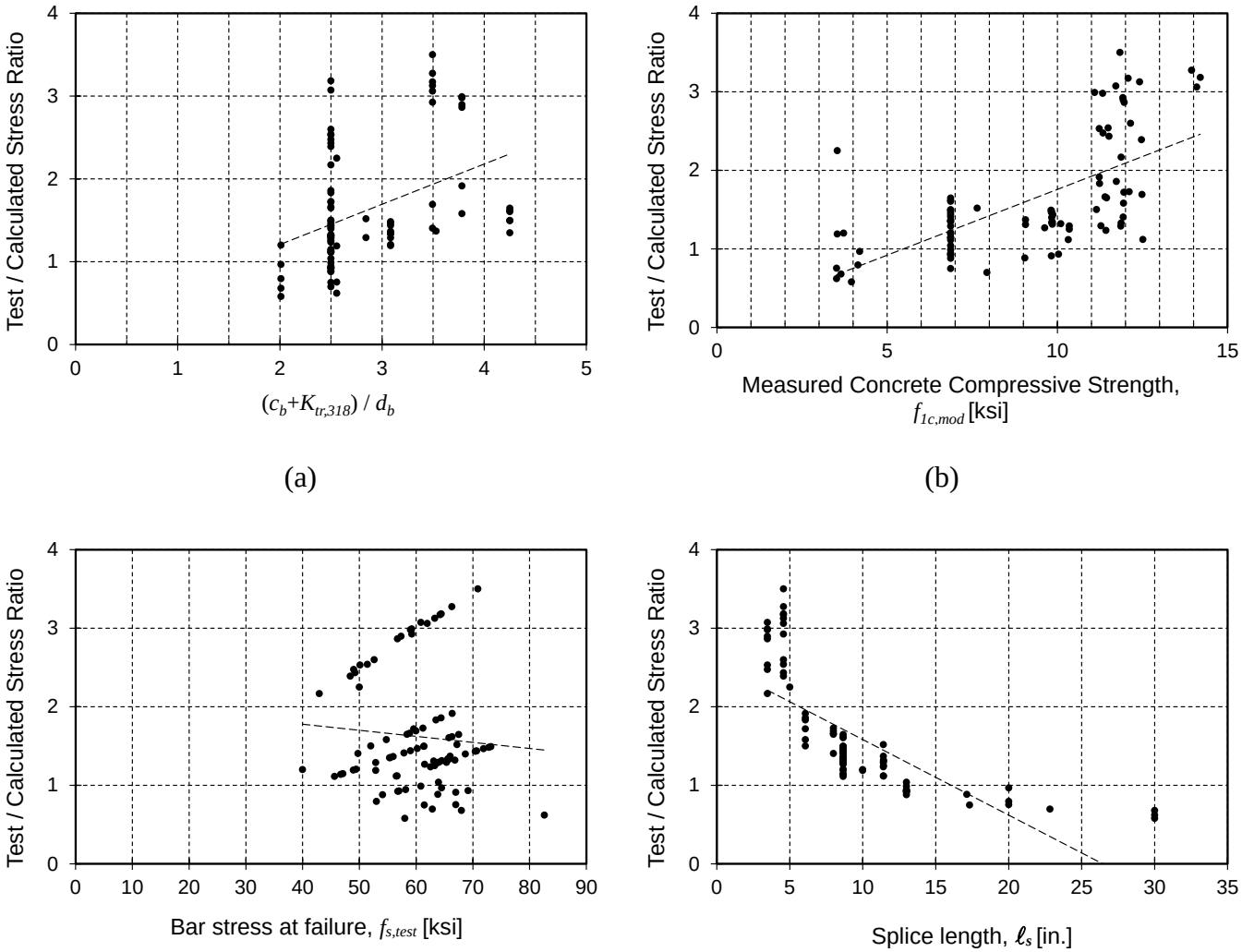

Figure 67 – ACI 318-19 [3] §25.4.9 Compression Development: *T*/*C* vs.: (a) $(c_b + K_{tr,318})/d_b$ (b) measured concrete compressive strength, $f_{1c,mod}$ (c) measured steel failure stress $f_{s,test}$ (d) provided splice length ℓ_s

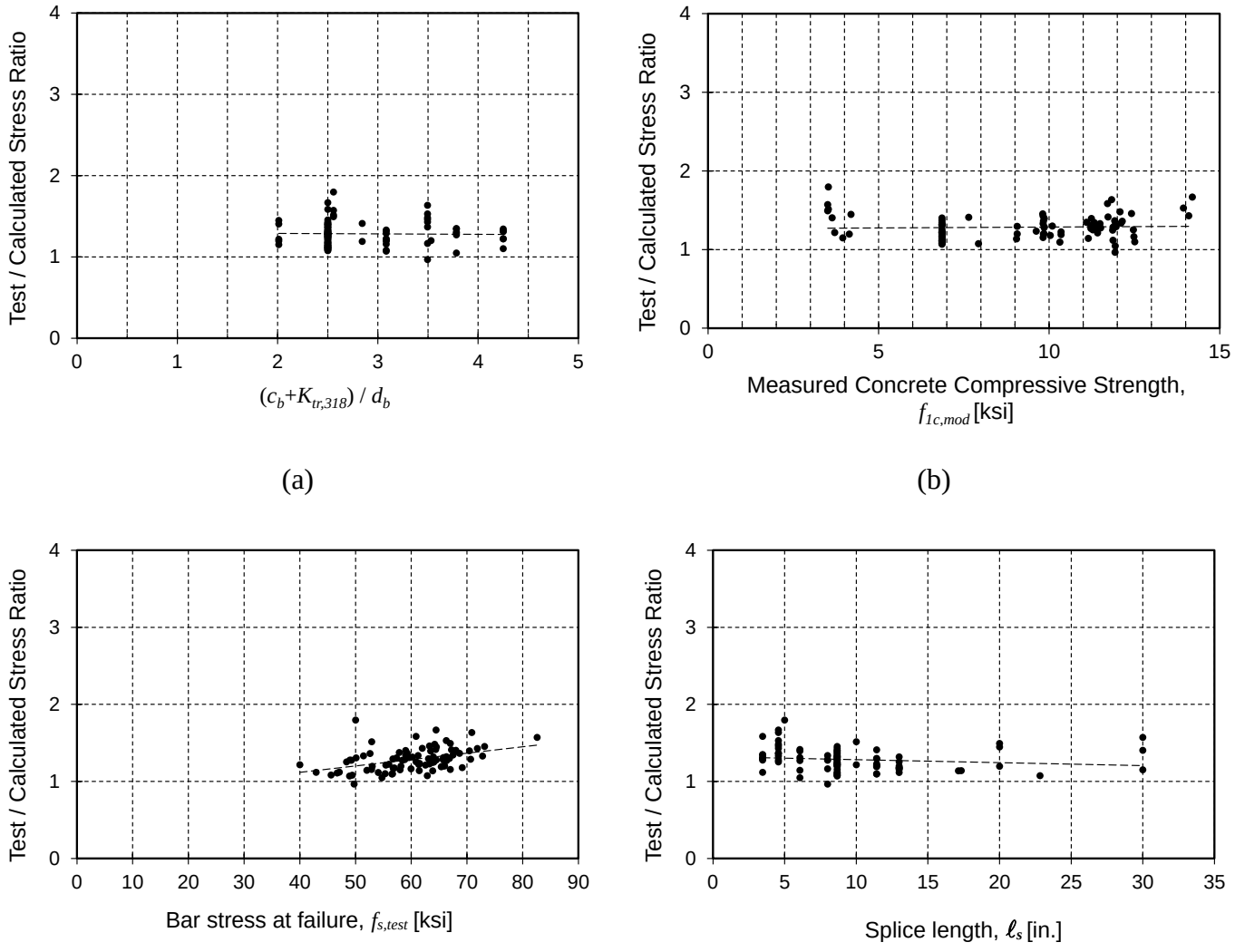

Figure 68 – Chun et al. [9] Compression Splice (Complex): T/C vs.: (a) $(c_b + K_{tr,318})/d_b$ (b) measured concrete compressive strength, $f_{1c,mod}$ (c) measured steel failure stress $f_{s,test}$ (d) provided splice length ℓ_s

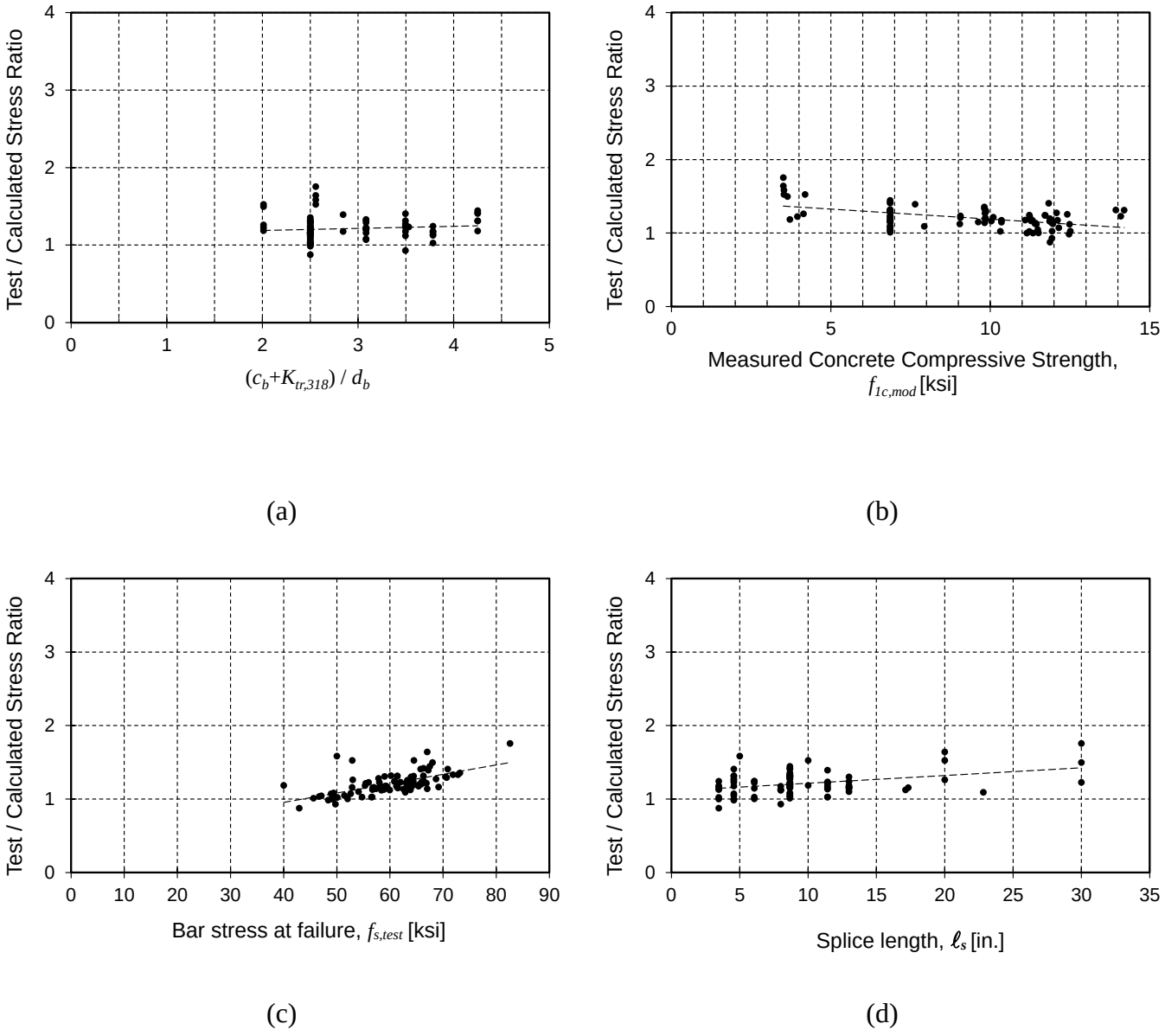

Figure 69 – Chun et al. [8] Compression Splice (Simplified): T/C vs.: (a) $(c_b + K_{tr,318})/d_b$ (b) measured concrete compressive strength, $f_{1c,mod}$ (c) measured steel failure stress $f_{s,test}$ (d) provided splice length ℓ_s

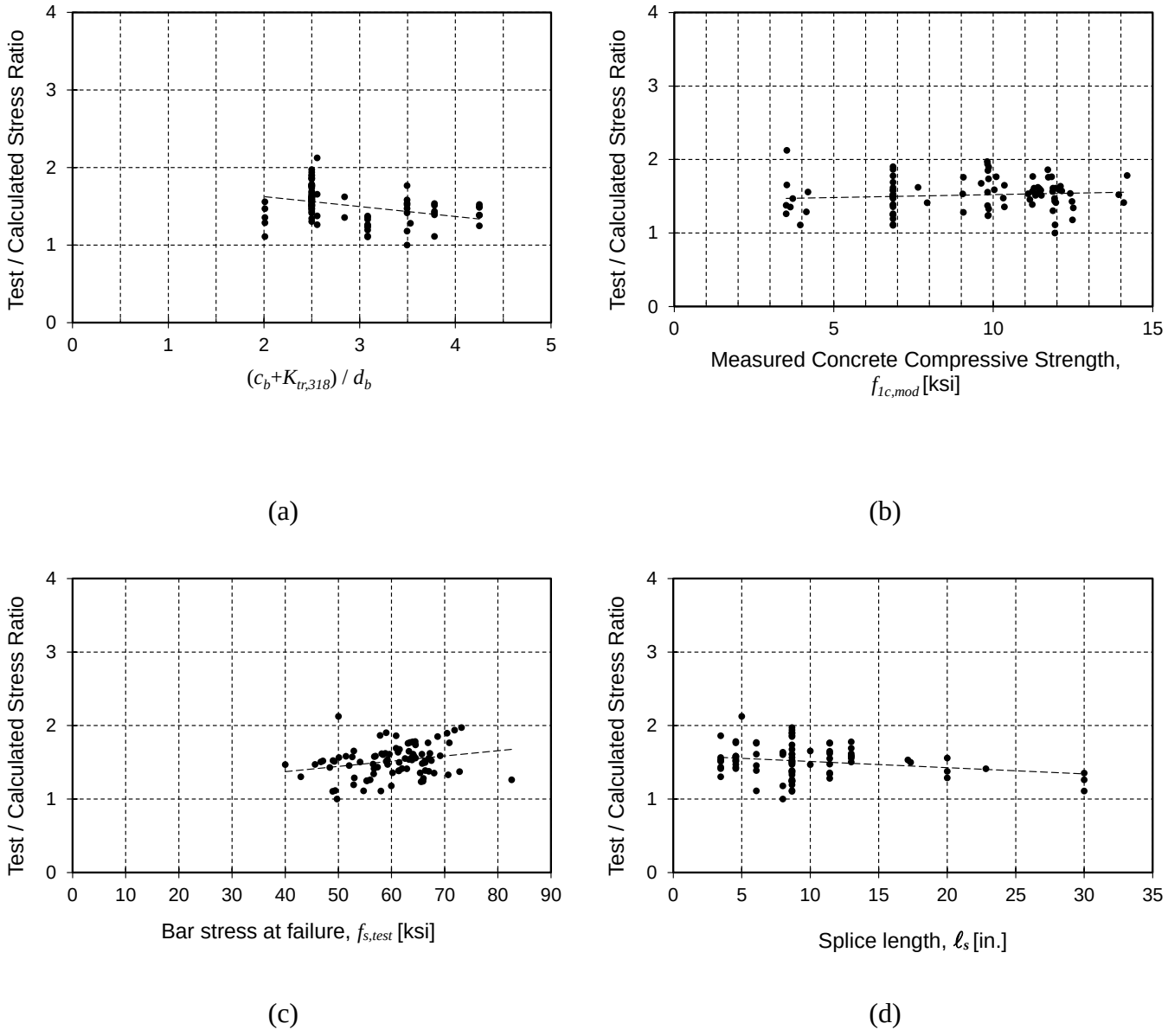

Figure 70 – Cairns Compression Splice: *T*/*C* vs.: (a) $(c_b + K_{tr,318})/d_b$ (b) measured concrete compressive strength, $f_{1c,mod}$ (c) measured steel failure stress $f_{s,test}$ (d) provided splice length ℓ_s

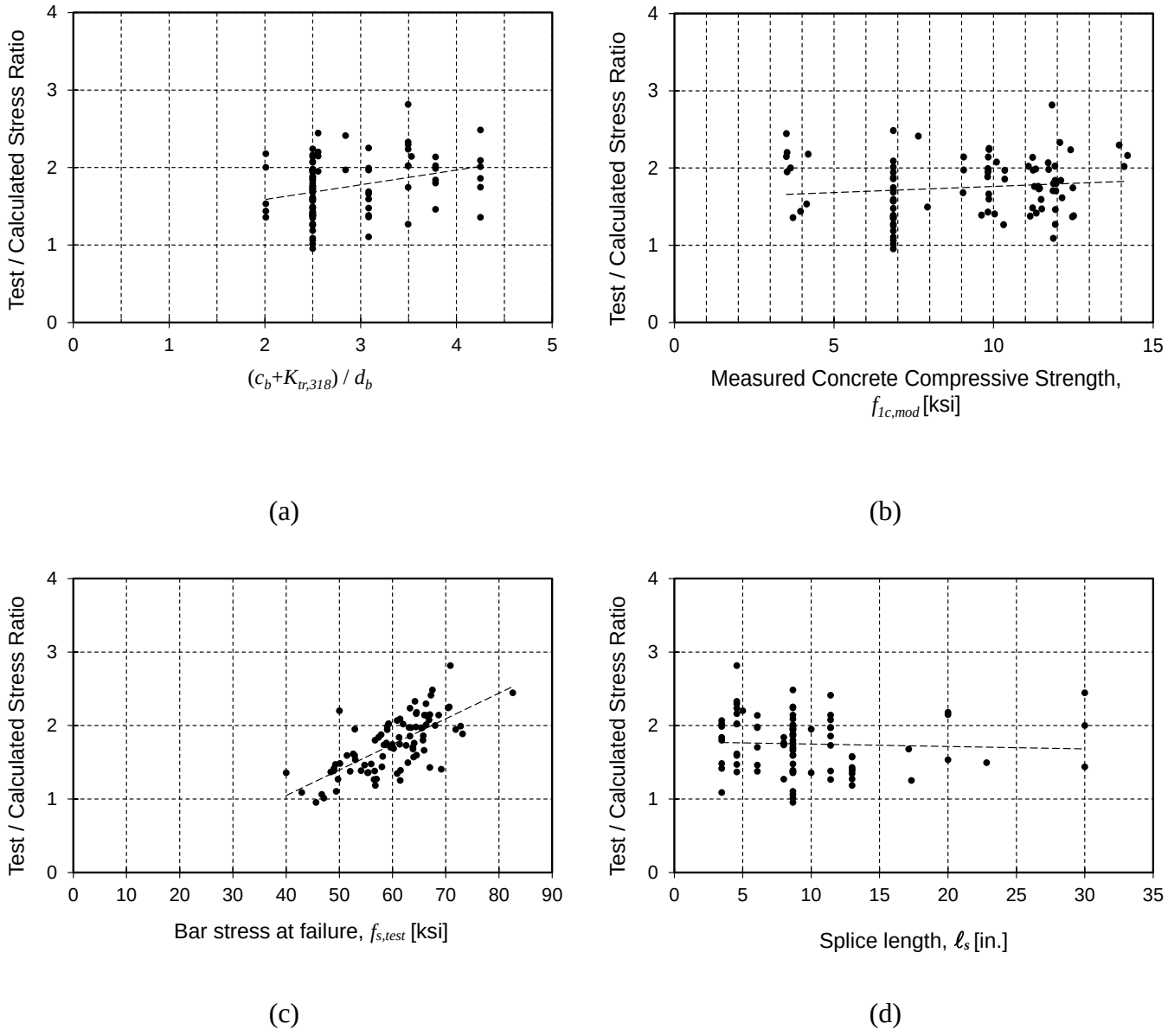

Figure 71 – fib MC 2010: T/C vs.: (a) $(c_b + K_{tr,318})/d_b$ (b) measured concrete compressive strength, $f_{1c,mod}$ (c) measured steel failure stress $f_{s,test}$ (d) provided splice length ℓ_s

Appendix D: Compression Lap Splices: Behavior of Tension Development Length Equations

Plots show the performance of the equations against the database in terms of T/C versus: (i) $(c_b + K_{tr,318})/d_b$ (ii) measured concrete compressive strength, $f_{1c,mod}$ (iii) measured steel failure stress $f_{s,test}$ (iv) provided splice length ℓ_s. The plots are organized showing the behavior of the original equation, the equation using the derived r_1 factor, and the derived r_2 factor.

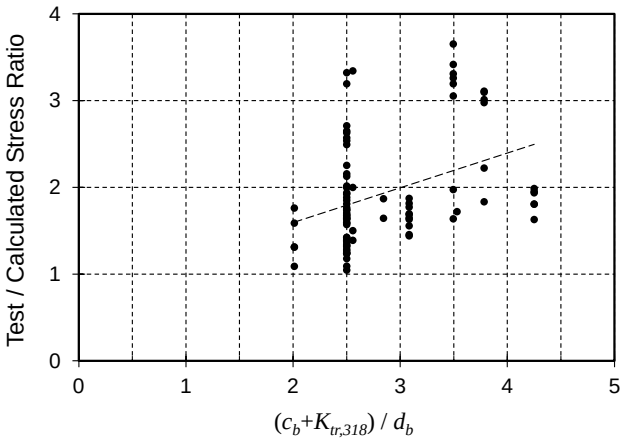

(a) ACI 318-19

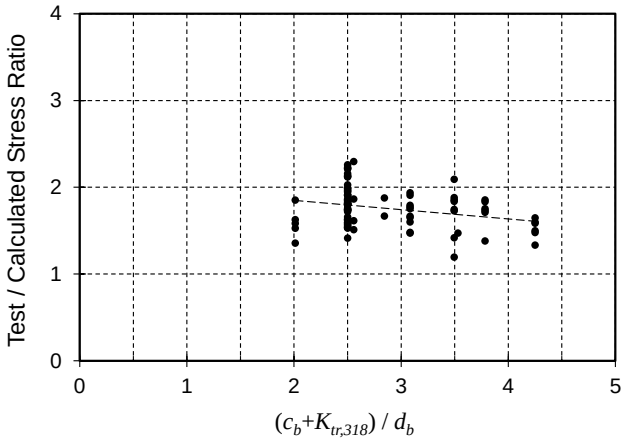

(b) ACI 408R-03

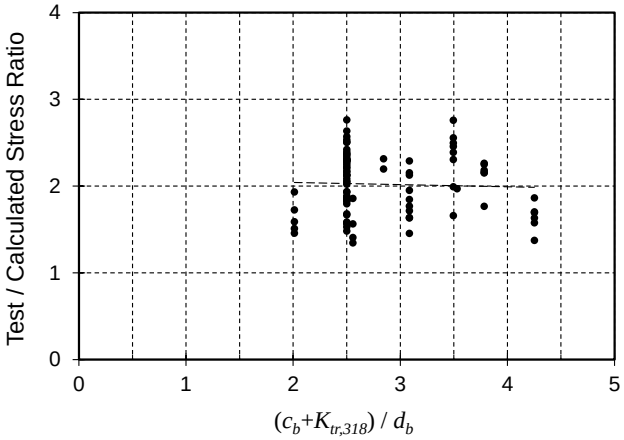

(c) Lepage et al.

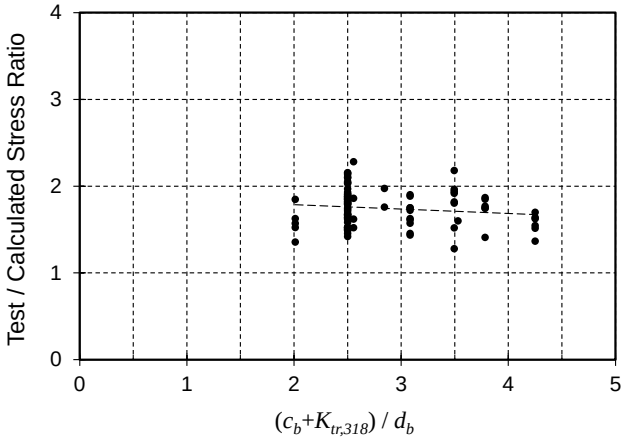

(d) Darwin et al.

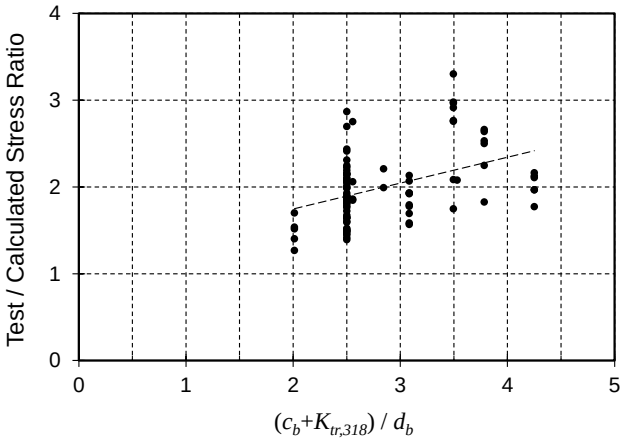

(e) Canbay and Frosch

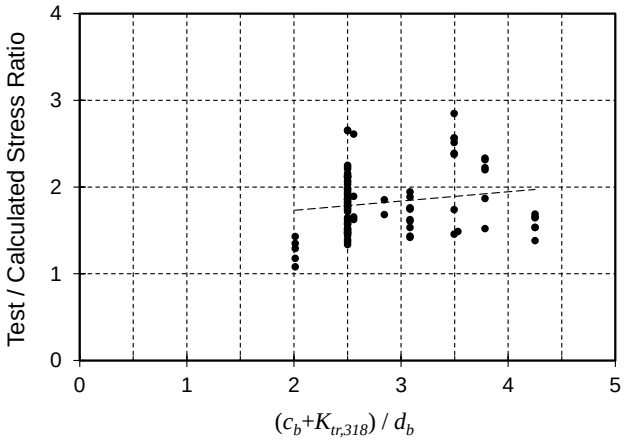

(f) Frosch et al.

Figure 72 - T/C vs. $(c_b + K_{tr,318})/d_b$ for tension development length equations

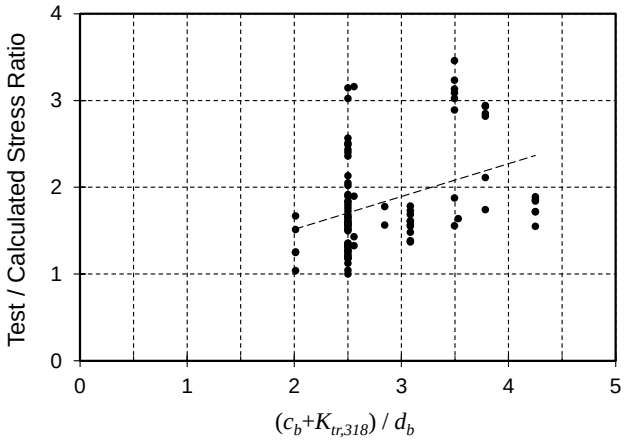

(a) ACI 318-19. r_1 = 0.94

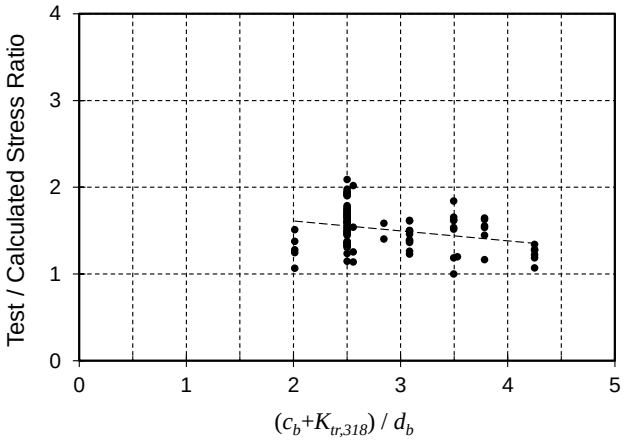

(b) ACI 408R-03. r_1 = 0.69

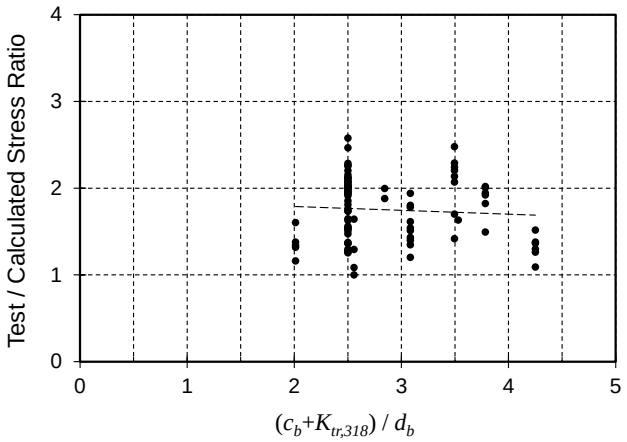

(c) Lepage et al. r_1 = 0.66

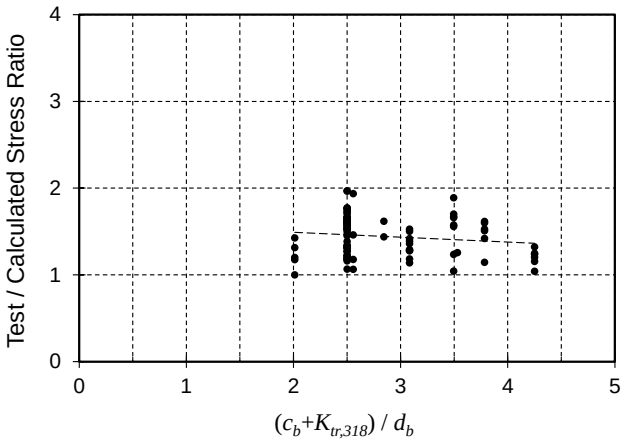

(d) Darwin et al. r_1 = 0.63

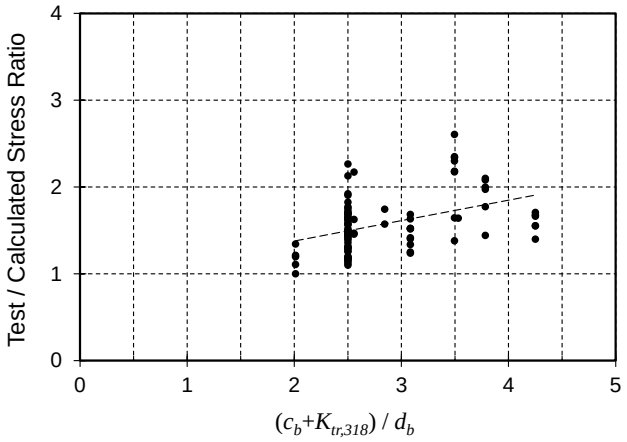

(e) Canbay and Frosch. r_1 = 0.62

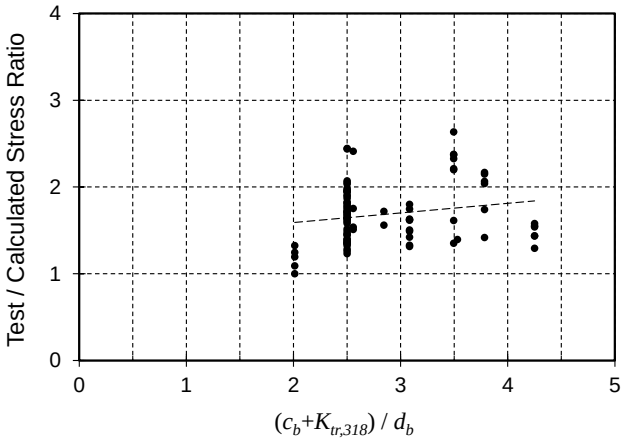

(f) Frosch et al. r_1 = 0.85

Figure 73 - T/C vs. $(c_b + K_{tr,318})/d_b$ for tension development length equations with r_1 factor

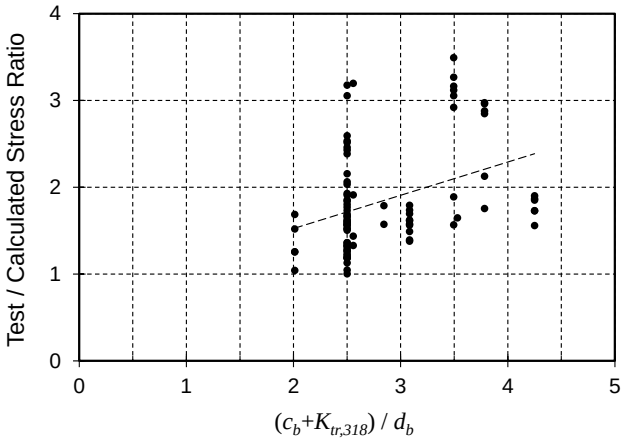

(a) ACI 318-19. r_2 = 0.96

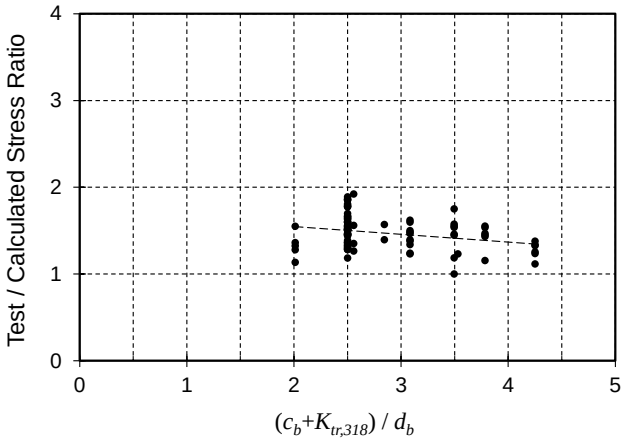

(b) ACI 408R-03. r_2 = 0.84

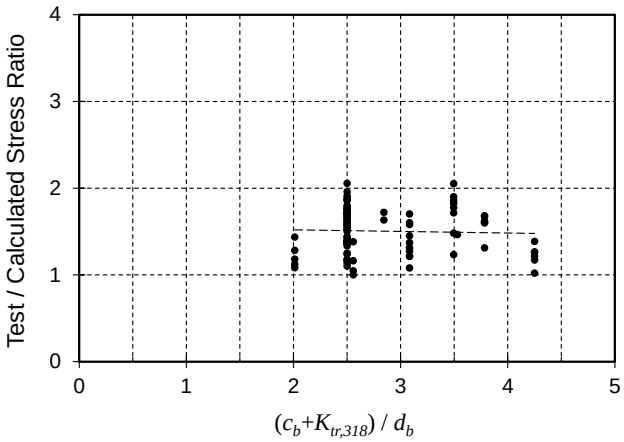

(c) Lepage et al. r_2 = 0.74

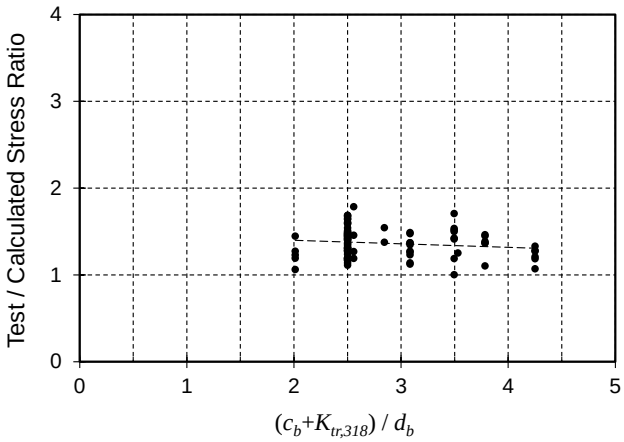

(d) Darwin et al. r_2 = 0.78

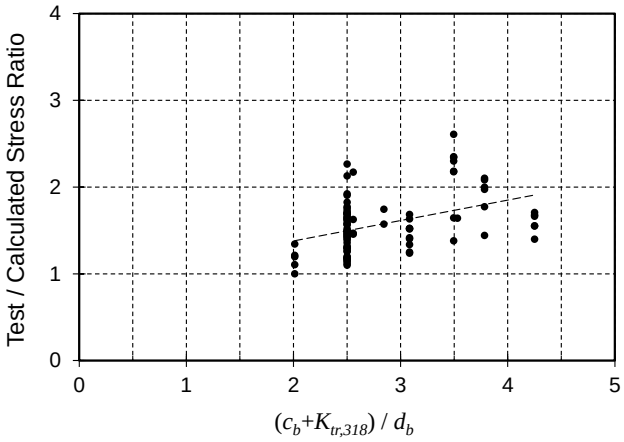

(e) Canbay and Frosch. r_2 = 0.79

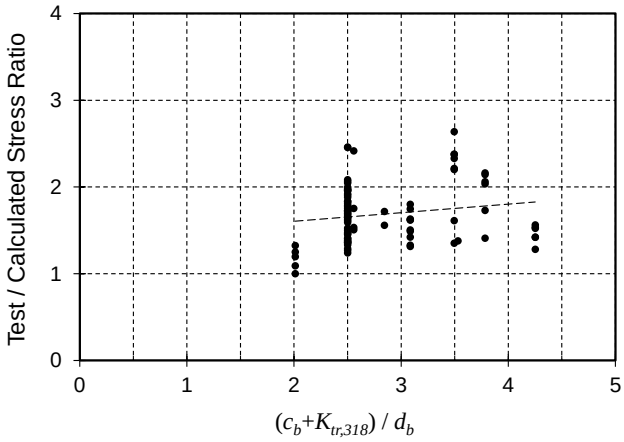

(f) Frosch et al. r_2 = 0.93

Figure 74 - T/C vs. $(c_b + K_{tr,318})/d_b$ for tension development length equations with r_2 factor

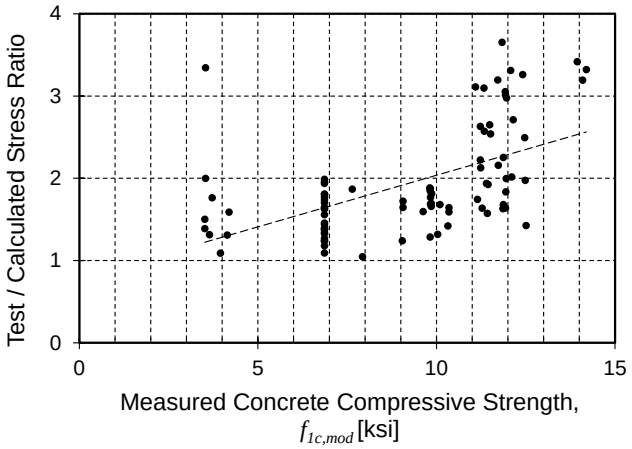

(a) ACI 318-19

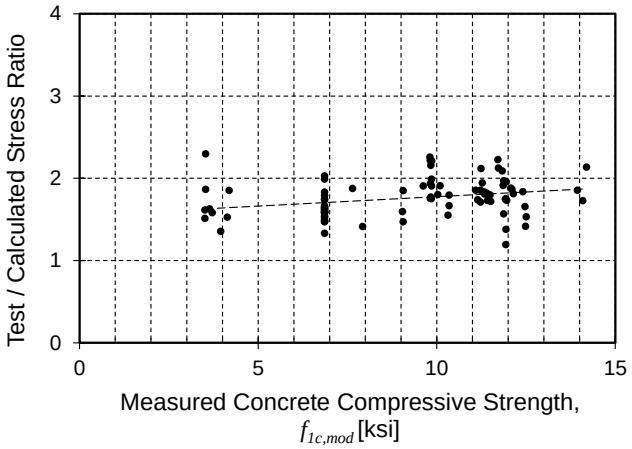

(b) ACI 408R-03

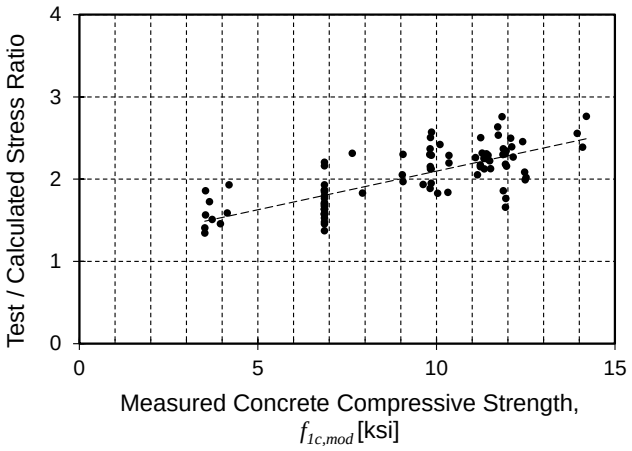

(c) Lepage et al.

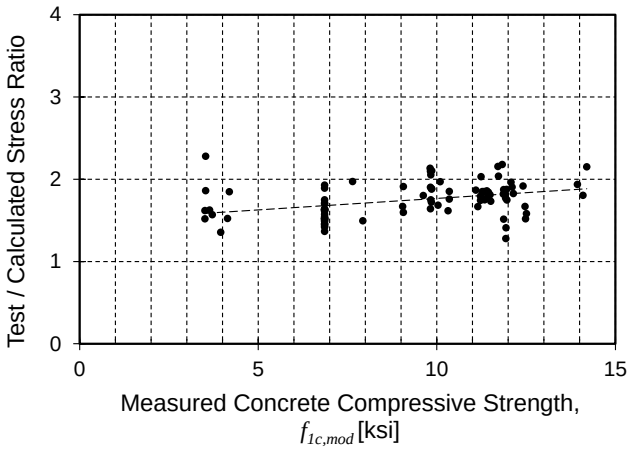

(d) Darwin et al.

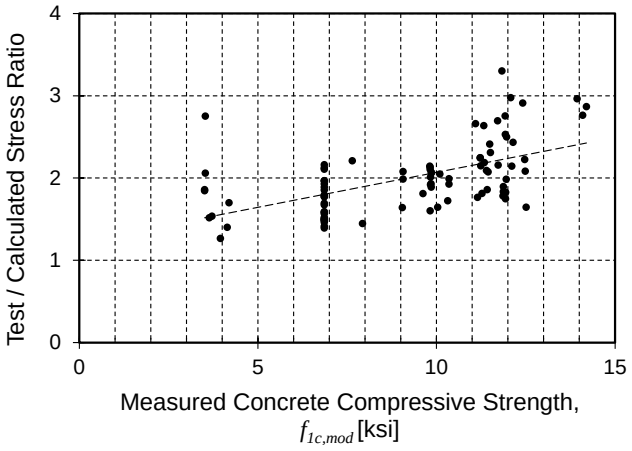

(e) Canbay and Frosch

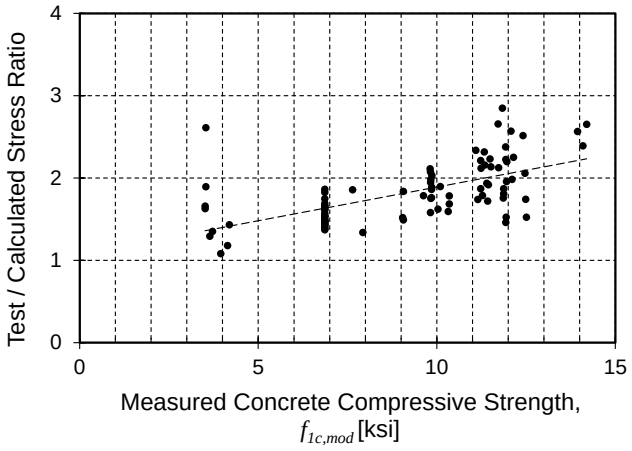

(f) Frosch et al.

Figure 75 - *T*/*C* vs. measured concrete compressive strength, $f_{1c,mod}$, for tension development length equations

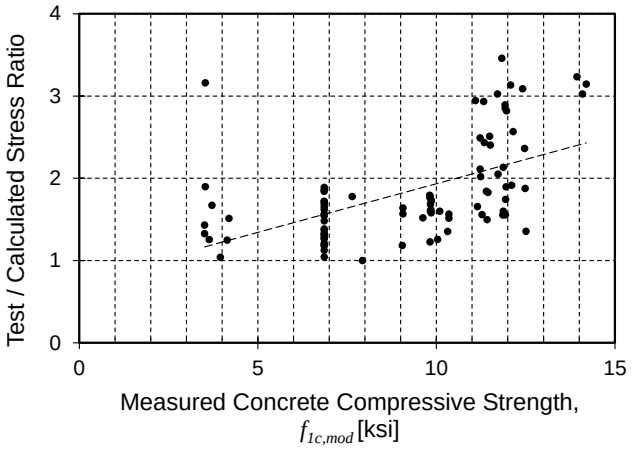

(a) ACI 318-19. r_1 = 0.94

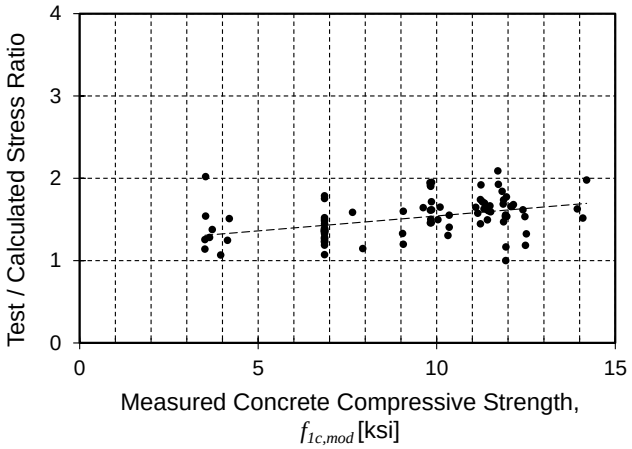

(b) ACI 408R-03. r_1 = 0.69

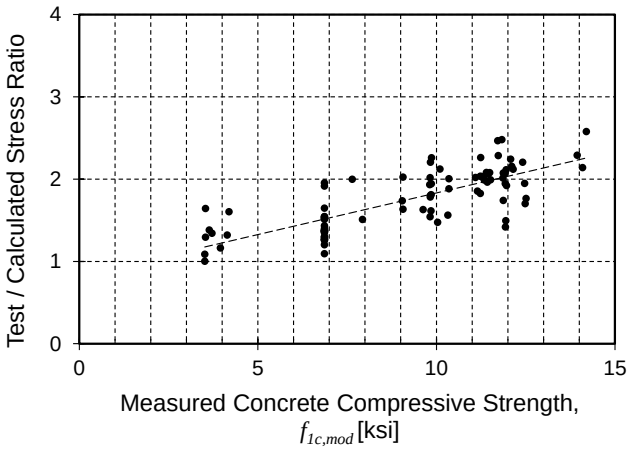

(c) Lepage et al. r_1 = 0.66

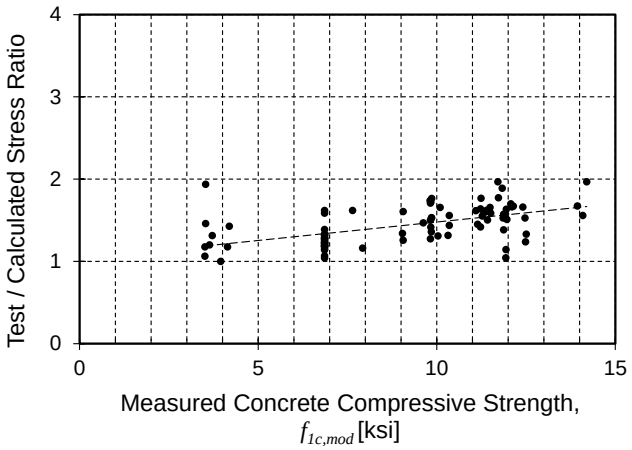

(d) Darwin et al. r_1 = 0.63

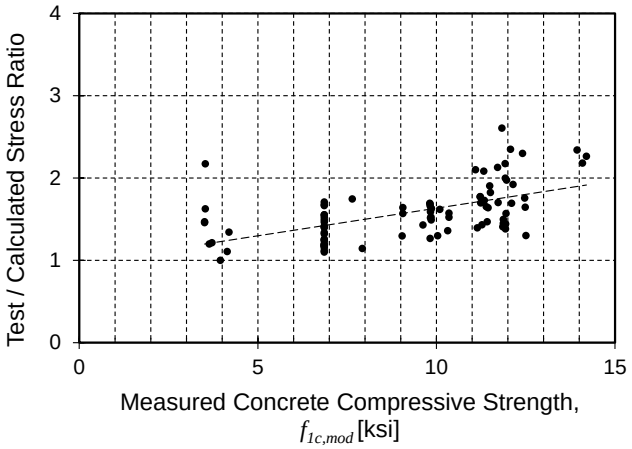

(e) Canbay and Frosch. r_1 = 0.62

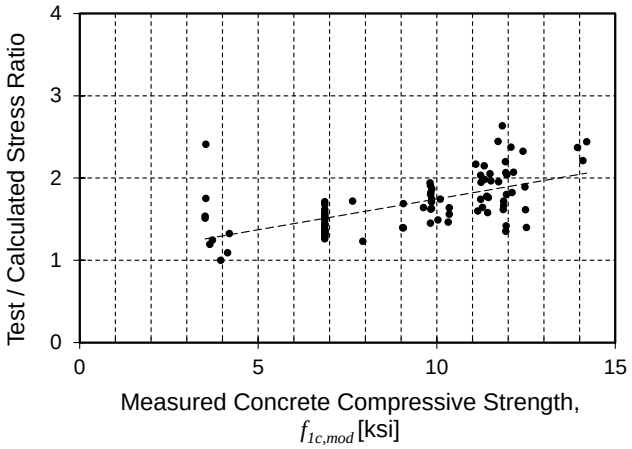

(f) Frosch et al. r_1 = 0.85

Figure 76 - *T*/*C* vs. measured concrete compressive strength, $f_{1c,mod}$, for tension development length equations with r_1 factor

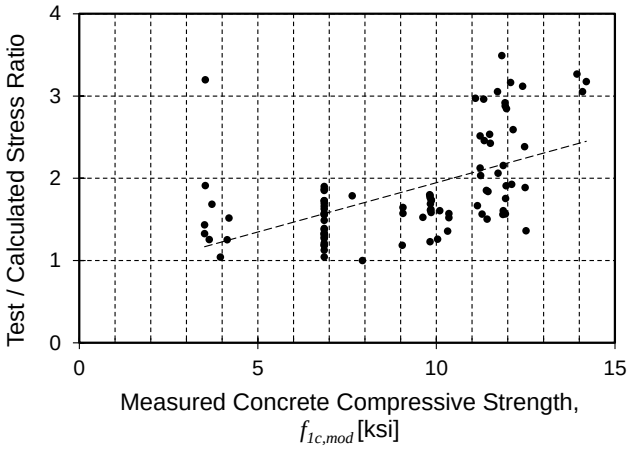

(a) ACI 318-19. r_2 = 0.96

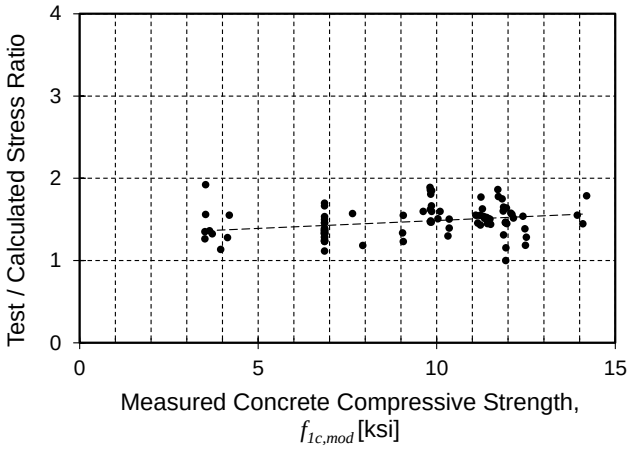

(b) ACI 408R-03. r_2 = 0.84

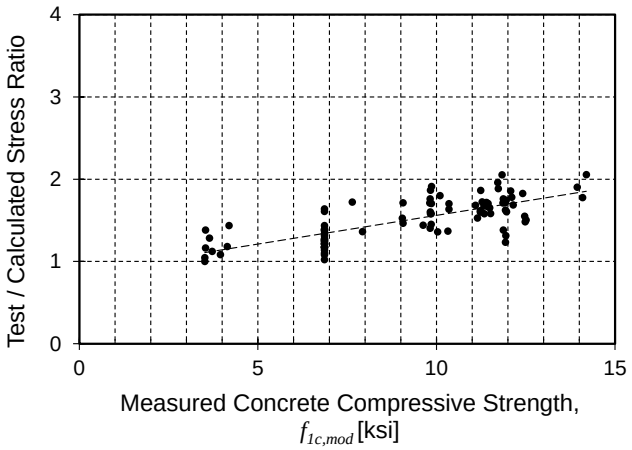

(c) Lepage et al. r_2 = 0.74

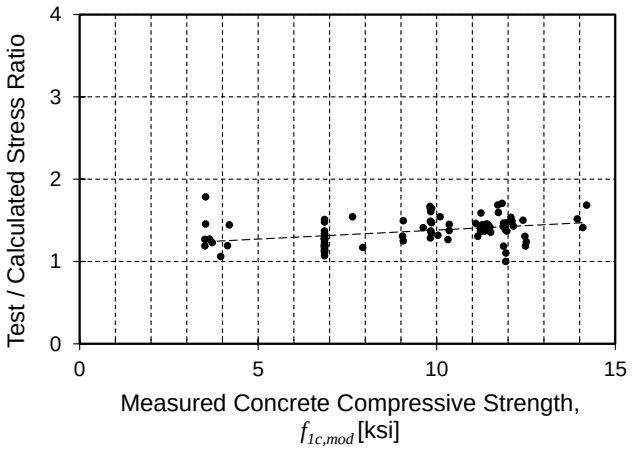

(d) Darwin et al. r_2 = 0.78

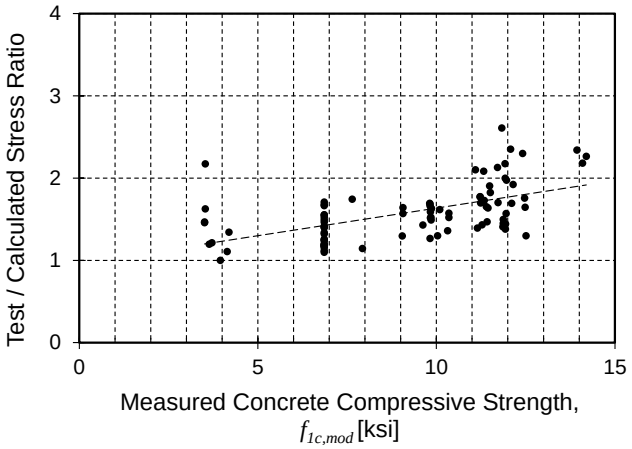

(e) Canbay and Frosch. r_2 = 0.79

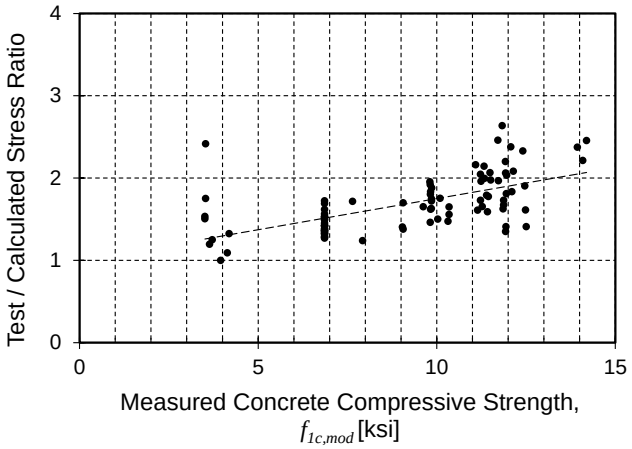

(f) Frosch et al. r_2 = 0.93

Figure 77 - *T*/*C* vs. measured concrete compressive strength, $f_{1c,mod}$, for tension development length equations with r_2 factor

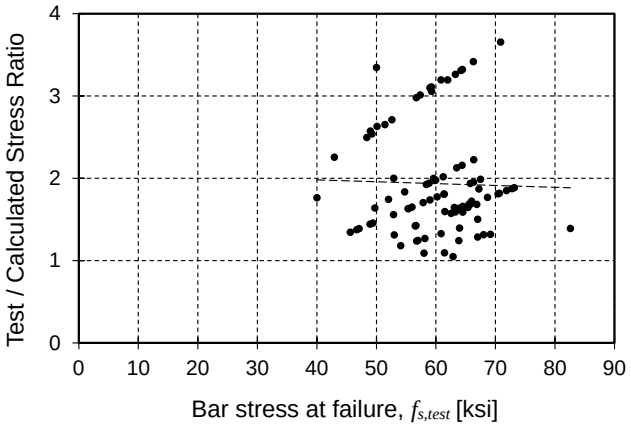

(a) ACI 318-19

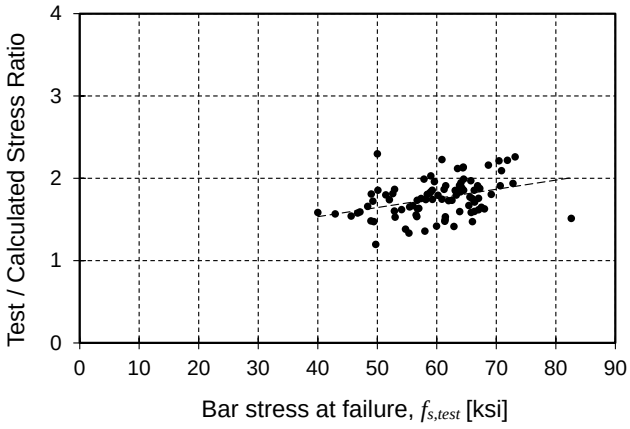

(b) ACI 408R-03

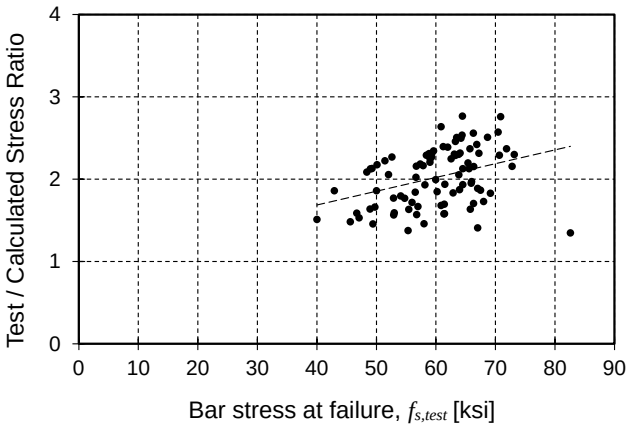

(c) Lepage et al.

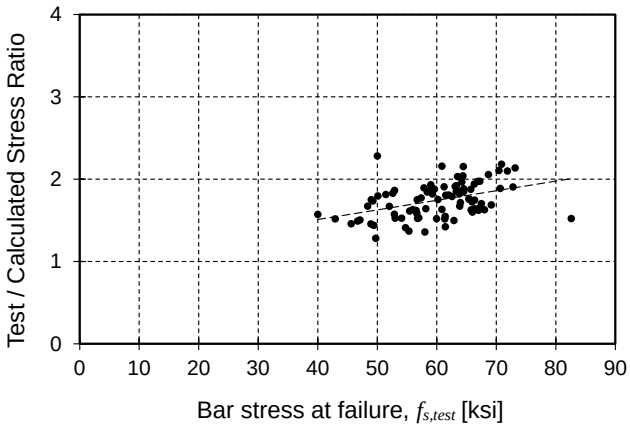

(d) Darwin et al.

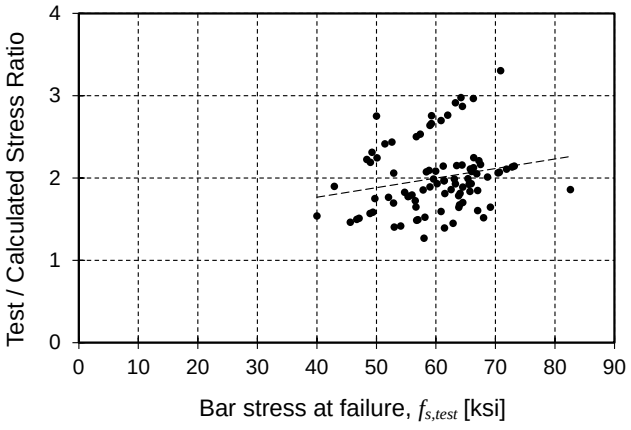

(e) Canbay and Frosch

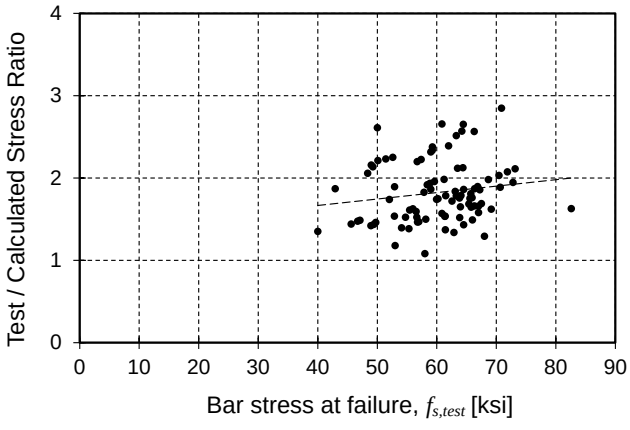

(f) Frosch et al.

Figure 78 - *T*/*C* vs. measured steel failure stress $f_{s,test}$ for tension development length equations

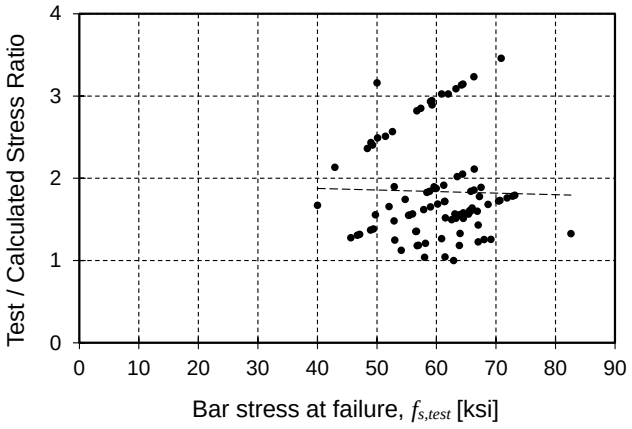

(a) ACI 318-19 r_1 = 0.94

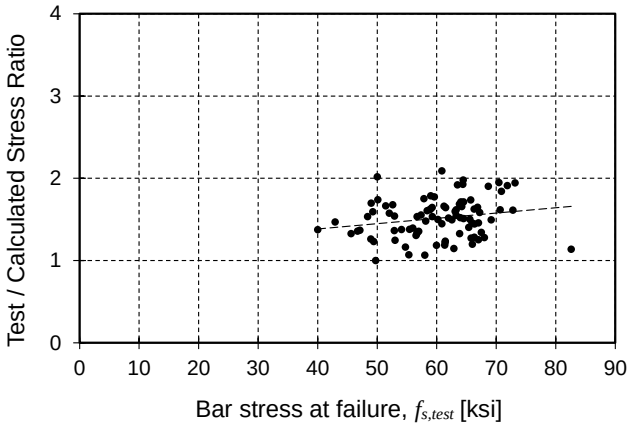

(b) ACI 408R-03 r_1 = 0.69

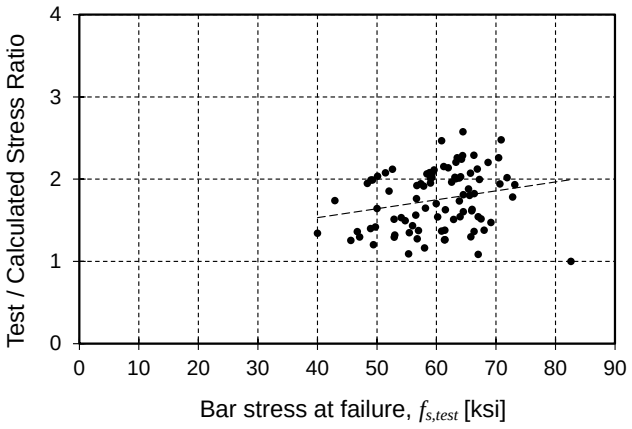

(c) Lepage et al. r_1 = 0.66

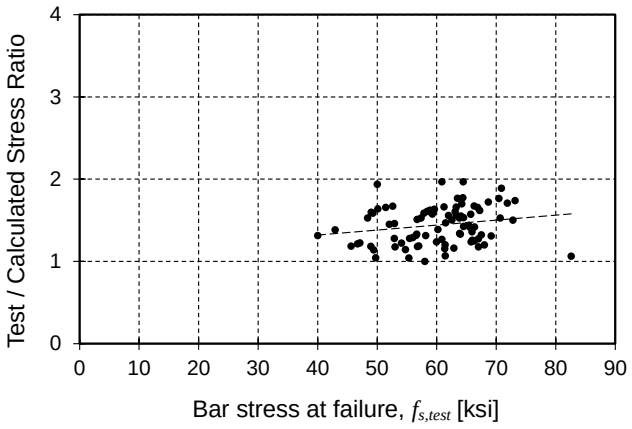

(d) Darwin et al. r_1 = 0.63

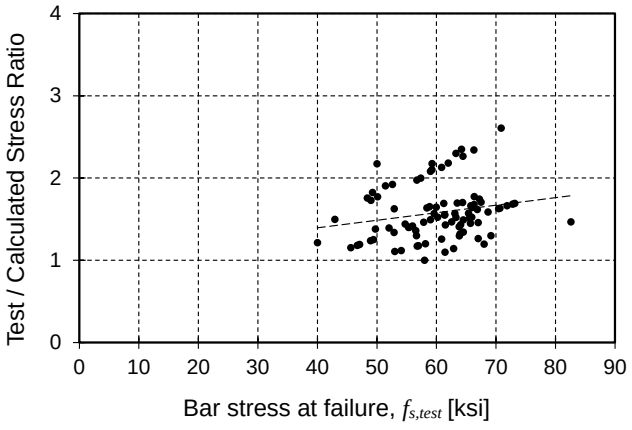

(e) Canbay and Frosch. r_1 = 0.62

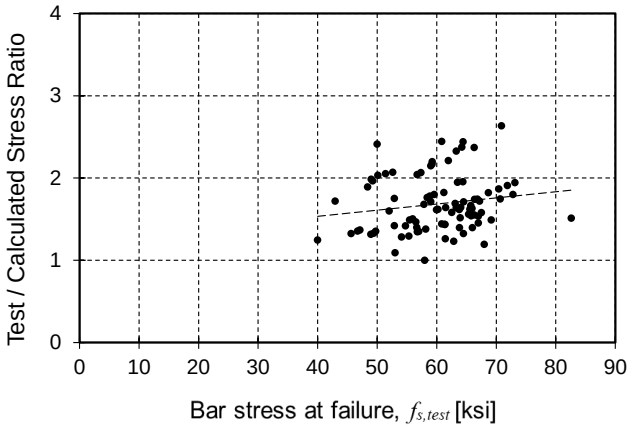

(f) Frosch et al. r_1 = 0.85

Figure 79 - *T*/*C* vs. measured steel failure stress $f_{s,test}$ for tension development length equations with r_1 factor

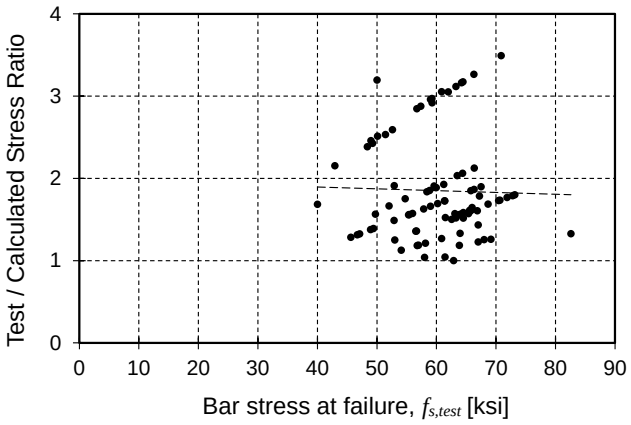

(a) ACI 318-19. r_2 = 0.96

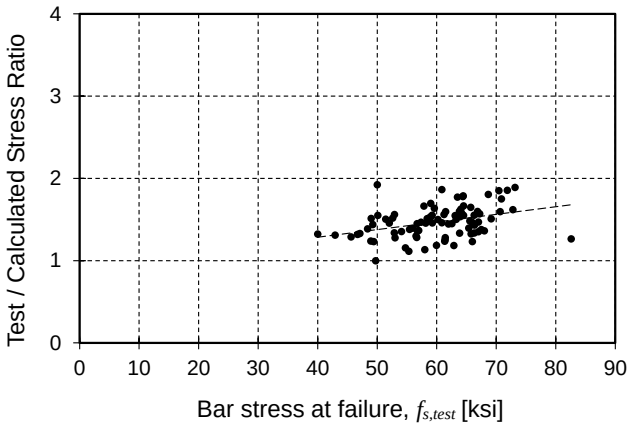

(b) ACI 408R-03. r_2 = 0.84

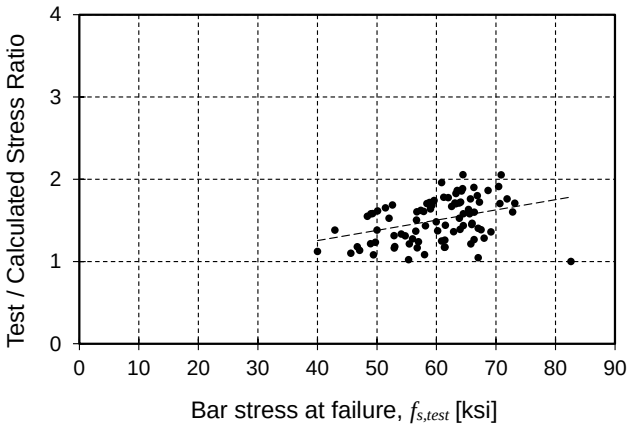

(c) Lepage et al. with r_2 = 0.74

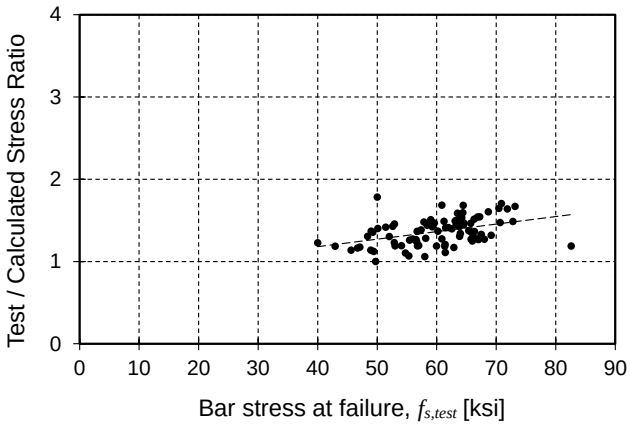

(d) Darwin et al. with r_2 = 0.78

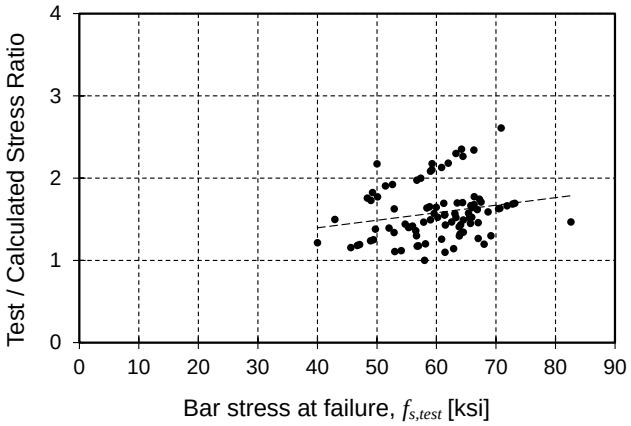

(e) Canbay and Frosch. with r_2 = 0.79

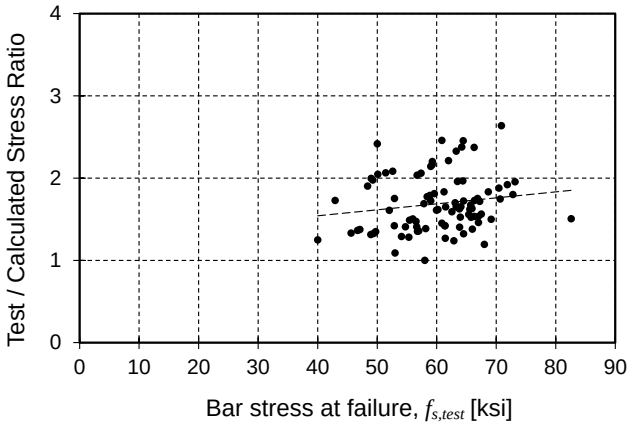

(f) Frosch et al. with r_2 = 0.93

Figure 80 - *T*/*C* vs. measured steel failure stress $f_{s,test}$ for tension development length equations with r_2 factor

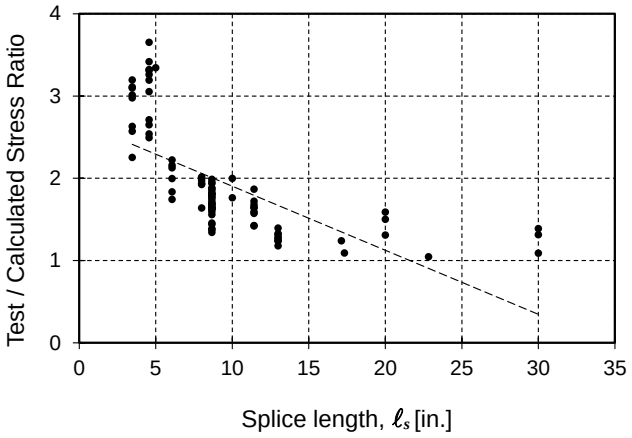

(a) ACI 318-19

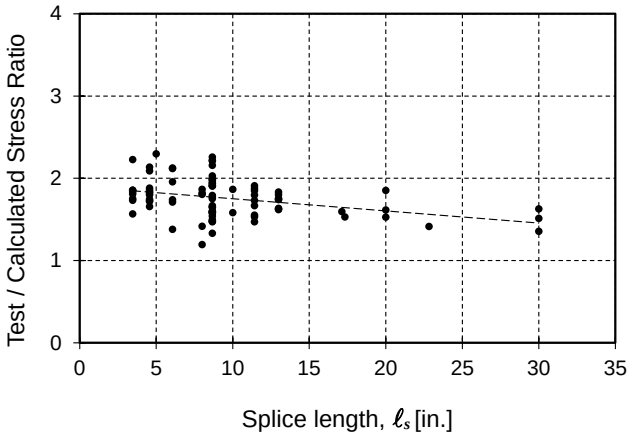

(b) ACI 408R-03

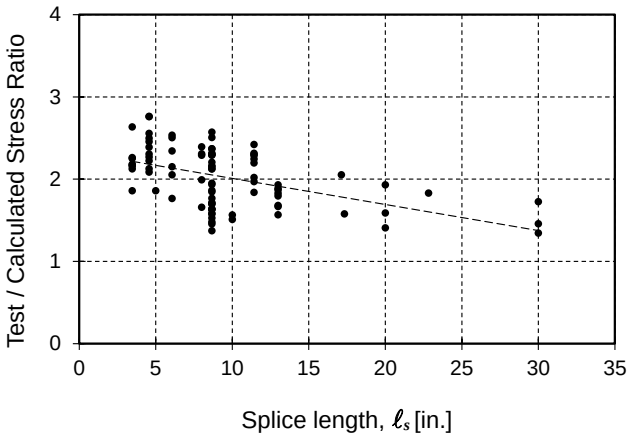

(c) Lepage et al.

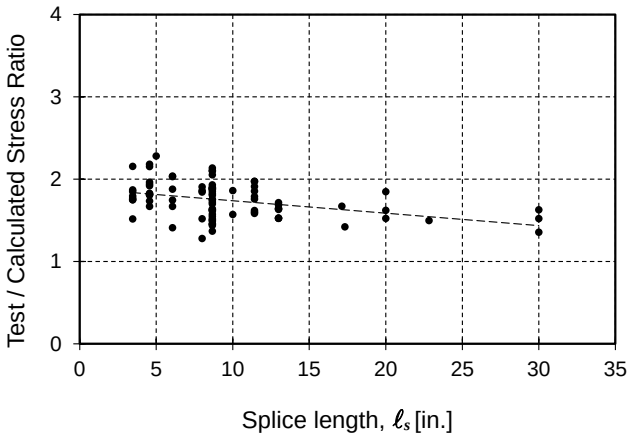

(d) Darwin et al.

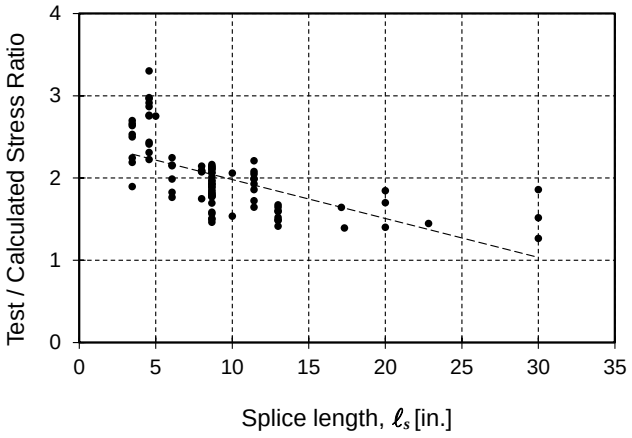

(e) Canbay and Frosch

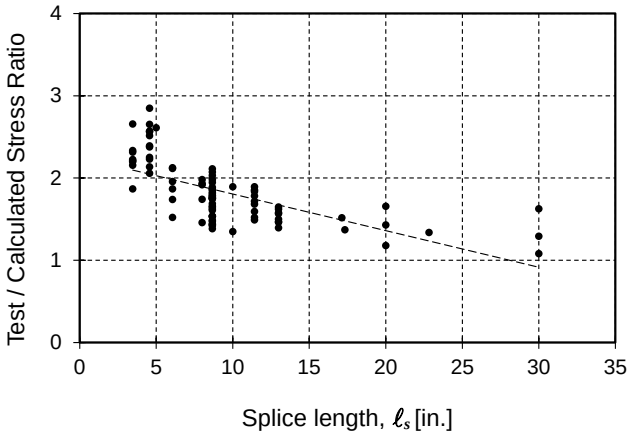

(f) Frosch et al.

Figure 81 - *T*/*C* vs. provided splice length ℓ_s for tension development length equations

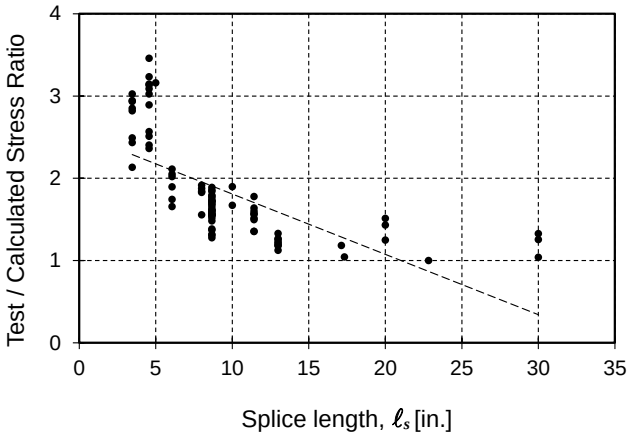

(a) ACI 318-19. r_1 = 0.94

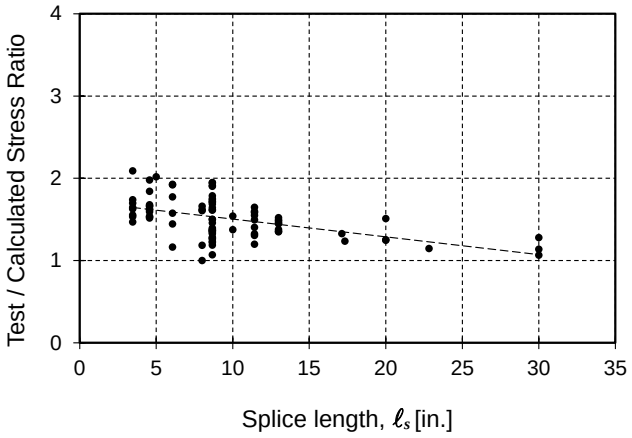

(b) ACI 408R-03. r_1 = 0.69

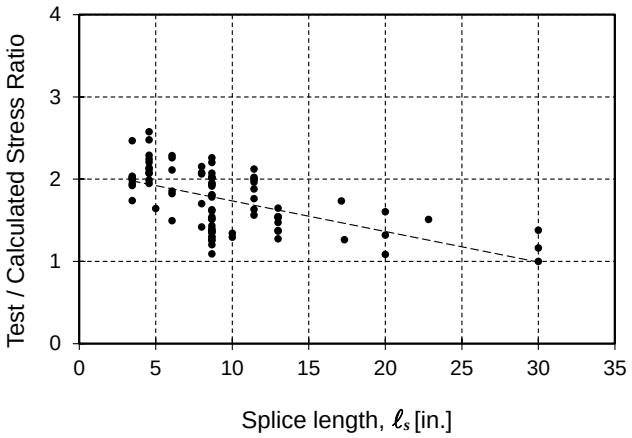

(c) Lepage et al. r_1 = 0.66

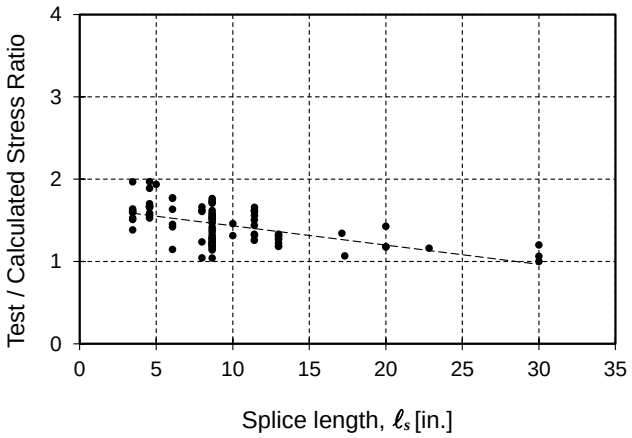

(d) Darwin et al. r_1 = 0.63

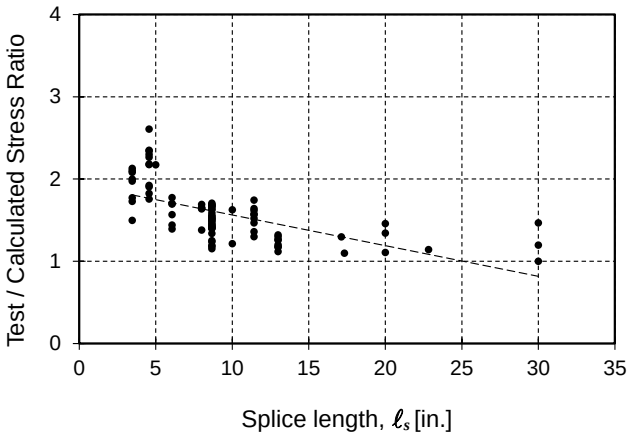

(e) Canbay and Frosch. r_1 = 0.62

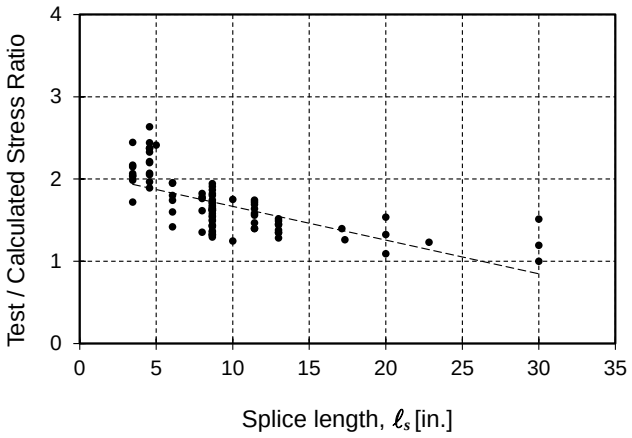

(f) Frosch et al. r_1 = 0.85

Figure 82 - T/C vs. $(c_b + K_{tr,318})/d_b$ for tension development length equations with r_1 factor

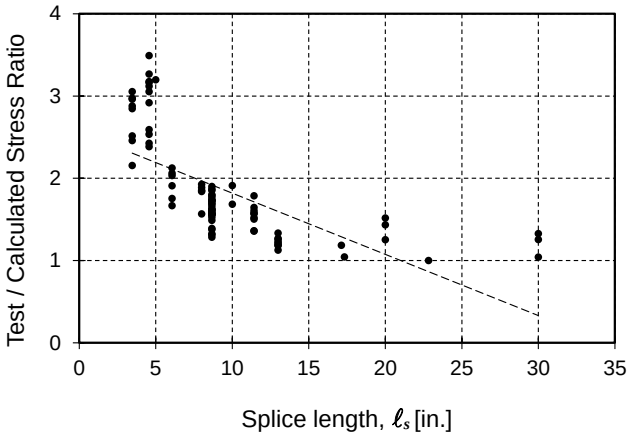

(a) ACI 318-19. r_2 = 0.96

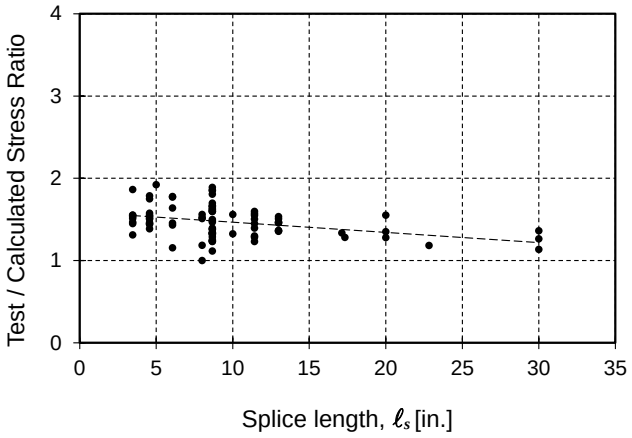

(b) ACI 408R-03. r_2 = 0.84

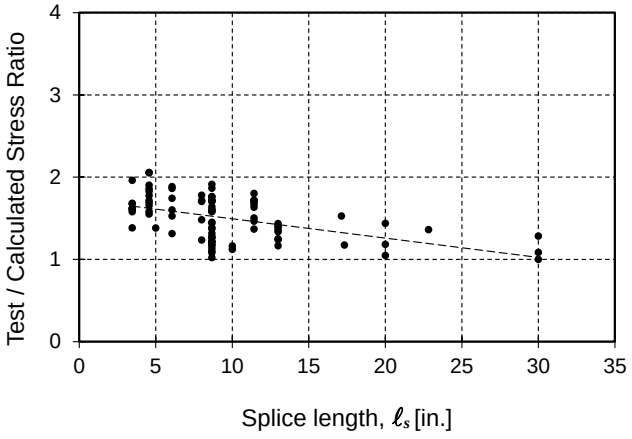

(c) Lepage et al. r_2 = 0.74

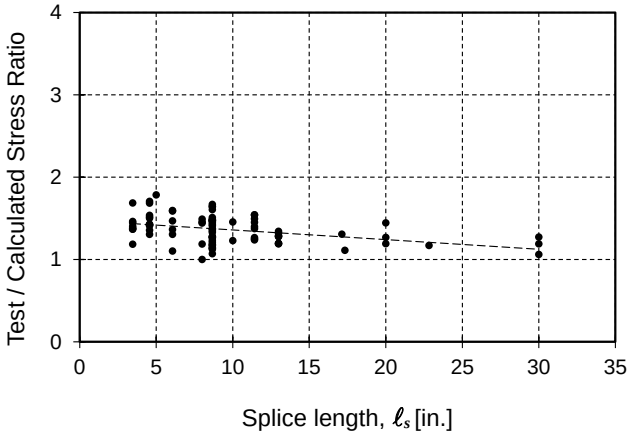

(d) Darwin et al. r_2 = 0.78

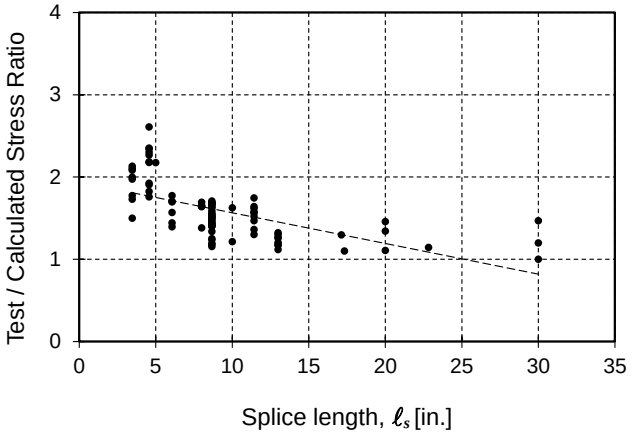

(e) Canbay and Frosch. r_2 = 0.79

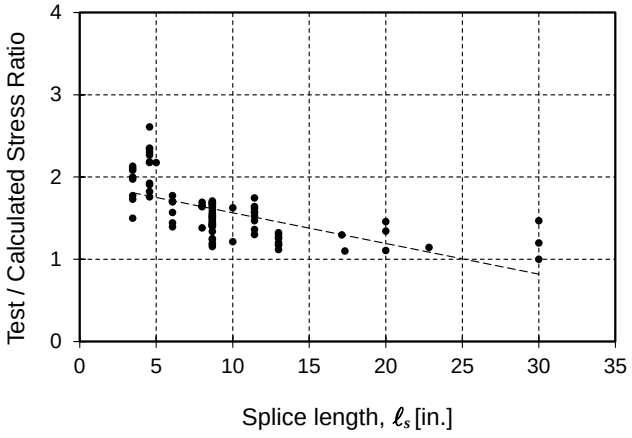

(f) Frosch et al. r_2 = 0.93

Figure 83 - T/C vs. $(c_b + K_{tr,318})/d_b$ for tension development length equations with r_2 factor

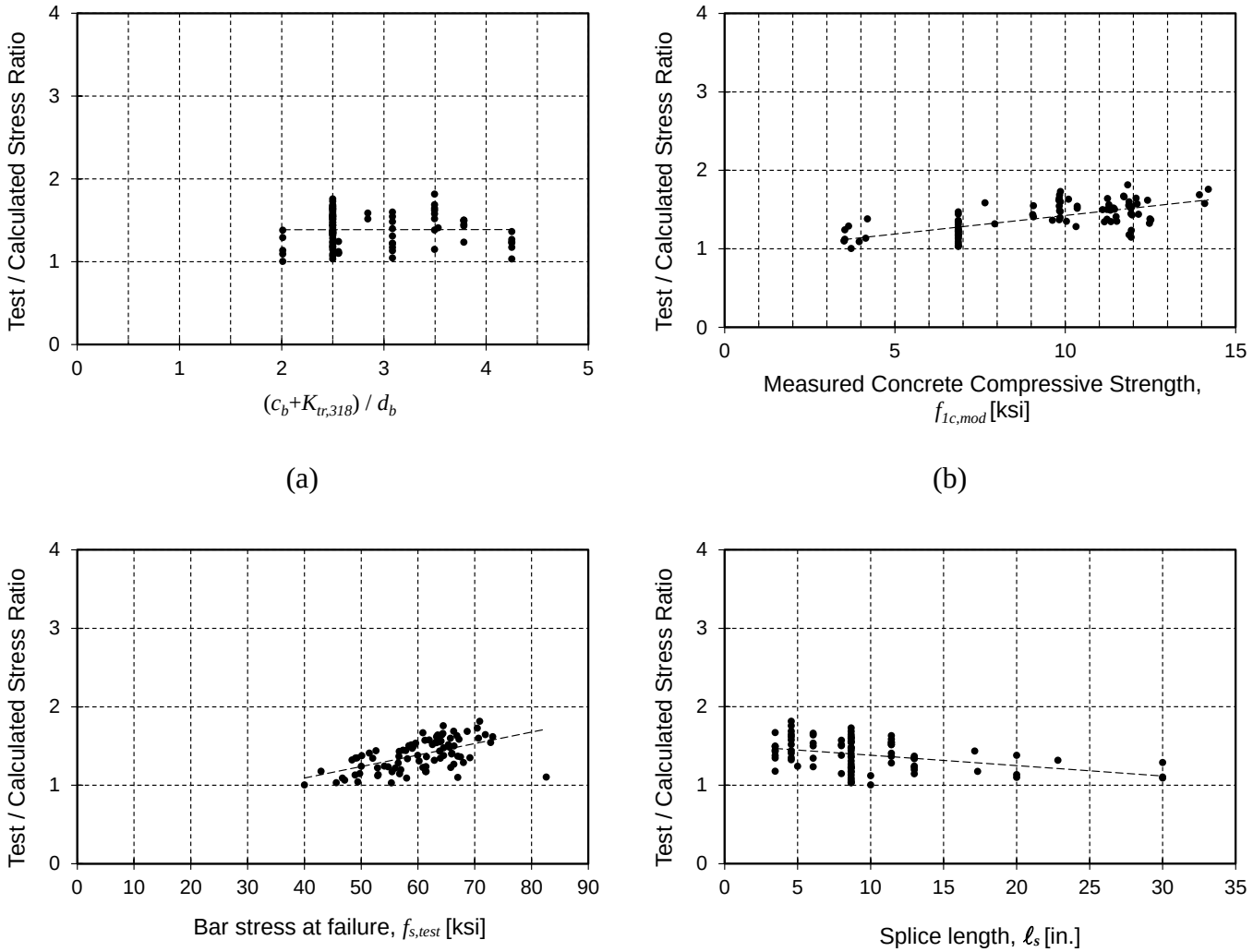

Figure 84 – Lepage et al. [16] with modified ψ_y: T/C vs.: (a) $(c_b + K_{tr,318})/d_b$ (b) measured concrete compressive strength, $f_{1c,mod}$ (c) measured steel failure stress $f_{s,test}$ (d) provided splice length ℓ_s

Appendix E: Headed Bars: Summary of Database

[1]	[2]	[3]	[4]	[5]	[6]	[7]	[8]
Authors	I.D	F.M.	f_{cm} (psi)	f_y (ksi)	h_c [in.]	h_b [in.]	b_b [in.]
Murakami et al. [29]	No. 100	I	5700	53.6	11.8	15.7	10.2
	No. 101	I	5700	53.6	11.8	15.7	10.2
Takeuchi et al. [30]	0-3	I	3520	54.7	15.7	17.7	13.8
Tazaki et al. [31]	E1	I	4410	55.0	11.8	11.8	11.8
	E2	I	4410	55.0	11.8	11.8	11.8
Chun et al. [23]	JM-1	I	8950	58.5	19.7	19.7	13.8
	JM-2	I	8720	58.5	19.7	19.7	13.8
Bashandy [22]	Specimen	I	4290	64.8	15.0	18.0	10.0
Takeuchi et al. [30]	0-1	I	6400	64.5	15.7	17.7	13.8
	0-4	I	6400	64.5	15.7	17.7	13.8
Chun et al. [23]	JM-No.11-1a	I	4760	66.4	20.5	19.9	17.7
	JM-No.11-1b	I	4760	66.4	20.5	19.9	17.7
Lee and Yu [27]	W0-M1	I	4450	68.6	16.0	18.0	12.0
	W150-M1	I	5190	68.6	16.0	18.0	12.0
Wallace et al. [32]	BCEJ1	I	5190	70.0	18.0	24.0	18.0
Kang et al. [25]	JH	I	4220	69.8	17.7	21.3	17.7
Murakami et al. [29]	B8-M	I	4280	74.1	11.8	15.7	10.2
	B7-M	I	4280	74.1	11.8	15.7	10.2
Adachi et al. [21]	J30-12-P1	I	4480	76.0	17.7	17.7	13.8
	J30-12-P2	I	4480	76.0	17.7	17.7	13.8
	J60-12-P2	I	9150	76.0	17.7	17.7	13.8
Yoshida et al. [33]	No.1	I	5470	81.5	13.8	15.7	11.8
	No.2	I	5470	81.5	13.8	15.7	11.8
	No.3	I	4500	81.5	13.8	15.7	11.8
Kato [26]	No.1	I	8820	75.6	18.7	17.7	12.8
	No.2	I	10270	73.2	18.7	17.7	12.8
Ishida et al. [24]	P2	II	3480	76.0	15.7	15.7	31.5
	P3	II	3480	76.0	15.7	15.7	31.5
	P4	II	4480	76.0	15.7	15.7	39.5
Adachi et al. [21]	J30-12-0	II	9150	76.0	17.7	17.7	13.8
	J60-12-0	II	9150	76.0	17.7	17.7	13.8
	J60-12-P1	II	4770	79.9	17.7	17.7	13.8
Matsushima et al. [28]	H	II	4770	79.9	15.7	18.9	13.8
	Hs	II	8830	85.0	15.7	18.9	13.8
Takeuchi et al. [30]	0-2	II	5700	53.6	15.7	17.7	13.8

F.M. = Failure Mode. I = Category–I (member flexural hinging followed by modest joint deterioration); II = Category–II (member flexural hinging followed by joint failure)

[1]	[2]	[7]	[8]	[9]	[10]	[11]
Authors	I.D	Bar Size	d_b (in.)	A_b (in.^{2})	n	A_{hs} (in.^{2})
Murakami et al. [29]	No. 100	D16	0.625	0.31	4	1.24
	No. 101	D16	0.625	0.31	4	1.24
Takeuchi et al. [30]	0-3	D25	1.000	0.79	3	2.37
Tazaki et al. [31]	E1	D16	0.625	0.31	6	1.85
	E2	D16	0.625	0.31	6	1.85
Chun et al. [23]	JM-1	D22/No.7	0.875	0.60	4	2.40
	JM-2	D22/No.7	0.875	0.60	8	4.80
Bashandy [22]	Specimen	D25	1.000	0.79	2	1.58
Takeuchi et al. [30]	0-1	D25	1.000	0.79	3	2.37
	0-4	D25	1.000	0.79	3	2.37
Chun et al. [23]	JM-No.11-1a	D36/No.11	1.410	1.56	3	4.68
	JM-No.11-1b	D36/No.11	1.410	1.56	3	4.68
Lee and Yu [27]	W0-M1	D22	0.875	0.60	4	2.40
	W150-M1	D22	0.875	0.60	4	2.40
Wallace et al. [32]	BCEJ1	No. 8	1.000	0.79	4	3.16
Kang et al. [25]	JH	D19	0.750	0.44	4	1.77
Murakami et al. [29]	B8-M	D19	0.750	0.44	3	1.32
	B7-M	2 D19, 1 D16	0.750,	0.44,0.312	3	1.19
Adachi et al. [21]	J30-12-P1	D25	1.000	0.79	4	3.16
	J30-12-P2	D25	1.000	0.79	4	3.16
	J60-12-P2	D25	1.000	0.79	6	4.74
Yoshida et al. [33]	No.1	D19	0.750	0.44	4	1.76
	No.2	D19	0.750	0.44	4	1.76
	No.3	D19	0.750	0.44	4	1.76
Kato [26]	No.1	D22	0.875	0.60	8	4.80
	No.2	D22	0.875	0.60	8	4.80
Ishida et al. [24]	P2	D22	0.875	0.60	7	4.20
	P3	D22	0.875	0.60	7	4.20
	P4	D22	1.000	0.60	9	5.40
Adachi et al. [21]	J30-12-0	D25	1.000	0.79	4	3.16
	J60-12-0	D25	1.000	0.79	6	4.74
	J60-12-P1	D25	1.000	0.79	6	4.74
Matsushima et al. [28]	H	D25	1.000	0.79	3	2.37
	Hs	D25	1.000	0.79	3	2.37
Takeuchi et al. [30]	0-2	D25	0.980	0.79	3	2.37

[1]	[2]	[23]	[24]	[12]	[25]	[28]	[31]
Authors	I.D	Confinement by transv. beams per ACI 318-19 §15.2.8	R_n	b_j (in.)	V_n (kip)	V_p [at column axis] (kip)	V_p/V_n
Murakami et al. [29]	No. 100	Not confined	12	11.8	126	60	0.48
	No. 101	Not confined	12	11.8	126	63	0.49
Takeuchi et al. [30]	0-3	Not confined	12	15.8	177	100	0.56
Tazaki et al. [31]	E1	Not confined	12	11.8	111	102	0.92
	E2	Not confined	12	11.8	111	89	0.80
Chun et al. [23]	JM-1	Not confined	12	25.6	572	146	0.26
	JM-2	Not confined	12	25.6	564	270	0.48
Bashandy [22]	Specimen	Not confined	12	13.0	153	94	0.62
Takeuchi et al. [30]	0-1	Not confined	12	15.8	238	120	0.51
	0-4	Not confined	12	15.8	238	127	0.53
Chun et al. [23]	JM-No.11-1a	Not confined	12	25.6	434	274	0.63
	JM-No.11-1b	Not confined	12	25.6	434	268	0.62
Lee and Yu [27]	W0-M1	Not confined	12	24.0	307	164	0.53
	W150-M1	Not confined	12	12.0	166	162	0.98
Wallace et al. [32]	BCEJ1	Not confined	12	18.0	280	202	0.72
Kang et al. [25]	JH	Not confined	12	17.7	245	122	0.50
Murakami et al. [29]	B8-M	Not confined	12	11.8	110	87	0.80
	B7-M	Not confined	12	11.8	110	88	0.80
Adachi et al. [21]	J30-12-P1	Not confined	12	17.7	252	191	0.76
	J30-12-P2	Not confined	12	17.7	252	194	0.77
	J60-12-P2	Not confined	12	17.7	360	295	0.82
Yoshida et al. [33]	No.1	Not confined	12	11.8	144	109	0.76
	No.2	Not confined	12	11.8	144	110	0.76
	No.3	Not confined	12	11.8	131	111	0.85
Kato [26]	No.1	Not confined	12	18.7	394	350	0.89
	No.2	Not confined	12	18.7	420	331	0.79
Ishida et al. [24]	P2	Confined	15	15.8	220	237	1.08
	P3	Confined	15	15.8	220	261	1.19
	P4	Confined	15	15.8	220	279	1.27
Adachi et al. [21]	J30-12-0	Not confined	12	17.7	252	190	0.75
	J60-12-0	Not confined	12	17.7	360	269	0.75
	J60-12-P1	Not confined	12	17.7	360	285	0.79
Matsushima et al. [28]	H	Not confined	12	15.8	206	166	0.81
	Hs	Not confined	12	15.8	206	156	0.76
Takeuchi et al. [30]	0-2	Not confined	12	15.8	280	141	0.50

[1]	[2]								
Authors	I.D	d (in.)	a (in.)	β_1	c (in.)	ε_s		f_y / E_s	Mn (kip-in.)
Murakami et al. [29]	No. 100	13.6	1.34	0.76	1.75	0.022	≥	0.0018	859
	No. 101	13.6	1.34	0.76	1.75	0.022	≥	0.0018	859
Takeuchi et al. [30]	0-3	15.6	3.14	0.85	3.69	0.012	≥	0.0019	1810
Tazaki et al. [31]	E1	10.0	2.30	0.83	2.77	0.010	≥	0.0019	896
	E2	10.0	2.30	0.83	2.77	0.010	≥	0.0019	896
Chun et al. [23]	JM-1	17.3	1.34	0.65	2.06	0.024	≥	0.0020	2330
	JM-2	16.8	2.75	0.65	4.23	0.011	≥	0.0020	4340
Bashandy [22]	Specimen	15.5	2.81	0.84	3.36	0.013	≥	0.0022	1440
Takeuchi et al. [30]	0-1	15.6	2.04	0.73	2.80	0.016	≥	0.0022	2220
	0-4	15.6	2.04	0.73	2.80	0.016	≥	0.0022	2220
Chun et al. [23]	JM-	17.1	4.34	0.81	5.34	0.009	≥	0.0023	4640
	JM-	17.1	4.34	0.81	5.34	0.009	≥	0.0023	4640
Lee and Yu [27]	W0-M1	16.0	3.63	0.83	4.38	0.010	≥	0.0024	2340
	W150-M1	16.0	3.11	0.79	3.93	0.011	≥	0.0024	2380
Wallace et al. [32]	BCEJ1	21.5	2.79	0.79	3.52	0.017	≥	0.0024	4450
Kang et al. [25]	JH	19.8	1.94	0.84	2.31	0.024	≥	0.0024	2320
Murakami et al. [29]	B8-M	13.6	2.63	0.84	3.14	0.012	≥	0.0026	1200
	B7-M	13.6	2.37	0.84	2.84	0.013	≥	0.0026	1090
Adachi et al. [21]	J30-12-P1	15.7	4.58	0.83	5.54	0.008	≥	0.0026	3230
	J30-12-P2	15.7	4.58	0.83	5.54	0.008	≥	0.0026	3230
	J60-12-P2	15.0	3.36	0.65	5.17	0.008	≥	0.0026	4780
Yoshida et al. [33]	No.1	14.0	2.61	0.78	3.37	0.012	≥	0.0028	1820
	No.2	14.0	2.61	0.78	3.37	0.012	≥	0.0028	1820
	No.3	14.0	3.18	0.83	3.85	0.010	≥	0.0028	1780
Kato [26]	No.1	15.5	3.78	0.65	5.82	0.007	≥	0.0026	4920
	No.2	15.5	3.15	0.65	4.84	0.009	≥	0.0025	4880
Ishida et al. [24]	P2	13.7	3.43	0.85	4.03	0.009	≥	0.0026	3840
	P3	13.7	3.43	0.85	4.03	0.009	≥	0.0026	3840
	P4	13.7	3.51	0.85	4.13	0.009	≥	0.0026	4920
Adachi et al. [21]	J30-12-0	15.7	4.58	0.83	5.54	0.008	≥	0.0026	3230
	J60-12-0	15.0	3.36	0.65	5.17	0.008	≥	0.0026	4780
	J60-12-P1	15.0	3.36	0.65	5.17	0.008	≥	0.0026	4780
Matsushima et al. [28]	H	15.1	3.39	0.81	4.18	0.010	≥	0.0028	2540
	Hs	15.1	3.39	0.81	4.18	0.010	≥	0.0028	2540
Takeuchi et al. [30]	0-2	15.6	1.95	0.65	3.00	0.015	≥	0.0029	2940

[1]	[2]				[29]	[30]	[32]
Authors	I.D	L_b (in.)	L_n (in.)	L_c (in.)	M_{peak} (kip.in.)	M_{peak}/M_n	$\delta_{0.8peak}$
Murakami et al.	No. 100	59.1	53.2	59.1	1030	1.20	0.080
Murakami et al.	No. 101	59.1	53.2	59.1	1070	1.24	0.083
Takeuchi et al.	0-3	66.9	59.1	57.1	1930	1.06	0.050
Tazaki et al.	E1	53.2	47.2	57.9	1080	1.21	0.060
Tazaki et al.	E2	53.2	47.2	57.9	951	1.06	0.060
Chun et al.	JM-1	88.6	78.7	102.6	2960	1.27	0.068
Chun et al.	JM-2	88.6	78.7	102.6	5040	1.16	0.040
Bashandy	Specimen	64.5	57.0	96.0	1590	1.10	0.053
Takeuchi et al.	0-1	66.9	59.1	57.1	2460	1.11	0.050
Takeuchi et al.	0-4	66.9	59.1	57.1	2590	1.17	0.050
Chun et al.	JM-No.11-1a	89.0	78.7	102.6	4890	1.06	0.075
Chun et al.	JM-No.11-1b	89.0	78.7	102.6	4780	1.03	0.065
Lee and Yu	W0-M1	84.7	76.7	106.3	2730	1.17	0.080
Lee and Yu	W150-M1	84.7	76.7	106.3	2750	1.16	0.080
Wallace et al.	BCEJ1	129.0	120.0	120.0	4950	1.11	0.048
Kang et al.	JH	103.4	94.5	141.7	2700	1.16	0.036
Murakami et al.	B8-M	59.1	53.2	59.1	1400	1.16	0.060
Murakami et al.	B7-M	59.1	53.2	59.1	1240	1.13	0.070
Adachi et al.	J30-12-P1	59.1	50.2	59.1	3510	1.09	0.045
Adachi et al.	J30-12-P2	59.1	50.2	59.1	3570	1.10	0.062
Adachi et al.	J60-12-P2	59.1	50.2	59.1	5320	1.11	0.067
Yoshida et al.	No.1	73.8	66.9	78.7	1680	0.92	0.040
Yoshida et al.	No.2	73.8	66.9	78.7	1700	0.93	0.040
Yoshida et al.	No.3	73.8	66.9	78.7	1670	0.94	0.040
Kato	No.1	78.7	69.4	88.6	5740	1.17	0.040
Kato	No.2	78.7	69.4	88.6	5580	1.14	0.080
Ishida et al.	P2	44.3	36.4	51.2	4000	1.04	0.030
Ishida et al.	P3	44.3	36.4	51.2	4400	1.15	0.030
Ishida et al.	P4	44.3	36.4	51.2	4680	0.95	0.030
Adachi et al.	J30-12-0	59.1	50.2	59.1	3490	1.08	0.032
Adachi et al.	J60-12-0	59.1	50.2	59.1	4850	1.01	0.033
Adachi et al.	J60-12-P1	59.1	50.2	59.1	5140	1.07	0.034
Matsushima et al.	H	78.7	70.9	97.6	2630	1.03	0.035
Matsushima et al.	Hs	78.7	70.9	97.6	2470	0.97	0.035
Takeuchi et al.	0-2	66.9	59.1	57.1	2900	0.99	0.033

Appendix F: Headed Bars: Average Length Ratios

Table 5 – Headed bars: Average length ratios: length in row / length in column

	ℓ_p	$\ell_{dt,318-14}$ no caps [Eq. (28)]	$\ell_{dt,25.4.4}$ [Eq. (21)]	$\ell_{dt,18.8.5.2}$ [Eq. (22)]	$\ell_{dc,25.4.9}$ [Eq. (23)]	ℓ_{ehy} [Eq. (31)]	ℓ_{dh} [Eq. (29)]	$0.7l_d$, Case I [Eq. (32)]	$0.7l_d$, Case II [Eq. (32)]
ℓ_p	1	0.87	0.72	0.58	0.65	1.32	0.91	0.46	0.80
$\ell_{dt,318-14}$, no caps [Eq. (28)]	1.15	1	0.83	0.67	0.78	1.55	1.04	0.53	0.92
$\ell_{dt,25.4.4}$ [Eq. (21)]	1.38	1.20	1	0.80	0.95	1.87	1.28	0.65	1.13
$\ell_{dt,18.8.5.2}$ [Eq. (22)]	1.73	1.50	1.25	1	1.18	2.34	1.60	0.81	1.41
$\ell_{dc,25.4.9}$ [Eq. (23)]	1.54	1.28	1.06	0.85	1	2.02	1.40	0.71	1.23
ℓ_{ehy} [Eq. (31)]	0.76	0.65	0.53	0.43	0.49	1	0.69	0.35	0.61
ℓ_{dh} [Eq. (29)]	1.10	0.96	0.78	0.63	0.72	1.45	1	0.51	0.88
$0.7l_d$, Case I [Eq. (32)]	2.17	1.89	1.54	1.23	1.42	2.89	1.97	1	1.79
$0.7l_d$, Case II [Eq. (32)]	1.25	1.09	0.89	0.71	0.82	1.65	1.13	0.56	1

Appendix G: Hooked Bars: Summary of Database

[1]	[2]	[3]	[4]	[5]	[6]	[7]	[8]	[9]
Authors	I.D	f_{cm} (psi)	f_y (ksi)	Beam bar size	d_b (in.)	A_b (in.^{2})	n	A_{hs} (in.^{2})
Hanson [35]	Specimen 3	5200	64.1	No. 8	1.00	0.79	4	3.16
	Specimen 4	5380	63.4	No. 8	1.00	0.79	4	3.16
	Specimen 5	5230	65.0	No. 8	1.00	0.79	4	3.16
Uzumeri [36]	Specimen #3	3920	50.8	No. 9	1.13	1.00	3	3.00
	Specimen #4	4490	50.6	No. 9	1.13	1.00	3	3.00
	Specimen #6	5250	51.1	No. 9	1.13	1.00	3	3.00
	Specimen #7	4460	51.1	No. 9	1.13	1.00	3	3.00
	Specimen #8	3820	51.1	No. 9	1.13	1.00	4	4.00
Scribner and Wight [37]	Specimen 9	4940	60.2	No. 8	1.00	0.79	4	3.16
	Specimen 11	4940	60.2	No. 8	1.00	0.79	4	3.16
Ehsani and Alameddine [38]	HL8	8100	62.0	No. 9	1.13	1.00	4	4.00
	HH8	8100	62.0	No. 9	1.13	1.00	4	4.00
	HL11	10700	52.0	No. 9	1.13	1.00	4	4.00
	HH11	10700	64.6	No. 9	1.13	1.00	4	4.00
	HH14	13600	65.3	No. 9	1.13	1.00	4	4.00
	LL8	8100	69.1	No. 8	1.00	0.79	4	3.16
	LH8	8100	67.3	No. 8	1.00	0.79	4	3.16
	LL11	10700	61.5	No. 8	1.00	0.79	4	3.16
	LH11	10700	75.5	No. 8	1.00	0.79	4	3.16
	LL14	13600	70.7	No. 8	1.00	0.79	4	3.16
	LH14	13600	71.9	No. 8	1.00	0.79	4	3.16
Kurose et al. [39]	J3	4700	67.2	No. 9	1.13	1.00	5	5.00
Hwang et al. [40]	3T44	11140	62.4	No. 8	1.00	0.79	4	3.16
	3T3	10010	62.4	No. 8	1.00	0.79	4	3.16
	2T4	10300	62.4	No. 8	1.00	0.79	4	3.16
	3T4	10900	71.2	No. 8	1.00	0.79	4	3.16
	2T5	11100	71.2	No. 8	1.00	0.79	4	3.16

[1]	[2]	[10]	[11]	[12]	[13]	[14]	[15]	[16]
Authors	I.D	h_c (in.)	b_c (in.)	h_b (in.)	b_b (in.)	side cover (in.)	c_{ch} (in.)	c_b (in.)
Hanson [35]	Specimen 3	15.0	15.0	20.0	12.0	2.41	3.00	1.25
	Specimen 4	15.0	15.0	20.0	12.0	2.41	3.00	1.25
	Specimen 5	15.0	15.0	20.0	12.0	2.41	3.00	1.25
Uzumeri [36]	Specimen #3	15.0	15.0	20.0	12.0	0.94	4.63	1.69
	Specimen #4	15.0	15.0	20.0	12.0	1.00	4.63	1.69
	Specimen #6	15.0	15.0	20.0	15.0	2.50	4.63	1.69
	Specimen #7	15.0	15.0	20.0	15.0	2.50	4.63	1.69
	Specimen #8	15.0	15.0	20.0	15.0	2.50	3.08	1.69
Scribner and Wight [37]	Specimen 9	18.0	12.0	14.0	10.0	1.55	1.63	0.80
	Specimen 11	18.0	12.0	14.0	10.0	1.55	1.63	0.80
Ehsani and Alameddine [38]	HL8	14.0	14.0	20.0	12.5	3.00	6.83	1.94
	HH8	14.0	14.0	20.0	12.5	3.00	6.83	1.94
	HL11	14.0	14.0	20.0	12.5	3.00	6.83	1.94
	HH11	14.0	14.0	20.0	12.5	3.00	6.83	1.94
	HH14	14.0	14.0	20.0	12.5	3.00	6.83	1.94
	LL8	14.0	14.0	20.0	12.5	3.00	6.83	2.00
	LH8	14.0	14.0	20.0	12.5	3.00	6.83	2.00
	LL11	14.0	14.0	20.0	12.5	3.00	6.83	2.00
	LH11	14.0	14.0	20.0	12.5	3.00	6.83	2.00
	LL14	14.0	14.0	20.0	12.5	3.00	6.83	2.00
	LH14	14.0	14.0	20.0	12.5	3.00	6.83	2.00
Kurose et al. [39]t	J3	20.0	20.0	20.0	16.0	2.63	2.44	1.50
Hwang et al. [40]	3T44	16.5	16.5	17.7	12.6	2.84	1.97	1.18
	3T3	16.5	16.5	17.7	12.6	2.84	2.05	1.18
	2T4	16.5	16.5	17.7	12.6	2.84	1.97	1.18
	3T4	17.7	17.7	17.7	12.6	2.84	1.97	1.18
	2T5	17.7	17.7	17.7	12.6	2.84	1.89	1.18

[1]	[2]	[17]	[18]	[19]	[20]	[21]	[22]
Authors	I.D	Column long. reinforcement			Joint transverse reinforcement		
		Bar size	d_b (in)	Type	Bar size	d_{bt} (in.)	s (in.)
Hanson [35]	Specimen 3	No. 11	1.41	hoops	No. 4	0.5	3.00
	Specimen 4	No. 11	1.41	hoops	No. 4	0.5	3.00
	Specimen 5	No. 11	1.41	hoops	No. 4	0.5	3.00
Uzumeri [36]	Specimen #3	No. 8	1.00	hoops	4 No. 3	0.38	3.00
	Specimen #4	No. 8	1.00	hoops	4 No. 4	0.5	3.00
	Specimen #6	No. 8	1.00	hoops	8 No. 4	0.5	1.75
	Specimen #7	No. 8	1.00	hoops	4 No. 4	0.5	3.00
	Specimen #8	No. 8	1.00	hoops	8 No. 4	0.5	1.75
Scribner and Wight [37]	Specimen 9	No. 6	0.75	hoops	4 No. 4	0.5	2.00
	Specimen 11	No. 6	0.75	hoops	4 No. 4	0.5	2.00
Ehsani and Alameddine [38]	HL8	No. 8	1.00	hoops	No. 4	0.5	2.50
	HH8	No. 8	1.00	hoops	No. 4	0.5	2.50
	HL11	No. 8	1.00	hoops	No. 4	0.5	2.50
	HH11	No. 8	1.00	hoops	No. 4	0.5	2.50
	HH14	No. 8	1.00	hoops	No. 4	0.5	2.50
	LL8	No. 8	1.00	hoops	No. 4	0.5	2.50
	LH8	No. 8	1.00	hoops	No. 4	0.5	2.50
	LL11	No. 8	1.00	hoops	No. 4	0.5	2.50
	LH11	No. 8	1.00	hoops	No. 4	0.5	2.50
	LL14	No. 8	1.00	hoops	No. 4	0.5	2.50
	LH14	No. 8	1.00	hoops	No. 4	0.5	2.50
Kurose et al. [39]	J3	No. 9	1.13	hoops	No. 4	0.5	4.00
Hwang et al. [40]	3T44	No. 10	1.27	hoops	3 sets 2 No. 4	0.5	3.82
	3T3	No. 10	1.27	hoops	3 sets No. 3	0.38	3.82
	2T4	No. 10	1.27	hoops	2 sets No. 4	0.5	5.75
	3T4	No. 10	1.27	hoops	3 sets No. 4	0.5	3.82
	2T5	No. 10	1.27	hoops	2 sets No. 5	0.63	5.75

[1]	[2]	[23]	[24]	[25]	[26]	[27]	[28]
Authors	I.D	Confinement by transv. beams per ACI 318-19 §15.2.8	R_n	b_j (in.)	V_n (kip)	V_p [at colum n axis] (kip)	V_p/V_n
Hanson [35]	Specimen 3	Not confined	12	12.0	156	224	1.44
	Specimen 4	Not confined	12	12.0	158	194	1.23
	Specimen 5	Not confined	12	12.0	156	214	1.37
Uzumeri [36]	Specimen #3	Not confined	12	12.0	135	135	1.00
	Specimen #4	Not confined	12	12.0	145	136	0.94
	Specimen #6	Not confined	12	15.0	196	143	0.73
	Specimen #7	Not confined	12	15.0	180	140	0.78
	Specimen #8	Not confined	12	15.0	167	182	1.09
Scribner and Wight [37]	Specimen 9	Not confined	12	10.0	152	225	1.48
	Specimen 11	Not confined	12	10.0	152	225	1.48
Ehsani and Alameddine [38]	HL8	Not confined	12	12.5	189	209	1.11
	HH8	Not confined	12	12.5	189	211	1.12
	HL11	Not confined	12	12.5	210	203	0.96
	HH11	Not confined	12	12.5	210	226	1.07
	HH14	Not confined	12	12.5	210	222	1.05
	LL8	Not confined	12	12.5	189	196	1.04
	LH8	Not confined	12	12.5	189	189	1.00
	LL11	Not confined	12	12.5	210	163	0.78
	LH11	Not confined	12	12.5	210	220	1.05
	LL14	Not confined	12	12.5	210	199	0.95
	LH14	Not confined	12	12.5	210	203	0.97
Kurose et al. [39]	J3	Confined	15	16.0	329	237	0.72
Hwang et al. [40]	3T44	Not confined	12	12.6	250	182	0.73
	3T3	Not confined	12	12.6	250	195	0.78
	2T4	Not confined	12	12.6	250	186	0.74
	3T4	Not confined	12	12.6	268	190	0.71
	2T5	Not confined	12	12.6	268	199	0.74

[1]	[2]	[29]	[30]	[31]	[32]	[33]		[34]	[35]
Authors	I.D	***d*** (in.)	***a*** (in.)	β_1	***c*** (in.)	ε_s		f_y / E_s	***Mn*** (kip-in.)
Hanson [35]	Specimen 3	18.0	3.82	0.85	4.49	0.011	≥	0.0022	3260
	Specimen 4	18.0	3.65	0.85	4.30	0.012	≥	0.0022	3240
	Specimen 5	18.0	3.85	0.85	4.53	0.011	≥	0.0022	3300
Uzumeri [36]	Specimen #3	18.3	3.81	0.85	4.48	0.012	≥	0.0018	2500
	Specimen #4	18.3	3.31	0.85	3.90	0.013	≥	0.0017	2530
	Specimen #6	18.3	2.29	0.85	2.69	0.019	≥	0.0018	2630
	Specimen #7	18.3	2.70	0.85	3.17	0.016	≥	0.0018	2600
	Specimen #8	18.3	4.20	0.85	4.94	0.011	≥	0.0018	3310
Scribner and Wight [37]	Specimen 9	12.1	4.53	0.85	5.33	0.006	≥	0.0021	1870
	Specimen 11	12.1	4.53	0.85	5.33	0.006	≥	0.0021	1870
Ehsani and Alameddine [38]	HL8	17.0	2.88	0.85	3.39	0.014	≥	0.0021	3860
	HH8	17.0	2.88	0.85	3.39	0.014	≥	0.0021	3860
	HL11	17.0	1.83	0.85	2.15	0.022	≥	0.0018	3350
	HH11	17.0	2.27	0.85	2.67	0.018	≥	0.0022	4100
	HH14	17.0	1.81	0.85	2.13	0.023	≥	0.0023	4200
	LL8	17.0	2.54	0.85	2.98	0.016	≥	0.0024	3440
	LH8	17.0	2.47	0.85	2.91	0.017	≥	0.0023	3350
	LL11	17.0	1.71	0.85	2.01	0.024	≥	0.0021	3140
	LH11	17.0	2.10	0.85	2.47	0.019	≥	0.0026	3810
	LL14	17.0	1.55	0.85	1.82	0.026	≥	0.0024	3630
	LH14	17.0	1.57	0.85	1.85	0.026	≥	0.0025	3680
Kurose et al. [39]	J3	17.9	5.26	0.85	6.18	0.008	≥	0.0023	5140
Hwang et al. [40]	3T44	15.1	1.65	0.85	1.94	0.022	≥	0.0022	2820
	3T3	15.1	1.84	0.85	2.16	0.020	≥	0.0022	2800
	2T4	15.1	1.79	0.85	2.10	0.020	≥	0.0022	2800
	3T4	15.1	1.93	0.85	2.27	0.019	≥	0.0025	3190
	2T5	15.1	1.89	0.85	2.23	0.019	≥	0.0025	3190

[1]	[2]	[36]	[37]	[38]	[39]	[40]	[41]
Authors	I.D	L_b (in.)	L_n (in.)	L_c (in.)	M_{peak} (kip.in.)	M_{peak}/M_n	$\delta_{0.8peak}$
Hanson [35]	Specimen 3	126	120	120	4200	1.29	N/R
	Specimen 4	126	120	120	3660	1.13	N/R
	Specimen 5	126	120	120	4000	1.21	N/R
Uzumeri [36]	Specimen #3	120	113	120	2590	1.04	≥ 3%
	Specimen #4	120	113	120	2650	1.05	≥ 3%
	Specimen #6	120	113	120	2890	1.10	≥ 3%
	Specimen #7	120	113	120	2800	1.08	≥ 3%
	Specimen #8	120	113	120	3460	1.04	≥ 3%
Scribner and Wight [37]	Specimen 9	72	63.0	96	2510	1.34	≥ 3%
	Specimen 11	72	63.0	96	2500	1.34	≥ 3%
Ehsani and Alameddine [38]	HL8	70	63	141	3710	0.96	N/R
	HH8	70	63	141	3740	0.97	N/R
	HL11	70	63	141	3730	1.12	≥ 3%
	HH11	70	63	141	4090	1.00	N/R
	HH14	70	63	141	4080	0.97	≥ 3%
	LL8	70	63	141	3520	1.02	N/R
	LH8	70	63	141	3400	1.01	N/R
	LL11	70	63	141	3020	0.96	≥ 3%
	LH11	70	63	141	4020	1.06	≥ 3%
	LL14	70	63	141	3700	1.02	≥ 3%
	LH14	70	63	141	3780	1.03	≥ 3%
Kurose et al. [39]	J3	96	86.0	165	4040	0.79	≥ 3%
Hwang et al. [40]	3T44	74.8	66.5	106	3070	1.09	≥ 3%
	3T3	74.8	66.5	106	3260	1.17	≥ 3%
	2T4	74.8	66.5	106	3110	1.11	≥ 3%
	3T4	74.8	65.9	106	3170	1.00	≥ 3%
	2T5	74.8	65.9	106	3320	1.04	≥ 3%

Appendix H: Hooked Bars: Average Length Ratios

Table 6 – Hooked bars: Average length ratios: length in row / length in column (all 27 specimens)

	ℓ_p	$\ell_{dh,318-14}$	$\ell_{dh,25.4.3}$	$\ell_{dc,25.4.9}$ + BR + d_b	ℓ_{ehy}	$\ell_{dh,18.8.5.1}$	0.7 $l_{d,408}$ Case I + BR + d_b	0.7 $l_{d,408}$ Case II + BR + d_b
ℓ_p	1	1.19	0.80	0.62	1.26	1.06	0.43	0.93
$\ell_{dh,318-14}$ [Eq. (39)]	0.84	1	0.69	0.55	1.13	0.94	0.37	0.82
$\ell_{dh,25.4.3}$ [Eq. (33)]	1.25	1.44	1	0.80	1.63	1.36	0.54	1.18
$\ell_{dc,25.4.9}$ [Eq. (35)] + BR + d_b	1.61	1.82	1.26	1	2.12	1.76	0.71	1.52
ℓ_{ehy} [Eq. (41)]	0.79	0.88	0.61	0.47	1	0.85	0.33	0.74
$\ell_{dh,18.8.5.1}$ [Eq. (34)]	0.94	1.06	0.73	0.57	1.18	1	0.40	0.87
0.7 $l_{d,408}$ Case I [Eq. (42)] + BR + d_b	2.34	2.71	1.86	1.41	3.01	2.47	1	2.31
0.7 $l_{d,408}$ Case II [Eq. (42)] + BR + d_b	1.08	1.22	0.84	0.66	1.36	1.15	0.43	1

BR =bend radius

Table 7 – Hooked bars: Average length ratios: length in row / length in column (specimens with $\delta_{0.8peak} \geq 3\%$: 19 specimens)

	ℓ_p	$\ell_{dh,318-14}$	$\ell_{dh,25.4.3}$	$\ell_{dc,25.4.9}$ + BR + d_b	ℓ_{ehy}	$\ell_{dh,18.8.5.1}$	0.7 $l_{d,408}$ Case I + BR + d_b	0.7 $l_{d,408}$ Case II + BR + d_b
ℓ_p	1	1.39	0.91	0.70	1.37	1.19	0.39	0.78
$\ell_{dh,318-14}$ [Eq. (39)]	0.72	1	0.66	0.52	1.02	0.87	0.29	0.57
$\ell_{dh,25.4.3}$ [Eq. (33)]	1.10	1.51	1	0.80	1.55	1.33	0.44	0.88
$\ell_{dc,25.4.9}$ [Eq. (35)] + BR + d_b	1.43	1.91	1.25	1	2.01	1.72	0.59	1.12
ℓ_{ehy} [Eq. (41)]	0.73	0.98	0.65	0.50	1	0.88	0.29	0.58
$\ell_{dh,18.8.5.1}$ [Eq. (34)]	0.84	1.15	0.75	0.58	1.14	1	0.34	0.66
0.7 $l_{d,408}$ Case I [Eq. (42)] + BR + d_b	2.54	3.47	2.27	1.71	3.50	2.94	1	2.08
0.7 $l_{d,408}$ Case II [Eq. (42)] + BR + d_b	1.28	1.74	1.14	0.89	1.73	1.51	0.48	1

BR =bend radius